OPTIMAL CONTROL OF UNCERTAIN EULER-LAGRANGE SYSTEMS

By

KEITH DUPREE

A DISSERTATION PRESENTED TO THE GRADUATE SCHOOL
OF THE UNIVERSITY OF FLORIDA IN PARTIAL FULFILLMENT
OF THE REQUIREMENTS FOR THE DEGREE OF
DOCTOR OF PHILOSOPHY

UNIVERSITY OF FLORIDA

2009

© 2009 Keith Dupree

To my wife Jennifer, my father Kevin, my mother Dorothy, my brother Patrick, and my dog Lucy, for their love, support, and patience

ACKNOWLEDGMENTS

I would like to thank my advisor, Dr. Warren Dixon, for his guidance and support. His example taught me to dedicate myself to everything I attempt, and to always seek to ways to improve my work. The opportunities he provided me are both unmeasurable and invaluable.

I would also like to thank my committee members: Dr. Norman Fitz-Coy, Dr. Jacob Hammer, and Dr. Prabir Barooah, for the time and help that they provided.

Finally, I would like to thank my NCR lab fellows for their friendship during the past four years. Specifically, I would like to thank Parag Patre for always having the time to answer a question, and Will MacKunis for making the lab a more lively environment.

TABLE OF CONTENTS

page

ACKNOWLEDGMENTS 4

LIST OF TABLES 7

LIST OF FIGURES 8

ABSTRACT 10

CHAPTER

1 INTRODUCTION 12

1.1 Motivation and Literature Review 12
1.2 Problem Statement 15
1.3 Contributions 18

2 OPTIMAL CONTROL OF UNCERTAIN NONLINEAR SYSTEMS USING A NEURAL NETWORK AND RISE FEEDBACK 20

2.1 Dynamic Model and Properties 20
2.2 Control Objective 22
2.3 Optimal Control Design 22
2.4 RISE Feedback Control Development 25
2.5 Stability Analysis 27
2.6 Neural Network Extension 31
2.7 Neural Networks 32
2.8 Stability Analysis 38
2.9 Simulation and Experimental Results 42
2.9.1 Simulation 42
2.9.2 Experiment 44
2.9.3 Discussion 54

3 INVERSE OPTIMAL CONTROL OF A NONLINEAR EULER-LAGRANGE SYSTEM 56

3.1 Dynamic Model and Properties 57
3.2 Control Development 58
3.3 Stability Analysis 60
3.4 Cost Functional Minimization 63
3.5 Simulation and Experimental Results 65
3.5.1 Simulation 65
3.5.2 Experiment 69
3.5.3 Discussion 72

4 INVERSE OPTIMAL CONTROL OF A NONLINEAR EULER-LAGRANGE SYSTEM USING OUTPUT FEEDBACK 74

4.1 Dynamic Model and Properties 74
4.2 Control Development 75
4.3 Stability Analysis 79
4.4 Cost Functional Minimization 82
4.5 Output Feedback Form of the Controller 84
4.6 Experimental Results 86
4.6.1 Experiment 86
4.6.2 Discussion 89

5 CONCLUSION 90

APPENDIX

A SOLUTION OF RICCATI DIFFERENTIAL EQUATION 92

B SOLUTION OF HAMILTON-JACOBI-BELLMAN EQUATION 93

C BOUND ON $\tilde{N}(t)$ 96

D BOUND ON $L(t)$ - PART 1 101

E BOUND ON $L(t)$ - PART 2 102

F REVIEW OF ADAPTIVE INVERSE OPTIMAL CONTROL: 104

REFERENCES 107

BIOGRAPHICAL SKETCH 111

LIST OF TABLES

Table page

2-1 Tabulated values for the 10 runs for the developed controllers. 50

3-1 Tabulated values for the adaptive inverse optimal controller 72

4-1 Tabulated values for the 10 runs of the output feedback adaptive inverse optimal controller 87

LIST OF FIGURES

Figure page

2-1 The simulated tracking errors for the RISE and optimal controller. 45

2-2 The simulated torques for the RISE and optimal controller. 45

2-3 The difference between the RISE feedback and the nonlinear effects and bounded disturbances. 46

2-4 The simulated tracking errors for the RISE, NN, and optimal controller. 46

2-5 The simulated torques for the RISE, NN, and optimal controller. 47

2-6 The difference between the RISE feedback and feedforward NN and the nonlinear effects and bounded disturbances (i.e., $.\left(\hat{f}_d + \mu\right) - (h + \tau_d)$). 47

2-7 The experimental testbed consists of a two-link robot. The links are mounted on two NSK direct-drive switched reluctance motors. 48

2-8 Tracking errors resulting from implementing the RISE and optimal controller. . 51

2-9 Torques resulting from implementing the RISE and optimal controller. 51

2-10 Tracking errors resulting from implementing the RISE, NN, and optimal controller. 52

2-11 Torques resulting from implementing the RISE, NN, and optimal controller. . . 52

2-12 Tracking errors resulting from implementing the controller developed in literature. 53

2-13 Torques resulting from implementing the controller developed in literature. . . . 53

3-1 The simulated tracking errors for the adaptive inverse optimal controller. 66

3-2 The simulated torques for the adaptive inverse optimal controller. 67

3-3 Unknown system parameter estimates for the adaptive inverse optimal controller. 67

3-4 The value of $l\left(x, \hat{\theta}\right)$ from Equation 3–30. 68

3-5 The integral part of the cost functional in Equation 3–29. 68

3-6 Tracking errors resulting from implementing the adaptive inverse optimal controller. 70

3-7 Torques resulting from implementing the adaptive inverse optimal controller. . . 70

3-8 Tracking errors resulting from implementing the adaptive inverse optimal controller for a slower trajectory. 71

3-9 Torques resulting from implementing the adaptive inverse optimal controller for a slower trajectory. 71

4-1 Tracking errors resulting from implementing the output feedback adaptive inverse optimal controller. 88

4-2 Torques resulting from implementing the output feedback adaptive inverse optimal controller. 88

4-3 Unknown system parameter estimates for the output feedback adaptive inverse optimal controller. 89

Abstract of Dissertation Presented to the Graduate School
of the University of Florida in Partial Fulfillment of the
Requirements for the Degree of Doctor of Philosophy

OPTIMAL CONTROL OF UNCERTAIN EULER-LAGRANGE SYSTEMS

By

Keith Dupree

May 2009

Chair: Warren E. Dixon
Major: Mechanical Engineering

Optimal control theory involves the design of controllers that can satisfy some tracking or regulation control objective while simultaneously minimizing some performance metric. A sufficient condition to solve an optimal control problem is to solve the Hamilton-Jacobi-Bellman (HJB) equation. For the special case of linear time-invariant systems, the solution to the HJB equation reduces to solving the algebraic Riccati equation. However, for general systems, the challenge is to find a value function that satisfies the HJB equation. Finding this value function has remained problematic because it requires the solution of a partial differential equation that can not be solved explicitly.

Chapter 2 illustrates the amalgamation of optimal control techniques with a recently developed continuous robust integral of the sign of the error (RISE) feedback term. Specifically, a system in which all terms are assumed known (temporarily) is feedback linearized and a control law is developed based on the HJB optimization method for a given quadratic performance index. Under the assumption that parametric uncertainty and unknown bounded disturbances are present in the dynamics, the control law is modified to contain the RISE feedback term which is used to identify the uncertainty. A Lyapunov stability analysis is included to show that the RISE feedback term asymptotically identifies the unknown dynamics (yielding semi-global asymptotic tracking) provided upper bounds on the disturbances are known and the control gains are selected appropriately. A feedforward neural network is then added to the previous

controller. The utility of combining these feedforward and feedback methods are twofold. Previous efforts indicate that modifying the RISE feedback with a feedforward term can reduce the control effort and improve the transient and steady state response of the RISE controller. Moreover, combining NN feedforward controllers with RISE feedback yields asymptotic results. Simulation as well as experimental results are provided to illustrate the developed controllers.

Inverse optimal control is an alternative method to solve the nonlinear optimal control problem by circumventing the need to solve the HJB equation. Adaptive inverse optimal control techniques have been developed that can handle structured (i.e., linear in the parameters (LP)) uncertainty for a particular class of nonlinear systems. In Chapter 3, an adaptive inverse optimal controller is developed to minimize a meaningful performance index while the generalized coordinates of a nonlinear Euler-Lagrange system asymptotically track a desired time-varying trajectory despite LP uncertainty. A Lyapunov analysis is provided to examine the stability of the developed optimal controller, and simulation and experimental results illustrate the performance of the controller.

Output feedback based controllers are more desirable than full-state feedback controllers because the necessary sensors for full-state feedback may not always be available and using numerical differentiation to obtain velocities can be problematic if position measurements are noisy. In Chapter 4, an adaptive output feedback IOC is developed which minimizes a meaningful cost, while the generalized coordinates of a nonlinear Euler-Lagrange system asymptotically tracks a desired time-varying trajectory. The new controller contains a desired compensation adaptation law (DCAL) based feedforward term and a feedback term that is shown to be implementable using only position measurements. A Lyapunov analysis is provided to prove the stability of the developed controller and to determine a meaningful cost functional. Experimental results are included to illustrate the performance of the controller. The dissertation is concluded in Chapter 5.

CHAPTER 1
INTRODUCTION

1.1 Motivation and Literature Review

Optimal controllers are controllers that minimize some cost while stabilizing a system. The design of an optimal controller generally involves solving the Hamilton-Jacobi-Bellman (HJB) equation, which reduces to an algebraic Riccati equation (ARE) for linear time-invariant systems. Due to the fact that the HJB equation is a partial differential equation, finding a value function that explicitly satisfies the HJB equation remains problematic.

One common technique in developing an optimal controller for a nonlinear system is to assume the nonlinear dynamics are exactly known, feedback linearize the system, and then apply optimal control techniques to the resulting system as in (1–3), and others. For example, dynamic feedback linearization was used in (1) to develop a control Lyapunov function to obtain a class of optimal controllers. A review of the optimality of nonlinear design techniques and general results involving feedback linearization as well as Jacobian linearization and other nonlinear design techniques are provided in (4; 5).

Motivated by the desire to eliminate the requirement for exact knowledge of the dynamics, (6) developed one of the first results to illustrate the interaction of adaptive control with an optimal controller. Specifically, (6) first used exact feedback linearization to cancel the nonlinear dynamics and produce an optimal controller. Then, a self-optimizing adaptive controller was developed to yield global asymptotic tracking despite linear-in-the parameters uncertainty. The analysis in (6) indicated that if the parameter estimation error could somehow converge to zero, then the controller would converge to the optimal solution.

Another method to compensate for system uncertainties is to employ neural networks (NN) to approximate the unknown dynamics. The universal approximation property states that a NN can identify a function up to some function reconstruction error. The use of

NN versus feedback linearization allows for general uncertain systems to be examined. However this added robustness comes at the expense of reduced steady-state error (i.e., generally resulting in a uniformly ultimately bounded (UUB) result). NN controllers were developed in results such as (7–12) to accommodate for the uncertainty in the system and to solve the HJB equation. Specifically the tracking errors are proven to be uniformly ultimately bounded (UUB) and the resulting state space system, for which the HJB optimal controller is developed, is only approximated.

The development in Chapter 2 is motivated by the desire to improve upon the UUB result previously found in literature. Specifically, this chapter illustrates how the inclusion of the Robust Integral of the Sign of the Error (RISE) method in (13; 14) can be used to identify the system and reject disturbances, while achieving asymptotic tracking and the convergence of a control term to the optimal controller. Chapter 2 also includes a NN extension to the previously designed controller as a modification to the results in (7–12) that allows for asymptotic stability and convergence to the optimal controller rather than to approximate the optimal controller.

Inverse optimal control (IOC) (15–21) is an alternative method to solve the nonlinear optimal control problem by circumventing the need to solve the HJB equation. Previous IOCs focus on finding a control Lyapunov function (CLF), which can be shown to also be a value function, and then developing a controller that optimizes a meaningful cost (i.e., a cost that puts a positive penalty on the states and actuation). The advantage of the IOC is that the controller does not have to converge to an optimal solution (like direct optimal controllers); however, the cost functional can not be chosen a priori. The cost functional is determined based on the value function.

Some adaptive IOC methods (22–26) have been developed to compensate for linear in the parameters (LP) uncertainty. Results such as (22) and (23), develop adaptive IOCs for a general class of nonlinear systems with unknown parameters. An inverse optimal adaptive attitude tracking controller is developed in (25) for rigid spacecraft with external

disturbances and a constant uncertain inertia matrix. In (26), an inverse optimal adaptive backstepping technique is applied to the design of a pitch control law for a surface-to-air nonlinear missile model with a constant inertia matrix. The results in Chapter 3 seek to apply adaptive inverse optimal control methods to an unknown Euler-Lagrange system with a state dependent inertia matrix.

Output feedback based controllers are more desirable than full-state feedback controllers, because the necessary sensors for full-state feedback may not always be available and using numerical differentiation to obtain velocities can be problematic if position measurements are noisy. Several researchers have developed output feedback optimal controllers. The researchers in (27), develop a finite dimensional dynamic output-feedback controller that achieves local near-optimality and semiglobal inverse optimality for a output-feedback system with input disturbances. However, the nonlinearities only depend on the measured output, and the system parameters are assumed to be known. An optimal trajectory tracking control is proposed in (28) for nonholonomic systems in chained form by using only output feedback information. The nonholonomic system in (28) is written in such a way that the state and control matrices are known. In (29), an output feedback optimal controller is designed using the certainty equivalence principle, where the states are estimated, but used in the control law as if they were the true states, resulting in a near optimal controller. The authors in Chapter 8 of (30), design an output feedback linear quadratic regulator, but for a linear system with known parameters.

Inspired by output feedback design methods developed in (31–34), an adaptive output feedback IOC is developed in Chapter 4. The new controller contains a DCAL based feedforward term and a feedback term that is shown to be implementable using only position measurements. Unlike the previous results in literature, the system contains an unknown state dependent inertia matrix. A Lyapunov analysis is provided to prove the stability of the developed controller and to determine a meaningful cost functional.

Experimental results are included to illustrate the performance of the controller. The dissertation is concluded in Chapter 5.

1.2 Problem Statement

In this dissertation, optimal control techniques are applied to uncertain nonlinear systems. The control objective is for the generalized coordinates of a system to track a desired trajectory while minimizing a cost functional. Depending on the problem, the cost may or may not be known a priori. For a direct optimal control problem the cost is determined in advance; while for an inverse optimal control problem, the cost functional is determined after the fact and is based on the value function.

The dissertation will address the following problems of interest: 1) RISE based optimal control of uncertain nonlinear systems; 2) RISE and NN based optimal control of uncertain nonlinear systems; 3) Adaptive inverse optimal control of uncertain nonlinear systems; and 4) Adaptive inverse optimal control of uncertain nonlinear systems using output feedback. The control development in the dissertation is proven by using nonlinear Lyapunov based methods and is demonstrated by Matlab simulation and/or experimental results.

1) *RISE based optimal control of uncertain nonlinear systems.*

Previous results rely on feedback linearization or NNs to cancel out nonlinearities or to identify them. Feedback linearization results are inherently not robust to plant uncertainty, and NNs result in an UUB stability result. Motivated by the desire to determine if it was possible to develop a controller which improved upon the UUB result previously found in literature, the controller developed in Chapter 2 incorporates optimal control elements with an implicit learning feedback control strategy developed in (35), that was later coined the Robust Integral of the Sign of the Error (RISE) method in (13; 14). The RISE method is used to identify the system and reject disturbances, while achieving asymptotic tracking and the convergence of a control term to the optimal controller. Inspired by the previous work in (6–12; 36; 37), a system in which all terms are

assumed known (temporarily) is feedback linearized and a control law is developed based on the HJB optimization method for a given quadratic performance index. Under the assumption that parametric uncertainty and unknown bounded disturbances are present in the dynamics, the control law is modified to contain the RISE feedback which is used to identify the uncertainty. Specifically, a Lyapunov stability analysis is included to show that the RISE feedback term asymptotically identifies the unknown dynamics (yielding semi-global asymptotic tracking) provided upper bounds on the disturbances are known and the control gains are selected appropriately. As in previous literature the control law converges to the optimal law, however because this result is asymptotic rather than UUB the control law converges exactly to the optimal law. Simulation as well as experimental results are provided to illustrate the developed controller.

2) *RISE and NN based optimal control of uncertain nonlinear systems.*

Motivated by the desire to improve the previous result, the amalgam of the robust RISE feedback method with NN methods to yield a direct optimal controller is investigated. The utility of combining these feedforward and feedback methods are twofold. Previous efforts in (13) indicate that modifying the RISE feedback with a feedforward term can reduce the control effort and improve the transient and steady state response of the RISE controller. Hence, the combined results should converge to the optimal controller faster. Moreover, combining NN feedforward controllers with RISE feedback yields asymptotic results (38). Hence, the efforts here provide a modification to the results in (7–12) that allows for asymptotic stability and convergence to the optimal controller rather than to approximate the optimal controller. Simulation and experimental results illustrate the performance of the controller.

3) *Adaptive inverse optimal control of uncertain nonlinear systems*

The result in Chapter 3 focuses on applying adaptive inverse optimal control techniques to uncertain nonlinear systems. Previous inverse optimal controllers are developed for classes of systems where the dynamics can be expressed in a specific form

to facilitate the development of a control Lyapunov function. Specifically, previous IOCs focus on the class problems modeled as

$$\dot{x} = f(x) + F(x)\theta + g(x)u, \tag{1–1}$$

for some state $x(t) \in \mathbb{R}^n$, where $f(x) \in \mathbb{R}^n$ is a smooth vector valued function, $F(x) \in \mathbb{R}^{n\times p}$, $g(x) \in \mathbb{R}^{n\times m}$ are smooth matrix valued functions, $\theta \in \mathbb{R}^p$ is a vector of unknown constants, and $u(t) \in \mathbb{R}^m$ is the control. In general, the input gain matrix $g(x)$ must be known. Systems with a constant inertia matrix, such as the applications in (25) and (26), can easily be transformed into Equation 1–1, unlike systems with an uncertain state-dependent inertia matrix or uncertainty in the input matrix. In order to determine if an IOC could be developed for a more practical engineering system (39), an adaptive IOC is developed in Chapter 3 based on the theoretical foundation presented in (22; 25; 40). The developed controller minimizes a meaningful performance index as the generalized coordinates of a nonlinear Euler-Lagrange system globally asymptotically track a desired time-varying trajectory despite LP uncertainty in the dynamics. The considered class of systems does not adhere to the model given in Equation 1–1. The unique ability to consider the IOC problem for uncertain Euler-Lagrange dynamics is due to a novel optimization analysis. A meaningful cost function (i.e., a positive function of the states and control input) is developed and an analysis is provided to prove the cost is minimized without having to prove the Lyapunov function is a CLF. To develop the optimal controller for the uncertain system, the open loop error system is segregated to include two adaptive terms. One adaptive term is based on the tracking error which contributes to the cost function, and the other adaptive term does not explicitly depend on the tracking error (and therefore does not explicitly contribute to the cost function). A Lyapunov analysis is provided to examine the stability of the developed controller and to determine a respective meaningful cost functional. Simulation as well as experimental results are provided to illustrate the developed controller.

4) *Adaptive inverse optimal control of uncertain nonlinear systems using output feedback*

Output feedback based controllers are more desirable than full-state feedback controllers, because the necessary sensors for full-state feedback may not always be available, and using numerical differentiation to obtain velocities can be problematic if position measurements are noisy. The controller in Chapter 4 is based on the desire to develop an adaptive controller for an uncertain Euler-Lagrange system that could minimize a meaningful cost, while the generalized coordinates of the system track a desired time-varying trajectory without using velocity measurements. Using the error system developed in (31–34) an adaptive IOC is developed that contains a DCAL based feedforward term and a feedback term that is shown to be implementable without velocity measurements. A Lyapunov analysis is provided to determine a meaningful cost functional and to prove the stability of the developed controller. Experimental results are included to illustrate the performance of the controller.

1.3 Contributions

The main contribution in this dissertation is the development of new optimal control techniques for uncertain nonlinear systems. Specifically, direct and adaptive inverse optimal control techniques are applied to an uncertain nonlinear system to develop continuous controllers that tracks a desired trajectory while minimizing a meaningful cost. In the process of achieving the main contribution, the following contributions were made:

1. For the first time ever, a direct optimal controller is developed that yields asymptotic tracking and convergence to an optimal controller.

2. Results exist in literature that use a NN with direct optimal control methods that result in UUB stability. The contribution in Chapter 2 is to illustrate how the previous methods could be augmented with RISE feedback to obtain asymptotic tracking.

3. An adaptive IOC is developed for a nonlinear Euler-Lagrange system. The use of an Euler-Lagrange system is motivated by the fact that the dynamics model a large class of contemporary engineering problems (39). The controller achieves asymptotic

tracking while minimizes a meaningful cost. The design is unique in that the model does not conform to the standard model used in literature.

4. An adaptive IOC is designed for a nonlinear Euler-Lagrange system that only requires position measurements. The controller achieves asymptotic tracking and minimizes a meaningful cost, while using a model that does not conform to the standard model used in literature. The controller consists of a DCAL feedforward term and a feedback term that can be implemented without velocity measurements.

CHAPTER 2
OPTIMAL CONTROL OF UNCERTAIN NONLINEAR SYSTEMS USING A NEURAL NETWORK AND RISE FEEDBACK

The development in this chapter is motivated by the desire to use optimal control techniques for uncertain nonlinear systems. Inspired by the previous work in (6–12; 36; 37), a system in which all terms are assumed known (temporarily) is feedback linearized and a control law is developed based on the HJB optimization method for a given quadratic performance index. The control law is then augmented to contain the RISE feedback term which is used to identify the parametric uncertainty and the unknown bounded disturbances that are present in the dynamics. The RISE feedback term is then shown, through a Lyapunov stability analysis, to asymptotically identify the unknown dynamics (yielding semi-global asymptotic tracking) provided upper bounds on the disturbances are known and the control gains are selected appropriately. Due to the fact that this result is asymptotic the control law converges to the optimal control law, rather than the UUB results in literature which only approximate the optimal control law.

The remainder of this chapter is organized as follows. In Section 2.1, the model is given along with several of its properties. In Section 2.2, the control objective is stated and an error system is formulated. In Section 2.3, an optimal controller is developed for a feedback linearized system. In Section 2.4, the RISE feedback term is developed. In Section 2.5, the stability of the controller is proven. In Section 2.6, the motivation behind including a NN is discussed. In Section 2.7, the properties of NN's are presented. In Section 2.8, the stability of the controller is proven. In Section 2.9, simulation and experimental results are presented.

2.1 Dynamic Model and Properties

The class of nonlinear dynamic systems considered in this chapter is assumed to be modeled by the following Euler-Lagrange (39) formulation:

$$M(q)\ddot{q} + V_m(q,\dot{q})\dot{q} + G(q) + F\left(\dot{q}\right) + \tau_d\left(t\right) = u(t). \tag{2–1}$$

In Equation 2–1, $M(q) \in \mathbb{R}^{n \times n}$ denotes the inertia matrix, $V_m(q, \dot{q}) \in \mathbb{R}^{n \times n}$ denotes the centripetal-Coriolis matrix, $G(q) \in \mathbb{R}^n$ denotes the gravity vector, $F(\dot{q}) \in \mathbb{R}^n$ denotes friction, $\tau_d(t) \in \mathbb{R}^n$ denotes a general nonlinear disturbance (e.g., unmodeled effects), $u(t) \in \mathbb{R}^n$ represents the input control vector, and $q(t)$, $\dot{q}(t)$, $\ddot{q}(t) \in \mathbb{R}^n$ denote the position, velocity, and acceleration vectors, respectively. The subsequent development is based on the assumption that $q(t)$ and $\dot{q}(t)$ are measurable and that $M(q)$, $V_m(q, \dot{q})$, $G(q)$, $F(\dot{q})$ and $\tau_d(t)$ are unknown. Moreover, the following properties will be exploited in the subsequent development.

Property 2.1 The Euler-Lagrange dynamics in Equation 2–1 along with the subsequent error system development is based on the assumption that the generalized coordinates, $q(t)$, are only defined for translations and rotations about a single axis.

Property 2.2: The inertia matrix $M(q)$ is symmetric, positive definite, and satisfies the following inequality $\forall \xi(t) \in \mathbb{R}^n$:

$$m_1 \|\xi\|^2 \leq \xi^T M(q) \xi \leq \bar{m}(q) \|\xi\|^2, \tag{2–2}$$

where $m_1 \in \mathbb{R}$ is a known positive constant, $\bar{m}(q) \in \mathbb{R}$ is a known positive function, and $\|\cdot\|$ denotes the standard Euclidean norm.

Property 2.3: The following skew-symmetric relationship is satisfied:

$$\xi^T \left(\dot{M}(q) - 2V_m(q, \dot{q}) \right) \xi = 0 \qquad \forall \xi \in \mathbb{R}^n. \tag{2–3}$$

Property 2.4: If $q(t)$, $\dot{q}(t) \in \mathcal{L}_\infty$, then $V_m(q, \dot{q})$, $F(\dot{q})$ and $G(q)$ are bounded. Moreover, if $q(t)$, $\dot{q}(t) \in \mathcal{L}_\infty$, then the first and second partial derivatives of the elements of $M(q)$, $V_m(q, \dot{q})$, $G(q)$ with respect to $q(t)$ exist and are bounded, and the first and second partial derivatives of the elements of $V_m(q, \dot{q})$, $F(\dot{q})$ with respect to $\dot{q}(t)$ exist and are bounded.

Property 2.5: The desired trajectory is assumed to be designed such that $q_d(t)$, $\dot{q}_d(t)$, $\ddot{q}_d(t)$, $\dddot{q}_d(t)$, $\ddddot{q}_d(t) \in \mathbb{R}^n$ exist, and are bounded.

Property 2.6: The nonlinear disturbance term and its first two time derivatives (i.e., $\tau_d(t)$, $\dot{\tau}_d(t)$, $\ddot{\tau}_d(t)$) are bounded by known constants.

2.2 Control Objective

The control objective is to ensure that the generalized coordinates of a system track a desired time-varying trajectory, denoted by $q_d(t) \in \mathbb{R}^n$, despite uncertainties in the dynamic model, while minimizing a given performance index. To quantify the tracking objective, a position tracking error, denoted by $e_1(t) \in \mathbb{R}^n$, is defined as

$$e_1 \triangleq q_d - q. \tag{2–4}$$

To facilitate the subsequent analysis, filtered tracking errors, denoted by $e_2(t)$, $r(t) \in \mathbb{R}^n$, are also defined as

$$e_2 \triangleq \dot{e}_1 + \alpha_1 e_1 \tag{2–5}$$

$$r \triangleq \dot{e}_2 + \alpha_2 e_2, \tag{2–6}$$

where $\alpha_1 \in \mathbb{R}^{n \times n}$, denotes a subsequently defined positive definite, constant, gain matrix, and $\alpha_2 \in \mathbb{R}$ is a positive constant. The filtered tracking error $r(t)$ is not measurable since the expression in Equation 2–6 depends on $\ddot{q}(t)$.

2.3 Optimal Control Design

In this section, a state-space model is developed based on the tracking errors in Equation 2–4 and Equation 2–5. Based on this model, a controller is developed that minimizes a quadratic performance index under the (temporary) assumption that the dynamics in Equation 2–1, including the additive disturbance, are known. The development in this section motivates the control design in Section 2.4, where a robust controller is developed to identify the unknown dynamics and additive disturbance.

To develop a state-space model for the tracking errors in Equation 2–4 and Equation 2–5, the time derivative of Equation 2–5 is premultiplied by the inertia matrix, and

substitutions are made from Equation 2–1 and Equation 2–4 to obtain

$$M\dot{e}_2 = -V_m e_2 - u + h + \tau_d, \tag{2–7}$$

where the nonlinear function $h\left(q,\dot{q},q_d,\dot{q}_d,\ddot{q}_d\right) \in \mathbb{R}^n$ is defined as

$$h \triangleq M\left(\ddot{q}_d + \alpha_1 \dot{e}_1\right) + V_m(\dot{q}_d + \alpha_1 e_1) + G + F. \tag{2–8}$$

Under the (temporary) assumption that the dynamics in Equation 2–1 are known, the control input can be designed as

$$u \triangleq h + \tau_d - u_o, \tag{2–9}$$

where $u_o\left(t\right) \in \mathbb{R}^n$ is an auxiliary control input that will be designed to minimize a subsequent performance index. By substituting Equation 2–9 into Equation 2–7 the closed-loop error system for $e_2(t)$ can be obtained as

$$M\dot{e}_2 = -V_m e_2 + u_o. \tag{2–10}$$

A state-space model for Equation 2–5 and Equation 2–10 can now be developed as

$$\dot{z} = A\left(q,\dot{q}\right) z + B\left(q\right) u_o, \tag{2–11}$$

where $A\left(q,\dot{q}\right) \in \mathbb{R}^{2n\times 2n}$, $B\left(q\right) \in \mathbb{R}^{2n\times n}$, and $z\left(t\right) \in \mathbb{R}^{2n}$ are defined as

$$A\left(q,\dot{q}\right) \triangleq \begin{bmatrix} -\alpha_1 & I_{n\times n} \\ 0_{n\times n} & -M^{-1}V_m \end{bmatrix},$$
$$B\left(q\right) \triangleq \begin{bmatrix} 0_{n\times n} & M^{-1} \end{bmatrix}^T,$$
$$z(t) \triangleq \begin{bmatrix} e_1^T & e_2^T \end{bmatrix}^T,$$

where $I_{n\times n}$ and $0_{n\times n}$ denote a $n \times n$ identity matrix and matrix of zeros, respectively. The quadratic performance index $J\left(u_o\right) \in \mathbb{R}$ to be minimized subject to the constraints in

Equation 2–11 is

$$J(u_o) \triangleq \int_0^\infty L(z, u_o) \quad dt = \int_0^\infty \left(\frac{1}{2} z^T Q z + \frac{1}{2} u_o^T R u_o \right) \quad dt, \tag{2–12}$$

where $L(z, u_o)$ is the Lagrangian. In Equation 2–12, $Q \in \mathbb{R}^{2n \times 2n}$ and $R \in \mathbb{R}^{n \times n}$ are positive definite symmetric matrices to weight the influence of the states and (partial) control effort, respectively. Furthermore, the matrix Q can be broken into blocks as follows:

$$Q = \begin{bmatrix} Q_{11} & Q_{12} \\ Q_{12}^T & Q_{22} \end{bmatrix}.$$

As stated in (7; 8), the fact that the performance index is only penalized for the auxiliary control $u_o(t)$ is practical since the gravity, Coriolis, and friction compensation terms in Equation 2–8 can not be modified by the optimal design phase.

To facilitate the subsequent development, let $P(q) \in \mathbb{R}^{2n \times 2n}$ be defined as

$$P(q) = \begin{bmatrix} K & 0_{n \times n} \\ 0_{n \times n} & M \end{bmatrix}, \tag{2–13}$$

where $K \in \mathbb{R}^{n \times n}$ denotes a gain matrix. If α_1, R, and K, introduced in Equation 2–5, Equation 2–12, and Equation 2–13, satisfy the following algebraic relationships

$$K = K^T = -\frac{1}{2} \left(Q_{12} + Q_{12}^T \right) > 0 \tag{2–14}$$

$$Q_{11} = \alpha_1^T K + K \alpha_1, \tag{2–15}$$

$$R^{-1} = Q_{22}, \tag{2–16}$$

where $Q_{ij} \in \mathbb{R}^{n \times n}$ denotes a block of Q, then $P(q)$ satisfies the Riccati differential equation[1] , and the value function $V(z,t) \in \mathbb{R}$

$$V = \frac{1}{2} z^T P z \tag{2–17}$$

satisfies the HJB equation. It can then be concluded that the optimal control $u_o(t)$ that minimizes Equation 2–12 subject to Equation 2–11 is[2]

$$u_o(t) = -R^{-1} B^T \left(\frac{\partial V(z,t)}{\partial z} \right)^T = -R^{-1} e_2. \tag{2–18}$$

2.4 RISE Feedback Control Development

In general, the bounded disturbance $\tau_d(t)$ and the nonlinear dynamics given in Equation 2–8 are unknown, so the controller given in Equation 2–9 can not be implemented. However, if the control input contains some method to identify and cancel these effects, then $z(t)$ will converge to the state space model in Equation 2–11 so that $u_o(t)$ minimizes the respective performance index. As stated in the introduction, several results have explored this strategy using function approximation methods such as neural networks, where the tracking control errors converge to a neighborhood near the state space model yielding a type of approximate optimal controller. In this section, a control input is developed that exploits RISE feedback to identify the nonlinear effects and bounded disturbances to enable $z(t)$ to asymptotically converge to the state space model.

To develop the control input, the error system in Equation 2–6 is premultiplied by $M(q)$ and the expressions in Equation 2–1, Equation 2–4, and Equation 2–5 are utilized to obtain

$$Mr = -V_m e_2 + h + \tau_d + \alpha_2 M e_2 - u. \tag{2–19}$$

[1] See Appendix A for details on these relationships and the Riccati differential equation

[2] See Appendix B for proof of optimality

Based on the open-loop error system in Equation 2–19, the control input is composed of the optimal control developed in Equation 2–18, plus a subsequently designed auxiliary control term $\mu(t) \in \mathbb{R}^n$ as

$$u = \mu - u_o. \tag{2–20}$$

The closed-loop tracking error system can be developed by substituting Equation 2–20 into Equation 2–19 as

$$Mr = -V_m e_2 + h + \tau_d + \alpha_2 M e_2 + u_o - \mu. \tag{2–21}$$

To facilitate the subsequent stability analysis the auxiliary function $f_d\left(q_d, \dot{q}_d, \ddot{q}_d\right) \in \mathbb{R}^n$, which is defined as

$$f_d \triangleq M(q_d)\ddot{q}_d + V_m(q_d, \dot{q}_d)\dot{q}_d + G(q_d) + F\left(\dot{q}_d\right), \tag{2–22}$$

is added and subtracted to Equation 2–21 to yield

$$Mr = -V_m e_2 + \bar{h} + f_d + \tau_d + u_o - \mu + \alpha_2 M e_2, \tag{2–23}$$

where $\bar{h}\left(q,\dot{q},q_d,\dot{q}_d,\ddot{q}_d\right) \in \mathbb{R}^n$ is defined as

$$\bar{h} \triangleq h - f_d. \tag{2–24}$$

The time derivative of Equation 2–23 can be written as

$$M\dot{r} = -\frac{1}{2}\dot{M}r + \tilde{N} + N_D - e_2 - R^{-1}r - \dot{\mu} \tag{2–25}$$

after strategically grouping specific terms. In Equation 2–25, the unmeasurable auxiliary terms $\tilde{N}(e_1, e_2, r, t)$, $N_D\left(t\right) \in \mathbb{R}^n$ are defined as

$$\tilde{N} \triangleq -\dot{V}_m e_2 - V_m \dot{e}_2 - \frac{1}{2}\dot{M}r + \dot{\bar{h}} + \alpha_2 \dot{M} e_2 + \alpha_2 M \dot{e}_2 + e_2 + \alpha_2 R^{-1} e_2$$

$$N_D \triangleq \dot{f}_d + \dot{\tau}_d.$$

Motivation for grouping terms into $\tilde{N}(e_1, e_2, r, t)$ and $N_D(t)$ comes from the subsequent stability analysis and the fact that the Mean Value Theorem, Property 2.4, Property 2.5, and Property 2.6 can be used to upper bound the auxiliary terms as[3]

$$\left\| \tilde{N}(t) \right\| \leq \rho(\|y\|) \|y\|, \tag{2–26}$$

$$\|N_D\| \leq \zeta_1, \qquad \left\| \dot{N}_D \right\| \leq \zeta_2, \tag{2–27}$$

where $y(t) \in \mathbb{R}^{3n}$ is defined as

$$y(t) \triangleq [e_1^T \quad e_2^T \quad r^T]^T, \tag{2–28}$$

the bounding function $\rho(\|y\|) \in \mathbb{R}$ is a positive globally invertible nondecreasing function, and $\zeta_i \in \mathbb{R}$ $(i = 1, 2)$ denote known positive constants. Based on Equation 2–25, the control term $\mu(t)$ is designed based on the RISE framework (see (13; 35; 41)) as

$$\mu(t) \triangleq (k_s + 1)e_2(t) - (k_s + 1)e_2(0) + \int_0^t [(k_s + 1)\alpha_2 e_2(\sigma) + \beta_1 sgn(e_2(\sigma))]d\sigma \tag{2–29}$$

where k_s, $\beta_1 \in \mathbb{R}$ are positive constant control gains. The closed loop error systems for $r(t)$ can now be obtained by substituting the time derivative of Equation 2–29 into Equation 2–25 as

$$M\dot{r} = -\frac{1}{2}\dot{M}r + \tilde{N} + N_D - e_2 - R^{-1}r - (k_s + 1)r - \beta_1 sgn(e_2). \tag{2–30}$$

2.5 Stability Analysis

The stability of the RISE and optimal controller given in Equation 2–20 can be examined through the following theorem.

Theorem 2.1: The controller given in Equation 2–20 ensures that all system signals are bounded under closed-loop operation, and the tracking errors are regulated in the sense that

$$\|e_1(t)\|, \|e_2(t)\|, \|r(t)\| \to 0 \qquad as \qquad t \to \infty. \tag{2–31}$$

[3] See Appendix C for details on this inequality

The boundedness of the closed loop signals and the result in Equation 2–31 can be obtained provided the control gain k_s introduced in Equation 2–29 is selected sufficiently large (see the subsequent stability analysis), and α_1, α_2 are selected according to the sufficient conditions

$$\lambda_{\min}(\alpha_1) > \frac{1}{2} \qquad \alpha_2 > 1, \tag{2–32}$$

where $\lambda_{\min}(\alpha_1)$ is the minimum eigenvalue of α_1, and β_1 is selected according to the following sufficient condition:

$$\beta_1 > \zeta_1 + \frac{1}{\alpha_2}\zeta_2, \tag{2–33}$$

where β_1 was introduced in Equation 2–29. Furthermore, $u(t)$ converges to an optimal controller that minimizes Equation 2–12 subject to Equation 2–11 provided the gain conditions given in Equation 2–14-Equation 2–16 are satisfied.

Remark: The control gain α_1 can not be arbitrarily selected, rather it is calculated using a Lyapunov equation solver. Its value is determined based on the value of Q and R. Therefore Q and R must be chosen such that Equation 2–32 is satisfied.

Proof: Let $\mathcal{D} \subset \mathbb{R}^{3n+1}$ be a domain containing $\Phi(t) = 0$, where $\Phi(t) \in \mathbb{R}^{3n+1}$ is defined as

$$\Phi(t) \triangleq [y^T(t) \quad \sqrt{O(t)}]^T. \tag{2–34}$$

In Equation 2–34, the auxiliary function $O(t) \in \mathbb{R}$ is defined as

$$O(t) \triangleq \beta \|e_2(0)\| - e_2(0)^T N_D(0) - \int_0^t L(\tau)d\tau, \tag{2–35}$$

where the auxiliary function $L(t) \in \mathbb{R}$ is defined as

$$L(t) \triangleq r^T(N_D(t) - \beta_1 sgn(e_2)), \tag{2–36}$$

where $\beta_1 \in \mathbb{R}$ is a positive constant chosen according to the sufficient conditions in Equation 2–33. As illustrated in Appendix D, provided the sufficient conditions introduced

in Equation 2–33 are satisfied, the following inequality can be obtained:

$$\int_0^t L(\tau)d\tau \leq \beta_1 \|e_2(0)\| - e_2(0)^T N_D(0). \tag{2–37}$$

Hence, Equation 2–37 can be used to conclude that $O(t) \geq 0$.

Let $V_L(\Phi, t) : \mathcal{D} \times [0, \infty) \rightarrow \mathbb{R}$ be a continuously differentiable positive definite function defined as

$$V_L(\Phi, t) \triangleq e_1^T e_1 + \frac{1}{2} e_2^T e_2 + \frac{1}{2} r^T M(q) r + O, \tag{2–38}$$

which satisfies the following inequalities:

$$U_1(\Phi) \leq V_L(\Phi, t) \leq U_2(\Phi), \tag{2–39}$$

provided the sufficient conditions introduced in Equation 2–33 are satisfied. In Equation 2–39, the continuous positive definite functions $U_1(\Phi)$, and $U_2(\Phi) \in \mathbb{R}$ are defined as $U_1(\Phi) \triangleq \lambda_1 \|\Phi\|^2$, and $U_2(\Phi) \triangleq \lambda_2(q) \|\Phi\|^2$, where λ_1, $\lambda_2(q) \in \mathbb{R}$ are defined as

$$\lambda_1 \triangleq \frac{1}{2} \min\{1, m_1\} \qquad \lambda_2(q) \triangleq \max\left\{\frac{1}{2}\bar{m}(q), 1\right\},$$

where m_1, $\bar{m}(q)$ are introduced in Equation 2–2. After taking the time derivative of Equation 2–38, $\dot{V}_L(\Phi, t)$ can be expressed as

$$\dot{V}_L(\Phi, t) = 2e_1^T \dot{e}_1 + e_2^T \dot{e}_2 + \frac{1}{2} r^T \dot{M}(q) r + r^T M(q) \dot{r} + \dot{O}.$$

After utilizing Equation 2–5, Equation 2–6, Equation 2–30, and substituting in for the time derivative of $O(t)$, $\dot{V}(\Phi, t)$ can be simplified as follows:

$$\begin{aligned} \dot{V}_L(\Phi, t) \leq & -2e_1^T \alpha_1 e_1 + 2e_2^T e_1 + r^T \tilde{N}(t) \\ & - \left(k_s + 1 + \lambda_{\min}\left(R^{-1}\right)\right) \|r\|^2 - \alpha_2 \|e_2\|^2. \end{aligned} \tag{2–40}$$

Based on the fact that

$$e_2^T e_1 \leq \frac{1}{2} \|e_1\|^2 + \frac{1}{2} \|e_2\|^2,$$

the expression in Equation 2–40 can be simplified as

$$\dot{V}_L(\Phi,t) \leq r^T \tilde{N}(t) - \left(k_s + 1 + \lambda_{\min}\left(R^{-1}\right)\right)\|r\|^2 \\ - \left(2\lambda_{\min}(\alpha_1) - 1\right)\|e_1\|^2 - (\alpha_2 - 1)\|e_2\|^2. \tag{2–41}$$

By using Equation 2–26, the expression in Equation 2–41 can be rewritten as

$$\dot{V}_L(\Phi,t) \leq -\lambda_3\|y\|^2 - \left[k_s\|r\|^2 - \rho(\|y\|)\|r\|\|y\|\right], \tag{2–42}$$

where $\lambda_3 \triangleq \min\{2\lambda_{\min}(\alpha_1) - 1, \alpha_2 - 1, 1 + \lambda_{\min}(R^{-1})\}$ and α_1 and α_2 are chosen according to the sufficient condition in Equation 2–32. After completing the squares for the terms inside the brackets in Equation 2–42, the following expression can be obtained

$$\dot{V}_L(\Phi,t) \leq -\lambda_3\|y\|^2 + \frac{\rho^2(\|y\|)\|y\|^2}{4k_s} \leq -U(\Phi), \tag{2–43}$$

where $U(\Phi) = c\|y\|^2$, for some positive constant c, is a continuous, positive semi-definite function that is defined on the following domain:

$$\mathcal{D} \triangleq \left\{\Phi \in \mathbb{R}^{3n+1} \mid \|\Phi\| \leq \rho^{-1}\left(2\sqrt{\lambda_3 k_s}\right)\right\}.$$

The inequalities in Equation 2–39 and Equation 2–43 can be used to show that $V_L(\Phi,t) \in \mathcal{L}_\infty$ in $\mathcal{D}$; hence, $e_1(t)$, $e_2(t)$, and $r(t) \in \mathcal{L}_\infty$ in $\mathcal{D}$. Given that $e_1(t)$, $e_2(t)$, and $r(t) \in \mathcal{L}_\infty$ in $\mathcal{D}$, standard linear analysis methods can be used to prove that $\dot{e}_1(t)$, $\dot{e}_2(t) \in \mathcal{L}_\infty$ in $\mathcal{D}$ from Equation 2–5 and Equation 2–6. Since $e_1(t)$, $e_2(t)$, $r(t) \in \mathcal{L}_\infty$ in $\mathcal{D}$, the property that $q_d(t)$, $\dot{q}_d(t)$, $\ddot{q}_d(t)$ exist and are bounded can be used along with Equation 2–4 - Equation 2–6 to conclude that $q(t)$, $\dot{q}(t)$, $\ddot{q}(t) \in \mathcal{L}_\infty$ in $\mathcal{D}$. Since $q(t)$, $\dot{q}(t) \in \mathcal{L}_\infty$ in $\mathcal{D}$, Property 2.4 can be used to conclude that $M(q)$, $V_m(q,\dot{q})$, $G(q)$, and $F(\dot{q}) \in \mathcal{L}_\infty$ in $\mathcal{D}$. Thus from Equation 2–1 and Property 2.5, we can show that $u(t) \in \mathcal{L}_\infty$ in $\mathcal{D}$. Given that $r(t) \in \mathcal{L}_\infty$ in $\mathcal{D}$, it can be shown that $\dot{\mu}(t) \in \mathcal{L}_\infty$ in $\mathcal{D}$. Since $\dot{q}(t)$, $\ddot{q}(t) \in \mathcal{L}_\infty$ in $\mathcal{D}$, Property 2.4 can be used to show that $\dot{V}_m(q,\dot{q})$, $\dot{G}(q)$, $\dot{F}(q)$ and $\dot{M}(q) \in \mathcal{L}_\infty$ in $\mathcal{D}$; hence, Equation 2–30 can

be used to show that $\dot{r}(t) \in \mathcal{L}_\infty$ in $\mathcal{D}$. Since $\dot{e}_1(t)$, $\dot{e}_2(t)$, $\dot{r}(t) \in \mathcal{L}_\infty$ in $\mathcal{D}$, the definitions for $U(y)$ and $z(t)$ can be used to prove that $U(y)$ is uniformly continuous in $\mathcal{D}$.

Let $\mathcal{S} \subset \mathcal{D}$ denote a set defined as follows:

$$\mathcal{S} \triangleq \left\{ \Phi(t) \subset \mathcal{D} \mid U_2(\Phi(t)) < \lambda_1 \left(\rho^{-1} \left(2\sqrt{\lambda_3 k_s} \right) \right)^2 \right\}. \tag{2–44}$$

The region of attraction in Equation 2–44 can be made arbitrarily large to include any initial conditions by increasing the control gain k_s (i.e., a semi-global type of stability result) (41). Theorem 8.4 of (42) can now be invoked to state that

$$c \left\| y(t) \right\|^2 \to 0 \qquad as \qquad t \to \infty \qquad \forall y(0) \in \mathcal{S}. \tag{2–45}$$

Based on the definition of $y(t)$, Equation 2–45 can be used to conclude the results in Equation 2–31 $\forall y(0) \in \mathcal{S}$.

Since $u\left(t\right) \to 0$ as $e_2\left(t\right) \to 0$ (see Equation 2–18), then Equation 2–23 can be used to conclude that

$$\mu \to \bar{h} + f_d + \tau_d \qquad \text{as } r\left(t\right), e_2(t) \to 0. \tag{2–46}$$

The result in Equation 2–46 indicates that the dynamics in Equation 2–1 converge to the state-space system in Equation 2–11. Hence, $u\left(t\right)$ converges to an optimal controller that minimizes Equation 2–12 subject to Equation 2–11 provided the gain conditions given in Equation 2–14 - Equation 2–16 are satisfied.

2.6 Neural Network Extension

The efforts in this section investigate the amalgam of the robust RISE feedback method with NN methods to yield a direct optimal controller. The utility of combining these feedforward and feedback methods are twofold. Previous efforts in (13) indicate that modifying the RISE feedback with a feedforward term can reduce the control effort and improve the transient and steady state response of the RISE controller. Hence, the combined results should converge to the optimal controller faster. Moreover, combining NN feedforward controllers with RISE feedback yields asymptotic results (38). Hence, the

efforts in this dissertation provide a modification to the results in (7–12) that allows for asymptotic stability and convergence to the optimal controller rather than to approximate the optimal controller.

Based on the previous work done in the chapter the unknown LP and non-LP dynamics are temporarily assumed to be known so that a controller can be developed for a residual system based on the HJB optimization method for a given quadratic performance index. The original uncertain nonlinear system is then examined, where the optimal controller is augmented to include the RISE feedback and NN feedforward terms to asymptotically cancel the uncertainties. A Lyapunov-based stability analysis is included to show that the RISE and NN components asymptotically identify the unknown dynamics (yielding semi-global asymptotic tracking) provided upper bounds on the disturbances are known and the control gains are selected appropriately. Moreover, the controller converges to the optimal controller for the a priori given quadratic performance index.

2.7 Neural Networks

The universal approximation property indicates that weights and thresholds exist such that some continuous function $f(x) \in \mathbb{R}^{N_1+1}$ can be represented by a three-layer NN as (43), (44)

$$f(x) = W^T \sigma\left(V^T x\right) + \varepsilon(x). \tag{2–47}$$

In Equation 2–47, $V \in \mathbb{R}^{(N_1+1)\times N_2}$ and $W \in \mathbb{R}^{(N_2+1)\times n}$ are bounded constant ideal weight matrices for the first-to-second and second-to-third layers respectively, where N_1 is the number of neurons in the input layer, N_2 is the number of neurons in the hidden layer, and n is the number of neurons in the third layer. The activation function[4] in Equation 2–47 is denoted by $\sigma(\cdot) : \mathbb{R}^{N_1+1} \to \mathbb{R}^{N_2+1}$, and $\varepsilon(x) : \mathbb{R}^{N_1+1} \to \mathbb{R}^n$ is the functional reconstruction error. Based on Equation 2–47, the typical three-layer NN approximation

[4] A variety of activation functions (e.g., sigmoid, hyperbolic tangent or radial basis) could be used for the control development.

for $f(x)$ is given as (43), (44)

$$\hat{f}(x) \triangleq \hat{W}^T \sigma\left(\hat{V}^T x\right), \tag{2–48}$$

where $\hat{V}(t) \in \mathbb{R}^{(N_1+1)\times N_2}$ and $\hat{W}(t) \in \mathbb{R}^{(N_2+1)\times n}$ are subsequently designed estimates of the ideal weight matrices. The estimate mismatches for the ideal weight matrices, denoted by $\tilde{V}(t) \in \mathbb{R}^{(N_1+1)\times N_2}$ and $\tilde{W}(t) \in \mathbb{R}^{(N_2+1)\times n}$, are defined as

$$\tilde{V} \triangleq V - \hat{V}, \quad \tilde{W} \triangleq W - \hat{W},$$

and the mismatch for the hidden-layer output error for a given $x(t)$, denoted by $\tilde{\sigma}(x) \in \mathbb{R}^{N_2+1}$, is defined as

$$\tilde{\sigma} \triangleq \sigma - \hat{\sigma} = \sigma\left(V^T x\right) - \sigma\left(\hat{V}^T x\right). \tag{2–49}$$

One of the NN estimate properties that facilitate the subsequent development is described as follows.

Property 2.7: (*Boundedness of the Ideal Weights*) The ideal weights are assumed to exist and be bounded by known positive values so that

$$\|V\|_F^2 = tr(V^T V) \leq \bar{V}_B \tag{2–50}$$

$$\|W\|_F^2 = tr(W^T W) \leq \bar{W}_B \tag{2–51}$$

where $\|\cdot\|_F$ is the Frobenius norm of a matrix, $tr(\cdot)$ is the trace of a matrix.

To develop the control input, the error system in Equation 2–6 is premultiplied by $M(q)$ and the expressions in Equation 2–1, Equation 2–4, and Equation 2–5 are utilized to obtain

$$Mr = -V_m e_2 + h + \tau_d + \alpha_2 M e_2 - u. \tag{2–52}$$

To facilitate the subsequent stability analysis the auxiliary function $f_d(q_d, \dot{q}_d, \ddot{q}_d) \in \mathbb{R}^n$, which is defined as

$$f_d \triangleq M(q_d)\ddot{q}_d + V_m(q_d, \dot{q}_d)\dot{q}_d + G(q_d) + F(\dot{q}_d), \tag{2–53}$$

is added and subtracted to Equation 2–52 to yield

$$Mr = -V_m e_2 + \bar{h} + f_d + \tau_d + \alpha_2 M e_2 - u, \tag{2–54}$$

where $\bar{h}\left(q,\dot{q},q_d,\dot{q}_d,\ddot{q}_d\right) \in \mathbb{R}^n$ is defined as

$$\bar{h} \triangleq h - f_d. \tag{2–55}$$

The expression in Equation 2–53 can be represented by a three-layer NN as

$$f_d = W^T \sigma\left(V^T x_d\right) + \varepsilon\left(x_d\right). \tag{2–56}$$

In Equation 2–56, the input $x_d(t) \in \mathbb{R}^{3n+1}$ is defined as $x_d(t) \triangleq [1 \;\; q_d^T(t) \;\; \dot{q}_d^T(t) \;\; \ddot{q}_d^T(t)]^T$ so that $N_1 = 3n$ where N_1 was introduced in Equation 2–47. Based on the Property 2.5 that the desired trajectory is bounded, the following inequalities hold

$$\left\|\varepsilon\left(x_d\right)\right\| \leq \varepsilon_{b_1} \qquad \left\|\dot{\varepsilon}\left(x_d, \dot{x}_d\right)\right\| \leq \varepsilon_{b_2} \tag{2–57}$$
$$\left\|\ddot{\varepsilon}\left(x_d, \dot{x}_d, \ddot{x}_d\right)\right\| \leq \varepsilon_{b_3},$$

where ε_{b_1}, ε_{b_2}, $\varepsilon_{b_3} \in \mathbb{R}$ are known positive constants.

Based on the open-loop error system in Equation 2–52, the control input is composed of the optimal control developed in Equation 2–18, a three-layer NN feedforward term, plus the RISE feedback term as

$$u = \hat{f}_d + \mu - u_o. \tag{2–58}$$

Specifically, $\mu(t) \in \mathbb{R}^n$ denotes the RISE feedback control term defined in Equation 2–29. The feedforward NN component in Equation 2–58, denoted by $\hat{f}_d(t) \in \mathbb{R}^n$, is generated as

$$\hat{f}_d \triangleq \hat{W}^T \sigma\left(\hat{V}^T x_d\right). \tag{2–59}$$

The estimates for the NN weights in Equation 2–59 are generated on-line (there is no off-line learning phase) as

$$\dot{\hat{W}} = proj(\Gamma_1 \hat{\sigma}' \hat{V}^T \dot{x}_d e_2^T) \tag{2–60}$$
$$\dot{\hat{V}} = proj(\Gamma_2 \dot{x}_d (\hat{\sigma}'^T \hat{W} e_2)^T)$$

where $\sigma'(\hat{V}^T x) \equiv d\sigma\left(V^T x\right)/d\left(V^T x\right)|_{V^T x = \hat{V}^T x}$, and $\Gamma_1 \in \mathbb{R}^{(N_2+1)\times(N_2+1)}$, $\Gamma_2 \in \mathbb{R}^{(3n+1)\times(3n+1)}$ are constant, positive definite, symmetric matrices. In Equation 2–60, $proj(\cdot)$ denotes a smooth convex projection algorithm that ensures $\hat{W}(t)$ and $\hat{V}(t)$ remain bounded inside known bounded convex regions. See Section 4.3 in (45) for further details.

The closed-loop tracking error system is obtained by substituting Equation 2–58 into Equation 2–52 as

$$Mr = -V_m e_2 + \alpha_2 M e_2 + f_d - \hat{f}_d + \bar{h} + \tau_d + u_o - \mu. \tag{2–61}$$

To facilitate the subsequent stability analysis, the time derivative of Equation 2–61 is determined as

$$M\dot{r} = -\dot{M}r - \dot{V}_m e_2 - V_m \dot{e}_2 + \alpha_2 \dot{M} e_2 + \alpha_2 M \dot{e}_2 + \dot{f}_d - \dot{\hat{f}}_d + \dot{\bar{h}} + \dot{\tau}_d + \dot{u}_o - \dot{\mu}. \tag{2–62}$$

Using Equation 2–47 and Equation 2–59, the closed-loop error system in Equation 2–62 can be expressed as

$$M\dot{r} = -\dot{M}r - \dot{V}_m e_2 - V_m \dot{e}_2 + \alpha_2 \dot{M} e_2 + \alpha_2 M \dot{e}_2 + W^T \sigma' V^T \dot{x}_d - \dot{\hat{W}}^T \hat{\sigma} \tag{2–63}$$
$$- \hat{W}^T \hat{\sigma}' \dot{\hat{V}}^T x_d - \hat{W}^T \hat{\sigma}' \hat{V}^T \dot{x}_d + \dot{\varepsilon} + \dot{\bar{h}} + \dot{\tau}_d + \dot{u}_o - \dot{\mu},$$

where the notations $\hat{\sigma}$ and $\tilde{\sigma}$ are introduced in Equation 2–49. Adding and subtracting the terms $W^T\hat{\sigma}'\hat{V}^T\dot{x}_d + \hat{W}^T\hat{\sigma}'\tilde{V}^T\dot{x}_d$ to Equation 2–63, yields

$$\begin{aligned} M\dot{r} = &-\dot{M}r - \dot{V}_m e_2 - V_m\dot{e}_2 + \alpha_2\dot{M}e_2 + \alpha_2 M\dot{e}_2 + \hat{W}^T\hat{\sigma}'\tilde{V}^T\dot{x}_d \\ &+ \tilde{W}^T\hat{\sigma}'\hat{V}^T\dot{x}_d - \dot{\hat{W}}^T\hat{\sigma} - \hat{W}^T\hat{\sigma}'\dot{\hat{V}}^T x_d + W^T\sigma'V^T\dot{x}_d \\ &- W^T\hat{\sigma}'\hat{V}^T\dot{x}_d - \hat{W}^T\hat{\sigma}'\tilde{V}^T\dot{x}_d + \dot{\varepsilon} + \dot{\bar{h}} + \dot{\tau}_d + \dot{u}_o - \dot{\mu}. \end{aligned} \tag{2–64}$$

Using Equation 2–18 and the NN weight tuning laws in Equation 2–60, the expression in Equation 2–64 can be rewritten as

$$M\dot{r} = -\frac{1}{2}\dot{M}(q)r + \tilde{N} + N - e_2 - R^{-1}r - (k_s+1)r - \beta_1 sgn(e_2), \tag{2–65}$$

where the fact that the time derivative of Equation 2–29 is given as

$$\dot{\mu} = (k_s+1)r + \beta_1 sgn(e_2) \tag{2–66}$$

was utilized, and where the unmeasurable auxiliary terms $\tilde{N}(e_1, e_2, r, t)$, $N\left(\hat{W}, \hat{V}, x_d, t\right) \in \mathbb{R}^n$ are defined as

$$\begin{aligned} \tilde{N} \triangleq &-\frac{1}{2}\dot{M}r + \dot{\bar{h}} + e_2 + \alpha_2 R^{-1}e_2 - \dot{V}_m e_2 - V_m\dot{e}_2 + \alpha_2\dot{M}e_2 + \alpha_2 M\dot{e}_2 \\ &- proj(\Gamma_1\hat{\sigma}'\hat{V}^T\dot{x}_d e_2^T)^T\hat{\sigma} - \hat{W}^T\hat{\sigma}'proj(\Gamma_2\dot{x}_d(\hat{\sigma}'^T\hat{W}e_2)^T)^T x_d \end{aligned} \tag{2–67}$$

$$N \triangleq N_D + N_B. \tag{2–68}$$

In Equation 2–68, $N_D(t) \in \mathbb{R}^n$ is defined as

$$N_D = W^T\sigma'V^T\dot{x}_d + \dot{\varepsilon} + \dot{\tau}_d, \tag{2–69}$$

while $N_B\left(\hat{W}, \hat{V}, x_d\right) \in \mathbb{R}^n$ is further segregated as

$$N_B = N_{B_1} + N_{B_2}, \tag{2–70}$$

where $N_{B_1}\left(\hat{W}, \hat{V}, x_d\right) \in \mathbb{R}^n$ is defined as

$$N_{B_1} = -W^T \hat{\sigma}' \hat{V}^T \dot{x}_d - \hat{W}^T \hat{\sigma}' \tilde{V}^T \dot{x}_d, \tag{2–71}$$

and the term $N_{B_2}\left(\hat{W}, \hat{V}, x_d\right) \in \mathbb{R}^n$ is defined as

$$N_{B_2} = \hat{W}^T \hat{\sigma}' \tilde{V}^T \dot{x}_d + \tilde{W}^T \hat{\sigma}' \hat{V}^T \dot{x}_d. \tag{2–72}$$

Segregating the terms as in Equation 2–69 - Equation 2–72 facilitates the development of the NN weight update laws and the subsequent stability analysis. For example, the terms in Equation 2–69 are grouped together because the terms and their time derivatives can be upper bounded by a constant and rejected by the RISE feedback, whereas the terms grouped in Equation 2–70 can be upper bounded by a constant but their derivatives are state dependent. The terms in Equation 2–70 are further segregated because $N_{B_1}\left(\hat{W}, \hat{V}, x_d\right)$ will be rejected by the RISE feedback, whereas $N_{B_2}\left(\hat{W}, \hat{V}, x_d\right)$ will be partially rejected by the RISE feedback and partially canceled by the adaptive update law for the NN weight estimates.

In a similar manner as in (41), the Mean Value Theorem can be used to develop the following upper bound[5]

$$\left\| \tilde{N}(t) \right\| \leq \rho\left(\|y\|\right) \|y\|, \tag{2–73}$$

where $y(t) \in \mathbb{R}^{3n}$ is defined as

$$y(t) \triangleq [e_1^T \quad e_2^T \quad r^T]^T, \tag{2–74}$$

and the bounding function $\rho(\|y\|) \in \mathbb{R}$ is a positive globally invertible nondecreasing function. The following inequalities can be developed based on Property 2.6, Equation

[5] See Appendix C for details on this inequality

2–50, Equation 2–51, Equation 2–57, Equation 2–60 and Equation 2–70 - Equation 2–72:

$$\|N_D\| \leq \zeta_1 \qquad \|N_B\| \leq \zeta_2 \qquad \left\|\dot{N}_D\right\| \leq \zeta_3 \tag{2–75}$$

$$\left\|\dot{N}_B\right\| \leq \zeta_4 + \zeta_5 \|e_2\| . \tag{2–76}$$

In Equation 2–75 and Equation 2–76, $\zeta_i \in \mathbb{R}$ $(i = 1, 2, ..., 5)$ are known positive constants.

2.8 Stability Analysis

The stability of the RISE, NN, and optimal controller given in Equation 2–58 and Equation 2–60 can be examined through the following theorem.

Theorem 2.2: The nonlinear optimal controller given in Equation 2–58 and Equation 2–60 ensures that all system signals are bounded under closed-loop operation and that the position tracking error is regulated in the sense that

$$\|e_1(t)\| \to 0 \qquad as \qquad t \to \infty. \tag{2–77}$$

The result in Equation 2–77 can be achieved provided the control gain k_s introduced in Equation 2–29 is selected sufficiently large, and α_1, α_2 are selected according to the following sufficient conditions:

$$\lambda_{\min}(\alpha_1) > \frac{1}{2} \qquad \alpha_2 > \beta_2 + 1, \tag{2–78}$$

where $\lambda_{\min}(\cdot) \in \mathbb{R}$ denotes the minimum eigenvalue, and β_i $(i = 1, 2)$ are selected according to the following sufficient conditions:

$$\beta_1 > \zeta_1 + \zeta_2 + \frac{1}{\alpha_2}\zeta_3 + \frac{1}{\alpha_2}\zeta_4 \qquad \beta_2 > \zeta_5, \tag{2–79}$$

where $\zeta_i \in \mathbb{R}$, $i = 1, 2, ..., 5$ are introduced in Equation 2–75 - Equation 2–76, β_1 was introduced in Equation 2–29, and β_2 is introduced in Equation 2–82. Furthermore, $u(t)$ converges to an optimal controller that minimizes Equation 2–12 subject to Equation 2–11 provided the gain conditions given in Equation 2–14 - Equation 2–16 are satisfied.

Remark: The control gain α_1 can not be arbitrarily selected, rather it is calculated using a Lyapunov equation solver. Its value is determined based on the value of Q and R. Therefore Q and R must be chosen such that Equation 2–32 is satisfied.

Proof: Let $\mathcal{D} \subset \mathbb{R}^{3n+2}$ be a domain containing $\Phi(t) = 0$, where $\Phi(t) \in \mathbb{R}^{3n+2}$ is defined as

$$\Phi(t) \triangleq [y^T(t) \quad \sqrt{O(t)} \quad \sqrt{G(t)}]^T. \tag{2–80}$$

In Equation 2–80, the auxiliary function $O(t) \in \mathbb{R}$ is defined as

$$O(t) \triangleq \beta_1 \sum_{i=1}^{n} |e_{2_i}(0)| - e_2(0)^T N(0) - \int_0^t L(\tau) d\tau, \tag{2–81}$$

where $e_{2_i}(0)$ is equal to the i^{th} element of $e_2(0)$ and the auxiliary function $L(t) \in \mathbb{R}$ is defined as

$$\begin{aligned} L(t) \triangleq r^T (N_{B_1}(t) + N_D(t) - \beta_1 sgn(e_2)) \\ + \dot{e}_2^T(t) N_{B_2}(t) - \beta_2 \|e_2(t)\|^2, \end{aligned} \tag{2–82}$$

where $\beta_i \in \mathbb{R}$ $(i = 1, 2)$ are positive constants chosen according to the sufficient conditions in Equation 2–79. Provided the sufficient conditions introduced in Equation 2–79 are satisfied[6]

$$\int_0^t L(\tau) d\tau \leq \beta_1 \sum_{i=1}^{n} |e_{2_i}(0)| - e_2(0)^T N_B(0). \tag{2–83}$$

Hence, Equation 2–83 can be used to conclude that $O(t) \geq 0$. The auxiliary function $G(t) \in \mathbb{R}$ in Equation 2–80 is defined as

$$G(t) = \frac{\alpha_2}{2} tr\left(\tilde{W}^T \Gamma_1^{-1} \tilde{W}\right) + \frac{\alpha_2}{2} tr\left(\tilde{V}^T \Gamma_2^{-1} \tilde{V}\right). \tag{2–84}$$

Since Γ_1 and Γ_2 are constant, symmetric, and positive definite matrices and $\alpha_2 > 0$, it is straightforward that $G(t) \geq 0$.

[6] See Appendix E for details on this inequality

Let $V_L(\Phi, t) : \mathcal{D} \times [0, \infty) \rightarrow \mathbb{R}$ be a continuously differentiable positive definite function defined as

$$V_L(\Phi, t) \triangleq e_1^T e_1 + \frac{1}{2} e_2^T e_2 + \frac{1}{2} r^T M(q) r + O + G, \tag{2–85}$$

which satisfies the following inequalities:

$$U_1(\Phi) \leq V_L(\Phi, t) \leq U_2(\Phi) \tag{2–86}$$

provided the sufficient conditions introduced in Equation 2–79 are satisfied. In Equation 2–86, the continuous positive definite functions $U_1(\Phi)$, and $U_2(\Phi) \in \mathbb{R}$ are defined as $U_1(\Phi) \triangleq \lambda_1 \|\Phi\|^2$, and $U_2(\Phi) \triangleq \lambda_2(q) \|\Phi\|^2$, where λ_1, $\lambda_2(q) \in \mathbb{R}$ are defined as

$$\lambda_1 \triangleq \frac{1}{2} \min\{1, m_1\} \qquad \lambda_2(q) \triangleq \max\left\{\frac{1}{2}\bar{m}(q), 1\right\},$$

where m_1, $\bar{m}(q)$ are introduced in Equation 2–2. After taking the time derivative of Equation 2–85, $\dot{V}_L(\Phi, t)$ can be expressed as

$$\dot{V}_L(\Phi, t) = 2e_1^T \dot{e}_1 + e_2^T \dot{e}_2 + \frac{1}{2} r^T \dot{M}(q) r + r^T M(q) \dot{r} + \dot{O} + \dot{G}.$$

By utilizing Equation 2–5, Equation 2–6, Equation 2–65, and substituting in for the time derivative of $P(t)$ and $G(t)$, $\dot{V}(\Phi, t)$ can be simplified as

$$\begin{aligned} \dot{V}_L(\Phi, t) = & -2e_1^T \alpha_1 e_1 - (k_s + 1) \|r\|^2 - r^T R^{-1} r 2e_2^T e_1 + \beta_2 \|e_2(t)\|^2 \\ & + r^T \tilde{N}(t) - \alpha_2 \|e_2\|^2 + \alpha_2 e_2^T \left[\hat{W}^T \hat{\sigma}' \tilde{V}^T \dot{x}_d + \tilde{W}^T \hat{\sigma}' \hat{V}^T \dot{x}_d\right] \\ & + tr\left(\alpha_2 \tilde{W}^T \Gamma_1^{-1} \dot{\tilde{W}}\right) + tr\left(\alpha_2 \tilde{V}^T \Gamma_2^{-1} \dot{\tilde{V}}\right). \end{aligned} \tag{2–87}$$

Based on the fact that

$$e_2^T e_1 \leq \frac{1}{2} \|e_1\|^2 + \frac{1}{2} \|e_2\|^2,$$

and using Equation 2–60, the expression in Equation 2–87 can be simplified as

$$\dot{V}_L(\Phi,t) \leq r^T \tilde{N}(t) - \left(k_s + 1 + \lambda_{\min}\left(R^{-1}\right)\right)\|r\|^2 \\ - \left(2\lambda_{\min}(\alpha_1) - 1\right)\|e_1\|^2 - \left(\alpha_2 - 1 - \beta_2\right)\|e_2\|^2. \tag{2–88}$$

By using Equation 2–73, the expression in Equation 2–88 can be rewritten as

$$\dot{V}_L(\Phi,t) \leq -\lambda_3\|y\|^2 - \left[k_s\|r\|^2 - \rho(\|y\|)\|r\|\|y\|\right], \tag{2–89}$$

where $\lambda_3 \triangleq \min\{2\lambda_{\min}(\alpha_1) - 1, \alpha_2 - 1 - \beta_2, 1 + \lambda_{\min}(R^{-1})\}$; hence, α_1, and α_2 must be chosen according to the sufficient condition in Equation 2–78. After completing the squares for the terms inside the brackets in Equation 2–89, the following expression can be obtained:

$$\dot{V}_L(\Phi,t) \leq -\lambda_3\|y\|^2 + \frac{\rho^2(\|y\|)\|y\|^2}{4k_s} \leq -U(\Phi), \tag{2–90}$$

where $U(\Phi) = c\|y\|^2$, for some positive constant c, is a continuous, positive semi-definite function that is defined on the following domain:

$$\mathcal{D} \triangleq \left\{\Phi \in \mathbb{R}^{3n+2} \mid \|\Phi\| \leq \rho^{-1}\left(2\sqrt{\lambda_3 k_s}\right)\right\}.$$

The inequalities in Equation 2–86 and Equation 2–90 can be used to show that $V_L(\Phi,t) \in \mathcal{L}_\infty$ in $\mathcal{D}$; hence, $e_1(t)$, $e_2(t)$, and $r(t) \in \mathcal{L}_\infty$ in $\mathcal{D}$. Given that $e_1(t)$, $e_2(t)$, and $r(t) \in \mathcal{L}_\infty$ in $\mathcal{D}$, standard linear analysis methods can be used to prove that $\dot{e}_1(t)$, $\dot{e}_2(t) \in \mathcal{L}_\infty$ in $\mathcal{D}$ from Equation 2–5 and Equation 2–6. Since $e_1(t)$, $e_2(t)$, $r(t) \in \mathcal{L}_\infty$ in $\mathcal{D}$, the property that $q_d(t)$, $\dot{q}_d(t)$, $\ddot{q}_d(t)$ exist and are bounded can be used along with Equation 2–4 - Equation 2–6 to conclude that $q(t)$, $\dot{q}(t)$, $\ddot{q}(t) \in \mathcal{L}_\infty$ in $\mathcal{D}$. Since $q(t)$, $\dot{q}(t) \in \mathcal{L}_\infty$ in $\mathcal{D}$, Property 2.4 can be used to conclude that $M(q)$, $V_m(q,\dot{q})$, $G(q)$, and $F(\dot{q}) \in \mathcal{L}_\infty$ in $\mathcal{D}$. Thus from Equation 2–1 and Property 2,5, we can show that $u(t) \in \mathcal{L}_\infty$ in $\mathcal{D}$. Given that $r(t) \in \mathcal{L}_\infty$ in $\mathcal{D}$, Equation 2–66 can be used to show that $\dot{\mu}(t) \in \mathcal{L}_\infty$ in $\mathcal{D}$. Since $\dot{q}(t)$, $\ddot{q}(t) \in \mathcal{L}_\infty$ in $\mathcal{D}$, Property 2.4 can be used to show that $\dot{V}_m(q,\dot{q})$, $\dot{G}(q)$, $\dot{F}(q)$ and $\dot{M}(q) \in \mathcal{L}_\infty$ in $\mathcal{D}$; hence, Equation 2–65 can be used to show that $\dot{r}(t) \in \mathcal{L}_\infty$ in $\mathcal{D}$. Since $\dot{e}_1(t)$, $\dot{e}_2(t)$,

$\dot{r}(t) \in \mathcal{L}_\infty$ in $\mathcal{D}$, the definitions for $U(y)$ and $z(t)$ can be used to prove that $U(y)$ is uniformly continuous in $\mathcal{D}$.

Let $\mathcal{S} \subset \mathcal{D}$ denote a set defined as follows:

$$\mathcal{S} \triangleq \left\{ \Phi(t) \subset \mathcal{D} \mid U_2(\Phi(t)) < \lambda_1 \left(\rho^{-1} \left(2\sqrt{\lambda_3 k_s} \right) \right)^2 \right\}. \tag{2–91}$$

The region of attraction in Equation 2–91 can be made arbitrarily large to include any initial conditions by increasing the control gain k_s (i.e., a semi-global type of stability result) (41). Theorem 8.4 of (42) can now be invoked to state that

$$c \left\| y(t) \right\|^2 \to 0 \qquad as \qquad t \to \infty \qquad \forall y(0) \in \mathcal{S}. \tag{2–92}$$

Based on the definition of $y(t)$, Equation 2–92 can be used to show that

$$\left\| e_1(t) \right\| \to 0 \qquad as \qquad t \to \infty \qquad \forall y(0) \in \mathcal{S}. \tag{2–93}$$

The result in Equation 2–92 indicates that as $t \to \infty$, Equation 2–61 reduces to

$$\hat{f}_d + \mu = h + \tau_d. \tag{2–94}$$

Therefore, dynamics in Equation 2–7 converge to the state-space system in Equation 2–11. Hence, $u(t)$ converges to an optimal controller that minimizes Equation 2–12 subject to Equation 2–11 provided the gain conditions given in Equation 2–14 - Equation 2–16, Equation 2–78, and Equation 2–79 are satisfied.

2.9 Simulation and Experimental Results

2.9.1 Simulation

To examine the performance of the controllers proposed in Equation 2–20 and Equation 2–58 a numerical simulation was performed. The simulation is based on the

dynamics for a two-link robot given as

$$\begin{aligned}\begin{bmatrix} u_1 \\ u_2 \end{bmatrix} &= \begin{bmatrix} p_1 + 2p_3c_2 & p_2 + p_3c_2 \\ p_2 + p_3c_2 & p_2 \end{bmatrix} \begin{bmatrix} \ddot{q}_1 \\ \ddot{q}_2 \end{bmatrix} \\ &+ \begin{bmatrix} -p_3s_2\dot{q}_2 & -p_3s_2\left(\dot{q}_1 + \dot{q}_2\right) \\ p_3s_2\dot{q}_1 & 0 \end{bmatrix} \begin{bmatrix} \dot{q}_1 \\ \dot{q}_2 \end{bmatrix} \\ &+ \begin{bmatrix} f_{d_1} & 0 \\ 0 & f_{d_2} \end{bmatrix} \begin{bmatrix} \dot{q}_1 \\ \dot{q}_2 \end{bmatrix} + \begin{bmatrix} \tau_{d_1} \\ \tau_{d_2} \end{bmatrix},\end{aligned} \tag{2–95}$$

where $p_1 = 3.473\ kg \cdot m^2$, $p_2 = 0.196\ kg \cdot m^2$, $p_3 = 0.242\ kg \cdot m^2$, $f_{d_1} = 5.3\ Nm \cdot \sec$, $f_{d_2} = 1.1\ Nm \cdot \sec$, c_2 denotes $cos(q_2)$, s_2 denotes $sin(q_2)$ and τ_{d_1}, τ_{d_2} denote bounded disturbances defined as

$$\begin{aligned}\tau_{d_1} &= 0.1\ \sin(t) + 0.15\ \cos(3t) \\ \tau_{d_2} &= 0.15\ \sin(2t) + 0.1\ \cos(t).\end{aligned} \tag{2–96}$$

The desired trajectory is given as

$$q_{d_1} = q_{d_2} = \frac{1}{2}\ \sin(2t), \tag{2–97}$$

and the initial conditions of the robot were selected as

$$\begin{aligned}q_1(0) &= q_2(0) = 14.3\ deg \\ \dot{q}_1(0) &= \dot{q}_2(0) = 28.6\ deg/\sec.\end{aligned}$$

The weighting matrixes for both controllers were chosen as

$$Q_{11} = \begin{bmatrix} 20 & 2 \\ 2 & 20 \end{bmatrix} \qquad Q_{12} = \begin{bmatrix} -4 & 5 \\ 3 & -6 \end{bmatrix}$$

$$Q_{22} = diag\left\{\ 35,\ \ 35\ \right\}.$$

which using Equation 2–14, Equation 2–15, and Equation 2–16 yielded the following values for K, α_1, and R

$$K = \begin{bmatrix} 4 & -4 \\ -4 & 6 \end{bmatrix} \qquad \alpha_1 = \begin{bmatrix} 8.1 & 5.6 \\ 5.6 & 5.4 \end{bmatrix}$$

$$R = diag\left\{ \frac{1}{35}, \quad \frac{1}{35} \right\}.$$

The control gains for both controllers were selected as

$$\alpha_2 = 20 \qquad \beta_1 = 20 \qquad k_s = 75.$$

The neural network update law weights were selected as

$$\Gamma_1 = 5I_{11} \qquad \Gamma_2 = 500I_7.$$

The tracking errors and the control inputs for the RISE and optimal controller are shown in Figure 2-1 and Figure 2-2, respectively. To show that the RISE feedback identifies the nonlinear effects and bounded disturbances, a plot of the difference is shown in Figure 2-3. As this difference goes to zero, the dynamics in Equation 2–1 converge to the state-space system in Equation 2–11, and the controller becomes optimal.

The tracking errors and the control inputs for the RISE, NN, and optimal controller are shown in Figure 2-4 and Figure 2-5, respectively. To show that the RISE feedback and feedforward NN identifies the nonlinear effects and bounded disturbances, a plot of the difference is shown in Figure 2-6. As this difference goes to zero, the dynamics in Equation 2–1 converge to the state-space system in Equation 2–11, and the controller becomes optimal.

2.9.2 Experiment

To test the validity of the controllers developed in Equation 2–20 and Equation 2–58 an experiment was performed on a two-link robot testbed as depicted in Figure 2-7. The testbed is composed of a two-link direct drive revolute robot consisting of two aluminum links, mounted on a 240.0 [Nm] (base joint) and 20.0 [Nm] (second joint) switched

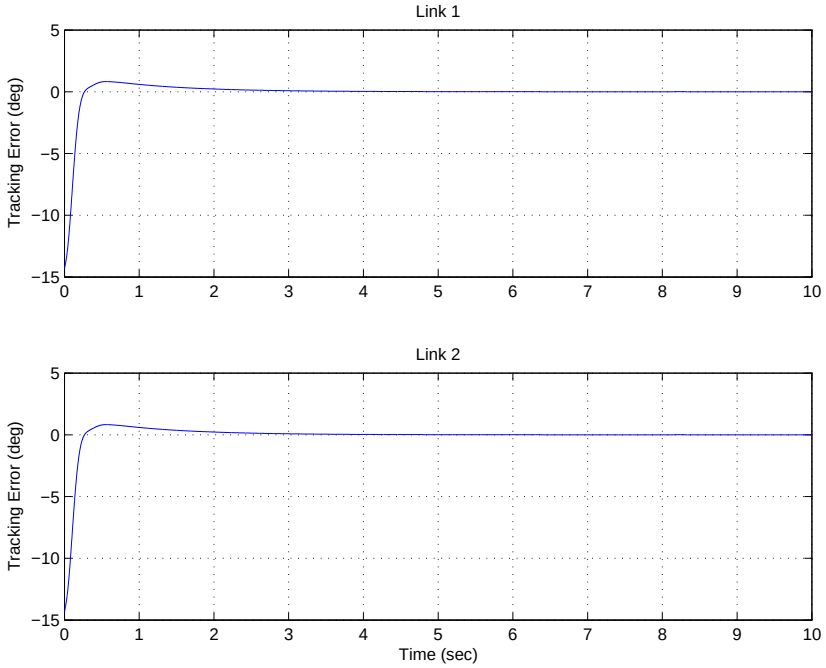

Figure 2-1. The simulated tracking errors for the RISE and optimal controller.

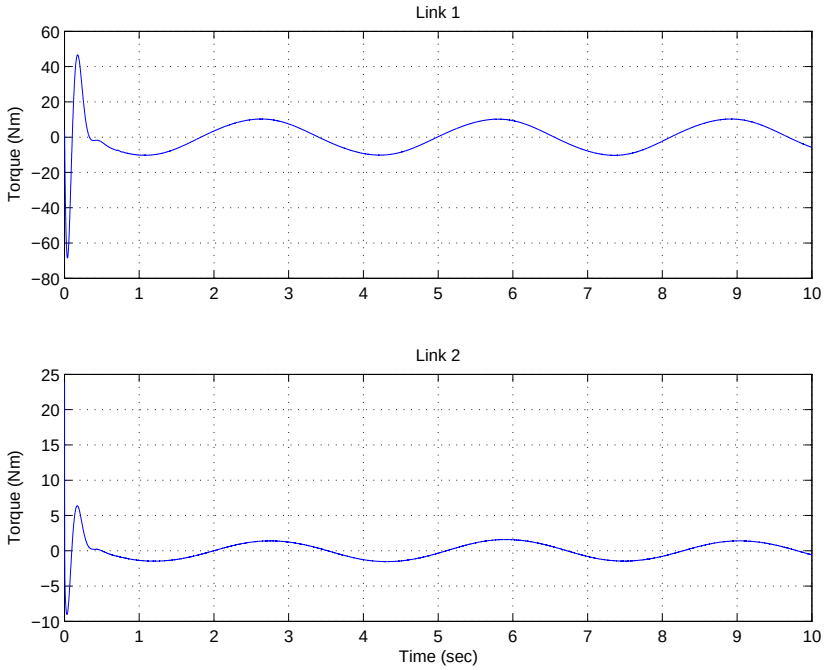

Figure 2-2. The simulated torques for the RISE and optimal controller.

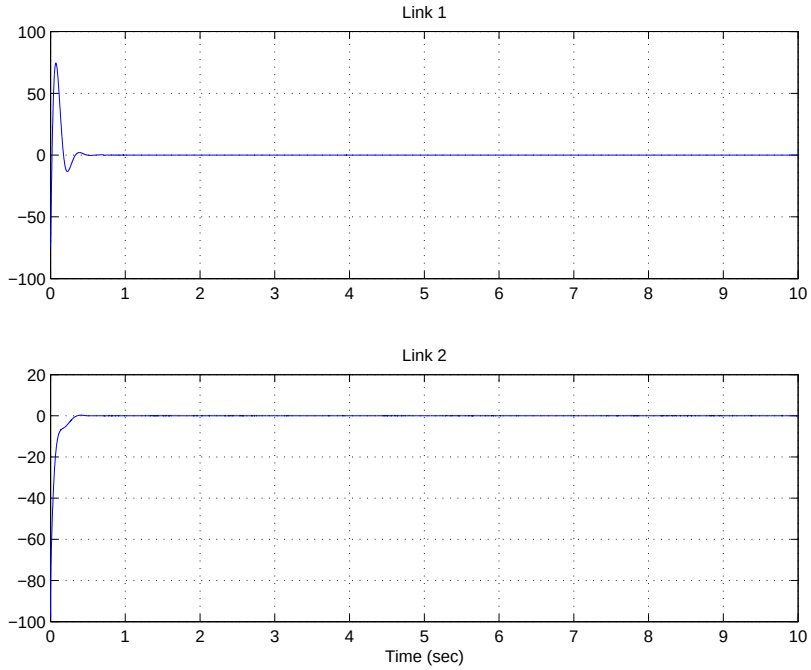

Figure 2-3. The difference between the RISE feedback and the nonlinear effects and bounded disturbances.

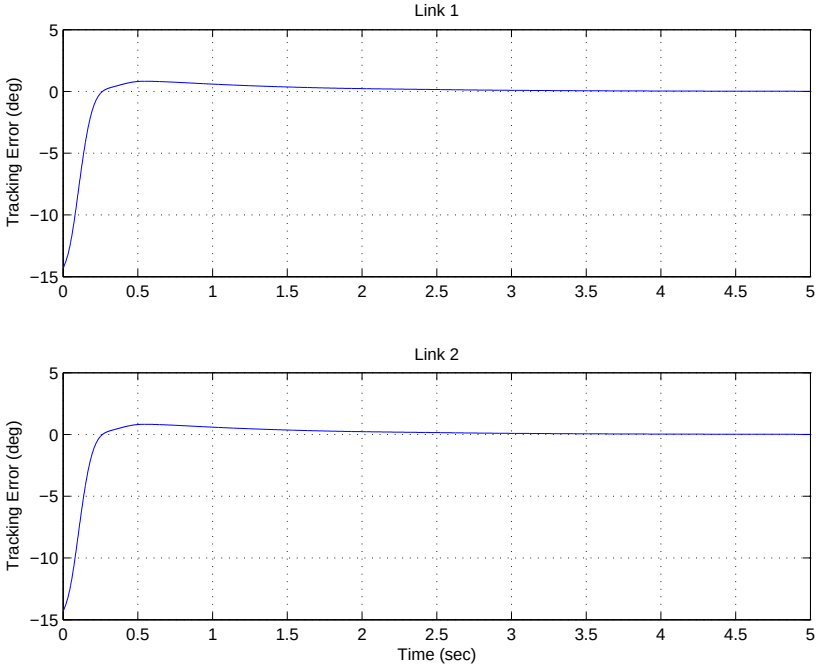

Figure 2-4. The simulated tracking errors for the RISE, NN, and optimal controller.

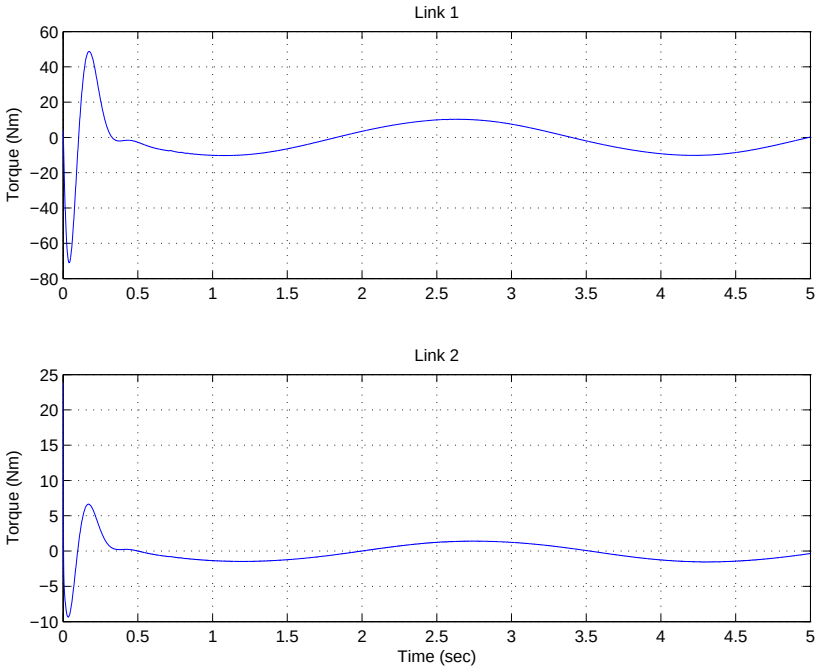

Figure 2-5. The simulated torques for the RISE, NN, and optimal controller.

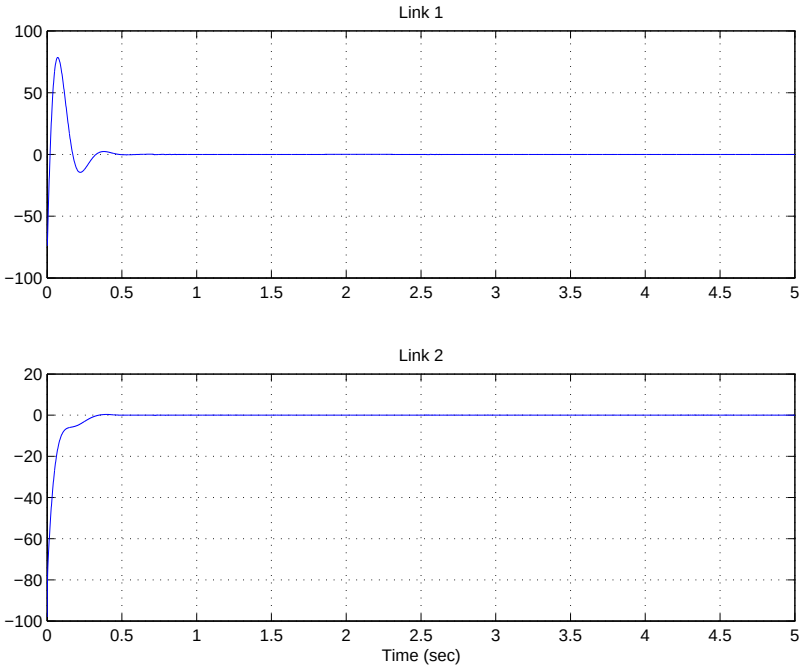

Figure 2-6. The difference between the RISE feedback and feedforward NN and the nonlinear effects and bounded disturbances (i.e., $.\left(\hat{f}_d + \mu\right) - (h + \tau_d)$).

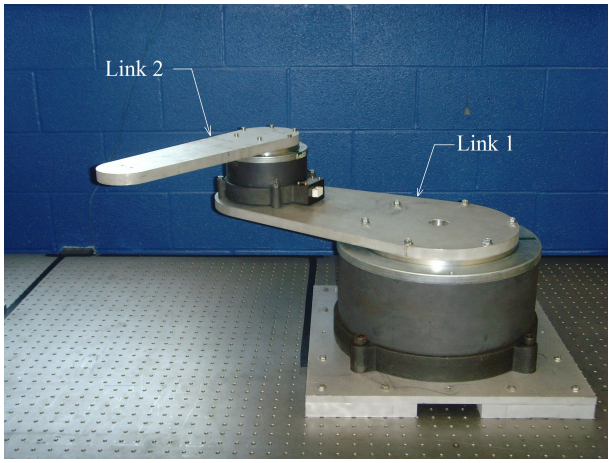

Figure 2-7. The experimental testbed consists of a two-link robot. The links are mounted on two NSK direct-drive switched reluctance motors.

reluctance motors. The motors are controlled through power electronics operating in torque control mode. The motor resolvers provide rotor position measurements with a resolution of 614400 pulses/revolution, and a standard backwards difference algorithm is used to numerically determine velocity from the encoder readings. A Pentium 2.8 GHz PC operating under QNX hosts the control algorithm, which was implemented via a custom graphical user-interface (46), to facilitate real-time graphing, data logging, and the ability to adjust control gains without recompiling the program. Data acquisition and control implementation were performed at a frequency of 1.0 kHz using the ServoToGo I/O board.

The control objective is to track the desired time-varying trajectory by using the proposed control laws. To achieve this control objective, the control gains α_2, k_s, and β_1 defined as scalars in Equation 2–6 and Equation 2–29, were implemented (with non-consequential implications to the stability result) as diagonal gain matrices. The weighting matrixes for both controllers were chosen as

$$Q_{11} = \begin{bmatrix} 40 & 2 \\ 2 & 40 \end{bmatrix} \qquad Q_{12} = \begin{bmatrix} -4 & 5 \\ 3 & -6 \end{bmatrix}$$

$$Q_{22} = diag\left\{ 4, \quad 4 \right\},$$

which using Equation 2–14, Equation 2–15, and Equation 2–16 yielded the following values for K, α_1, and R

$$K = \begin{bmatrix} 4 & -4 \\ -4 & 6 \end{bmatrix} \qquad \alpha_1 = \begin{bmatrix} 15.6 & 10.6 \\ 10.6 & 10.4 \end{bmatrix}$$

$$R = diag\left\{ \begin{array}{cc} 0.25, & 0.25 \end{array} \right\}.$$

The control gains for both controllers were selected as

$$\alpha_2 = diag\left\{ \begin{array}{cc} 60, & 35 \end{array} \right\} \qquad \beta_1 = diag\left\{ \begin{array}{cc} 5, & 0.1 \end{array} \right\}$$

$$k_s = diag\left\{ \begin{array}{cc} 140, & 20 \end{array} \right\}.$$

The neural network update law weights were selected as

$$\Gamma_1 = 25 I_{11} \qquad \Gamma_2 = 25 I_7.$$

The desired trajectories for both controllers was chosen as follows:

$$q_{d_1} = q_{d_2} = 60 \sin(2t) \left(1 - \exp\left(-0.01 t^3\right)\right). \tag{2–98}$$

To compare the developed controllers to the controllers in literature, the controller in (7) given by

$$u(t) = \hat{W}^T \sigma(x) - u_o - \eta, \tag{2–99}$$

was implemented. In Equation 2–99, $\eta(t) \in \mathbb{R}^n$ is robustifying term defined as

$$\eta = -k_{z1} \frac{r}{\|r\|},$$

where $k_{z1} \in \mathbb{R}$ and $\hat{W}(t)^T \sigma(x)$ is a functional link neural network estimate for Equation 2–8. The neural network update law is given by

$$\dot{\hat{W}} = \Gamma_1 \sigma(x) e_2^T - k_{z2} \|z\| \hat{W},$$

Table 2-1. Tabulated values for the 10 runs for the developed controllers.

	RISE	RISE + NN
Average Max Steady State Error (deg)- Link 1	0.0416	0.0416
Average Max Steady State Error (deg)- Link 2	0.0573	0.0550
Average RMS Error (deg) - Link 1	0.0128	0.0139
Average RMS Error (deg) - Link 2	0.0139	0.0143
Average RMS Torque (Nm) - Link 1	9.4217	9.4000
Average RMS Torque (Nm) - Link 2	1.7375	1.6825
Error Standard Deviation (deg) - Link 1	0.0016	0.0011
Error Standard Deviation (deg) - Link 2	0.0019	0.0015
Torque Standard Deviation (Nm) - Link 1	0.2775	0.3092
Torque Standard Deviation (Nm) - Link 2	0.0734	0.1746

where $k_{z1} \in \mathbb{R}$. The control gains relating to the optimal term were kept constant, however, the neural network update law weight and addition gains were selected as follows:

$$\Gamma_1 = 15 I_{15} \qquad k_{z2} = 0.1$$
$$k_{z1} = diag\left\{ 5, \quad 1 \right\}.$$

For all experiments, the rotor velocity signal is obtained by applying a standard backwards difference algorithm to the position signal. The integral structure for the RISE term in Equation 2–29 was computed on-line via a standard trapezoidal algorithm. In addition, all the states were initialized to zero. Each experiment (excluding the controller in Equation 2–99) using was performed ten times, and data from the experiments is displayed in Table 2-1.

Figure 2-8 and Figure 2-9 depict the tracking errors and control torques for one experimental trial for the RISE and optimal controller. Figure 2-10 and Figure 2-11 depict the tracking errors and control torques for one experimental trial for the RISE and optimal controller. Figure 2-12 and Figure 2-13 depict the tracking errors and control torques for controller in Equation 2–99. The experiment for the controller given in Equation 2–99 was run for a longer than the developed controllers, because more time was needed to gauge the control performance.

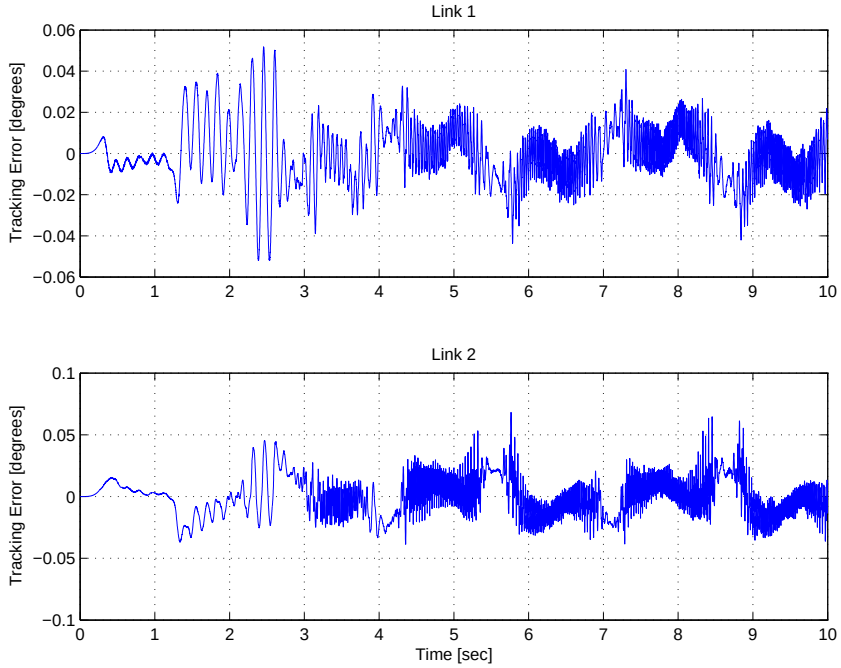

Figure 2-8. Tracking errors resulting from implementing the RISE and optimal controller.

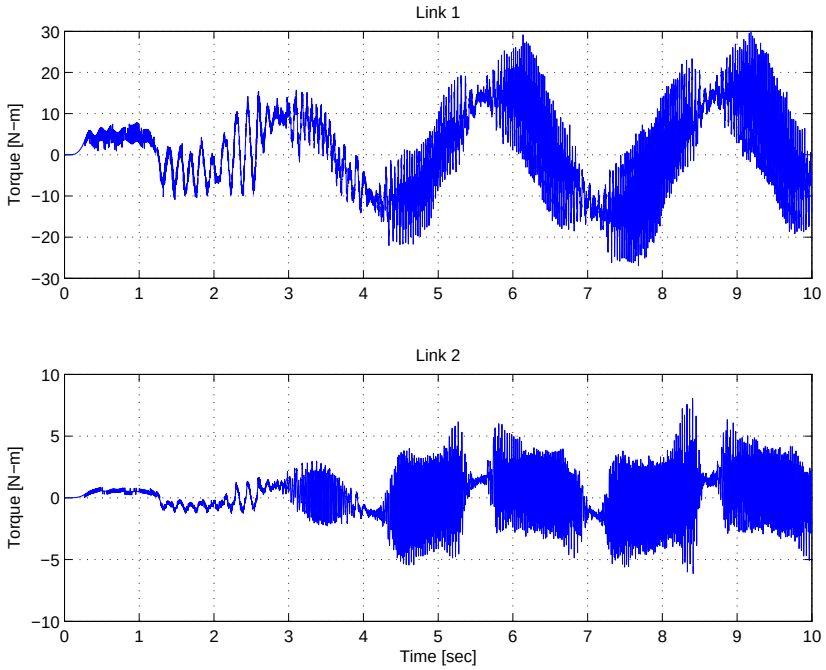

Figure 2-9. Torques resulting from implementing the RISE and optimal controller.

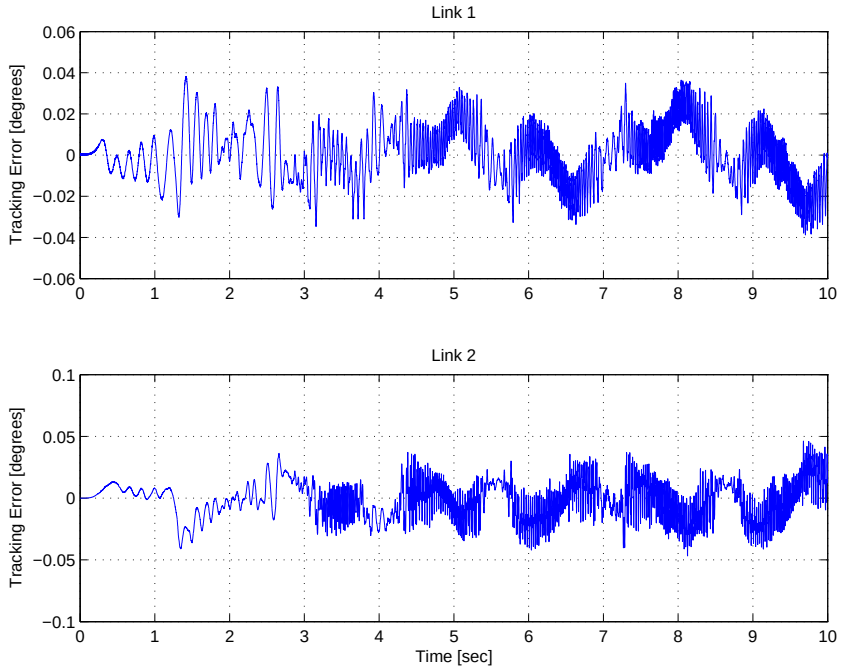

Figure 2-10. Tracking errors resulting from implementing the RISE, NN, and optimal controller.

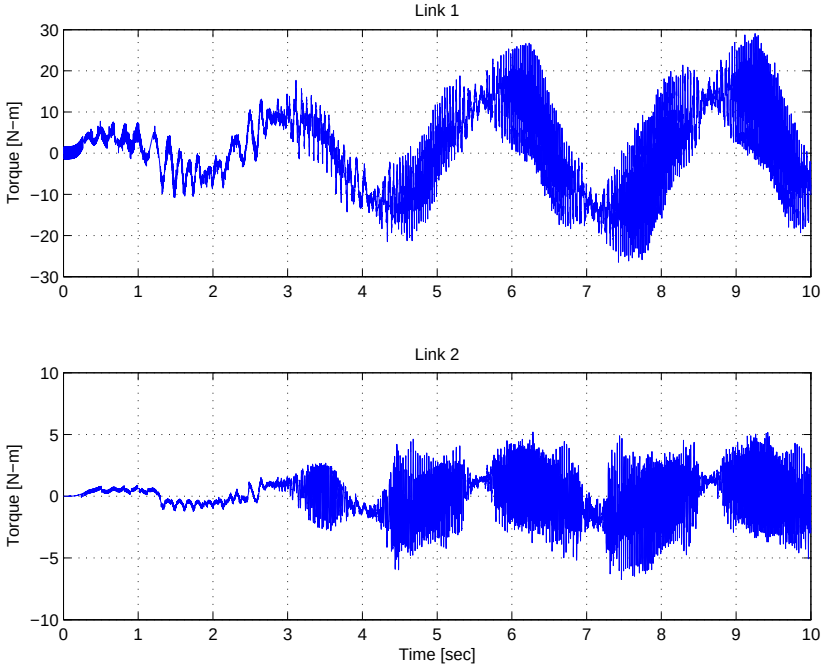

Figure 2-11. Torques resulting from implementing the RISE, NN, and optimal controller.

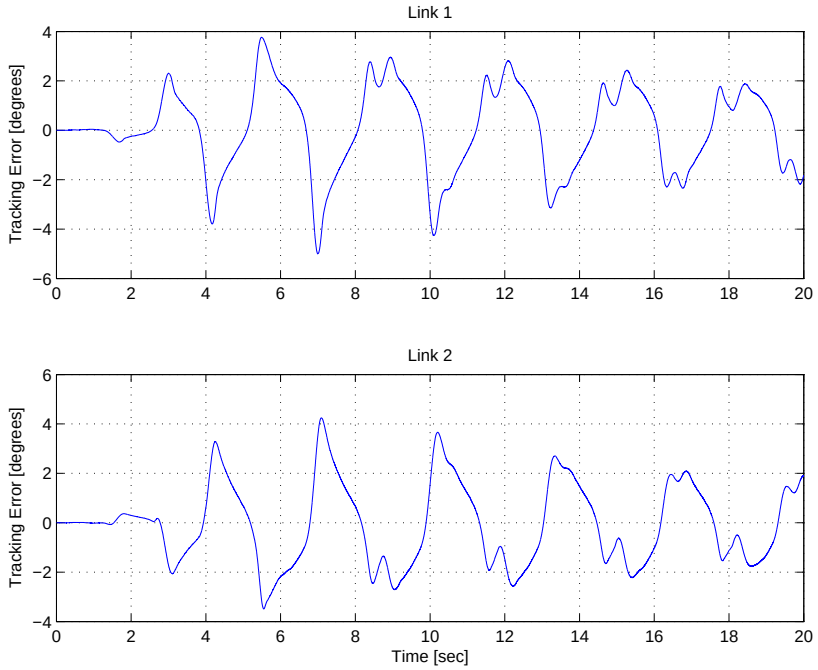

Figure 2-12. Tracking errors resulting from implementing the controller developed in literature.

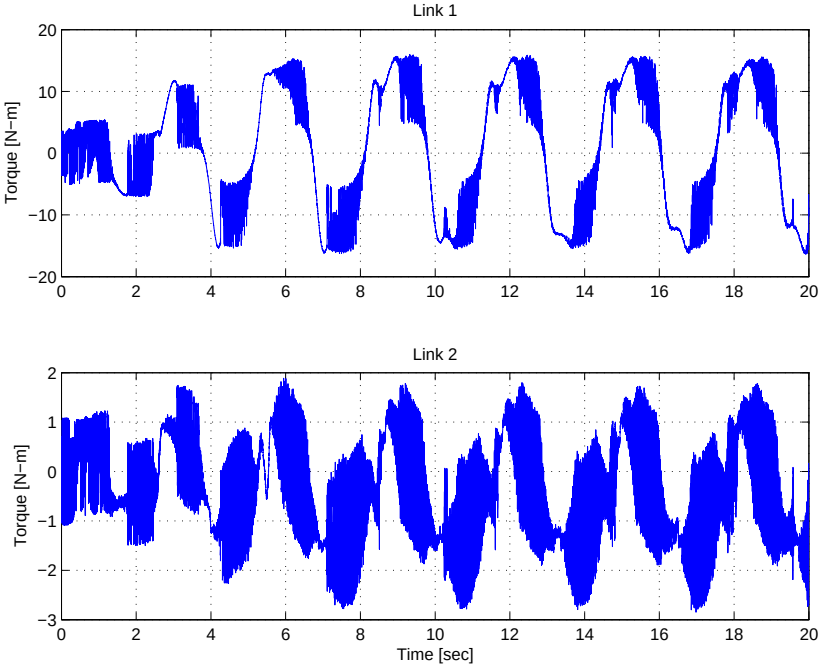

Figure 2-13. Torques resulting from implementing the controller developed in literature.

2.9.3 Discussion

The mismatch between the identifier and the disturbance can not be calculated in a physical system because the disturbance is not exactly known. Therefore, simulation results are use to show that the RISE feedback and RISE feedback plus a feedforward NN identifies the nonlinear effects and bounded disturbances. The simulation is also beneficial because it allows a comparison of how the optimal controllers perform in the presence of parametric uncertainty compared to the feedback linearized system in Equation 2–11, where as it is impossible to perfectly feedback linearize a real system. For the comparison, the contribution of the feedforward NN and RISE feedback term in Equation 2–20 and Equation 2–58 as well as contribution of $h\left(q,\dot{q},q_d,\dot{q}_d,\ddot{q}_d\right)$ and $\tau_d\left(t\right)$ in Equation 2–9 are not considered, since only the input $u_o\left(t\right)$ was included in the cost functional Equation 2–12. For the the feedback linearized system, assuming no uncertainty, $J\left(u_o\right)$ was calculated to be 40.41. For the RISE only controller, $J\left(u_o\right)$ was calculated to be 43.32. For the RISE and NN controller, $J\left(u_o\right)$ was calculated to be 42.43.

The experiments show that both controllers stabilize the system. Both controllers keep the average maximum steady state (defined as the last 5 seconds of the experiment) error under 0.05 degrees for the first link and under 0.06 degrees for the second link. The data in Table 2.1 indicates that the RISE and NN controller resulted in slightly more RMS error for each link, although a reduced or equal maximum steady state error, with a slightly reduced torque. The reduced standard deviation of the RISE and NN controller show that the results from each run were more alike than the RISE controller alone, but there was greater variance in the torque. Both controllers performed much better than the controller developed in (7) for the same cost. The controller in (7) may be able to achieve similar results for a different cost, however, changing the cost limits the comparisons that can be made between the controllers. Keeping the cost the same results in the optimal part of the controller being the same; the only part of the controller design to change is

the identifier. If the cost was changed, the optimal control portion would change and the controllers would be completely different.

CHAPTER 3
INVERSE OPTIMAL CONTROL OF A NONLINEAR EULER-LAGRANGE SYSTEM

Inverse optimal control (IOC) (15–21) was developed as a way to design optimal controllers for nonlinear systems without having to solve an HJB equation. In IOC design, a control Lyapunov function (CLF), which can be shown to also be a value function, is used to design a controller which stabilizes a system. It is then shown that the developed controller minimizes a meaningful cost (i.e., a cost that puts a positive penalty on the states and actuation). Due to the fact that the controller is designed before the cost, the cost can not be chosen a priori. However, an advantage of the IOC is that the controller does not have to converge to an optimal solution (like the previously developed controllers). Adaptive IOC methods (22–26) have been developed for systems that contain linear in the parameters (LP) uncertainty.

Previous IOCs focus on the class problems modeled as

$$\dot{x} = f(x) + F(x)\theta + g(x)u, \tag{3–1}$$

for some state $x(t) \in \mathbb{R}^n$, where $f(x) \in \mathbb{R}^n$ is a known smooth vector valued function, $F(x) \in \mathbb{R}^{n\times p}$, $g(x) \in \mathbb{R}^{n\times m}$ are smooth matrix valued functions, $\theta \in \mathbb{R}^p$ is a vector of unknown constants, and $u(t) \in \mathbb{R}^m$ is the control. In general, the input gain matrix $g(x)$ must be known. Classes of systems where the dynamics can be expressed as Equation 3–1 were used to develop inverse optimal controllers because that form facilitated the development of a control Lyapunov function. Systems with a constant inertia matrix, such as the applications in (25) and (26), can easily be transformed into Equation 3–1, unlike systems with an uncertain state-dependent inertia matrix or uncertainty in the input matrix.

Based on the theoretical foundation presented in (22; 25; 40), an adaptive IOC is developed in this Chapter. The class of systems considered in this Chapter are uncertain Euler-Lagrange systems, which do not adhere to the model given in Equation 3–1.

The developed controller achieves globally asymptotically tracking for the generalized coordinates of the system as it minimizes a meaningful (i.e., a positive function of the states and control input) performance index. To develop the optimal controller for the uncertain system, the open loop error system is segregated to include two adaptive terms: one based explicitly on the tracking error and one not. This is done because only terms that depend explicitly on the tracking error contribute to the cost functional. A Lyapunov analysis is provided to examine the stability of the developed controller and to determine a respective meaningful cost functional . It is then shown that the cost is minimized without having to prove the Lyapunov function is a CLF. Preliminary simulation results are included to illustrate the performance of the controller.

The remainder of this chapter is organized as follows. In Section 3.1, the model is given along with several of its properties. In Section 3.2, the control objective is stated and an error system is formulated. In Section 3.3, the stability of the controller is proven. In Section 3.4, a meaningful cost is developed and shown to be minimized by the control. In Section 3.5, simulation and experimental results are presented.

3.1 Dynamic Model and Properties

The class of nonlinear dynamic systems considered in this chapter is assumed to be modeled by the following Euler-Lagrange (39) formulation:

$$M(q)\ddot{q} + V_m(q,\dot{q})\dot{q} + G(q) + F_d\dot{q} = u(t), \tag{3–2}$$

where, $M(q)$, $V_m(q,\dot{q})$, $G(q)$, $q(t)$, $\dot{q}(t)$, $\ddot{q}(t)$, and $u(t)$ are defined in Section 2.1, and $F_d \in \mathbb{R}^{n\times n}$ denotes the constant, diagonal, positive-definite, viscous friction coefficient matrix. The subsequent development is based on the assumption that $q(t)$ and $\dot{q}(t)$ are measurable and that $M(q)$, $V_m(q,\dot{q})$, $G(q)$, and F_d are unknown. In addition to Properties 2.1, 2.2, and 2.3 the following properties will be exploited in the subsequent development.

Property 3.1: If $q(t)$, $\dot{q}(t) \in \mathcal{L}_\infty$, then $M(q)$, $V_m(q,\dot{q})$, and $G(q)$ are bounded.

Property 3.2: There exists a positive scalar constant $\zeta_f \in \mathbb{R}$ such that

$$\|F_d\| \leq \zeta_f.$$

Property 3.3: The desired trajectory is assumed to be designed such that $q_d(t)$, $\dot{q}_d(t)$, and $\ddot{q}_d(t) \in \mathbb{R}^n$ exist, and are bounded.

Property 3.4: The dynamics in Equation 3–2 can be linear parameterized as

$$Y\left(q, \dot{q}, \ddot{q}\right)\theta = M(q)\ddot{q} + V_m(q, \dot{q})\dot{q} + G(q) + F_d\dot{q}, \tag{3–3}$$

where $\theta \in \mathbb{R}^p$ contains the unknown constant system parameters, and the nonlinear regression matrix $Y\left(q, \dot{q}, \ddot{q}\right) \in \mathbb{R}^{n \times p}$ contains known functions of the link position, velocity, and acceleration, $q\left(t\right)$, $\dot{q}\left(t\right)$, $\ddot{q}\left(t\right) \in \mathbb{R}^n$, respectively.

3.2 Control Development

As in Chapter 2, the control objective is to ensure that the generalized coordinates of a system track a desired time-varying trajectory despite uncertainties in the dynamic model, while minimizing a performance index. To quantify the tracking objective, a position tracking error denoted by $e(t) \in \mathbb{R}^n$, is defined as

$$e \triangleq q_d - q. \tag{3–4}$$

To facilitate the subsequent control design and stability analysis, a filtered tracking error denoted by $r(t) \in \mathbb{R}^n$, is defined as

$$r = \dot{e} + \alpha e, \tag{3–5}$$

where $\alpha \in \mathbb{R}$ is a positive, constant gain. By taking the time derivative of $r(t)$ and premultipling by $M\left(q\right)$ the following open-loop error system can be obtained:

$$M\left(q\right)\dot{r} = M\left(q\right)\ddot{q}_d + V_m\left(q, \dot{q}\right)\dot{q} + G\left(q\right) + F_d\dot{q} + \alpha M\left(q\right)\dot{e} - u, \tag{3–6}$$

where Equation 3–2, Equation 3–4, and Equation 3–5 were used. The expression in Equation 3–6 can then be rewritten as

$$M(q)\dot{r} = -V_m(q,\dot{q})\,r + Y_1\theta + Y_2\theta - u, \tag{3–7}$$

where

$$Y_1\theta = \alpha V_m(q,\dot{q})\,e + \alpha M(q)\,\dot{e} - F_d\dot{e} \tag{3–8}$$

$$Y_2\theta = M(q)\,\ddot{q}_d + V_m(q,\dot{q})\,\dot{q}_d + G(q) + F_d\dot{q}_d. \tag{3–9}$$

In Equation 3–8 and Equation 3–9 $Y_1(q,\dot{q})$, and $Y_2(q,\dot{q},\dot{q}_d,\ddot{q}_d) \in \mathbb{R}^{n\times p}$, are nonlinear regression matrices that contain known functions of the position, velocity, desired velocity, and desired acceleration. Segregating the terms in Equation 3–8 and Equation 3–9 is not required to achieve the tracking control objective, rather the terms are segregated to facilitate the development of the optimal control law. Although both terms contain the same unknown parameters, Equation 3–8 explicitly depends on the tracking error, while Equation 3–9 does not (it is dependent the position and desired position but not dependent on their difference). Therefore, the total control $u(t)$ is made up of two parts: $u_f(t)$ based on Equation 3–9 which is independent of the tracking error and therefore the optimization, and the feedback law $u_o(t)$ based on Equation 3–8 which is later shown to minimize a meaningful cost (i.e., a cost that puts a positive penalty on the states and actuation). The control is defined as

$$u_f = Y_2\hat{\theta} \tag{3–10}$$

$$u = u_f - u_0 = Y_2\hat{\theta} - u_0, \tag{3–11}$$

where u_f, $u_o \in \mathbb{R}^n$ and $\hat{\theta}(t) \in \mathbb{R}^p$ is an estimate for θ. The parameter estimate $\hat{\theta}(t)$ in Equation 3–10 and Equation 3–11 is generated by the adaptive update law

$$\dot{\hat{\theta}} = \Gamma(Y_1 + Y_2)^T r, \tag{3–12}$$

where $\Gamma \in \mathbb{R}^{p\times p}$ is a constant, positive definite, symmetric, gain matrix. Substituting Equation 3–11 into Equation 3–7 yields

$$M(q)\dot{r} = -V_m(q,\dot{q})\, r + Y_1\theta + Y_2\tilde{\theta} + u_0, \tag{3–13}$$

where the parameter estimation error $\tilde{\theta}(t) \in \mathbb{R}^p$ is defined as

$$\tilde{\theta} = \theta - \hat{\theta}. \tag{3–14}$$

Based on Equation 3–13 and the subsequent stability analysis, the control input is designed as

$$u_o = -R^{-1}r = -\left(K_1 + \frac{\Psi_1^T\Psi_1}{2} + \frac{\Psi_2^T K_1^{-1}\Psi_2}{2}\right) r, \tag{3–15}$$

where $R^{-1}\left(x,\hat{\theta}\right)$, $K_1 \in \mathbb{R}^{n\times n}$ are positive definite and symmetric, and $\Psi_1(t)$, $\Psi_2(t) \in \mathbb{R}^{n\times n}$ are defined as

$$\Psi_1 = \left[\frac{1}{\sqrt{\alpha}} I_n + \sqrt{\alpha}\hat{V}_m(q,\dot{q}) - \sqrt{\alpha^3}\hat{M}(q) + \sqrt{\alpha}\hat{F}_d\right]^T \tag{3–16}$$

$$\Psi_2 = \left[\alpha\hat{M}(q) - \hat{F}_d\right], \tag{3–17}$$

where $I_n \in \mathbb{R}^{n\times n}$ is an identity matrix.

3.3 Stability Analysis

The stability of the controller given in Equation 3–10 - Equation 3–12, and Equation 3–15 can be examined through the following theorem.

Theorem 3.1: The adaptive update law given by Equation 3–12 and the feedback law given by Equation 3–15 ensures global asymptotic tracking of the system in Equation 3–13 in the sense that

$$\|e(t)\| \to 0 \qquad \|r(t)\| \to 0 \quad as \quad t \to \infty.$$

Proof: Let $V_a(e, r, \tilde{\theta}, t) \in \mathbb{R}$ denote a positive definite, radially unbounded function defined as

$$V_a = V + \frac{1}{2}\tilde{\theta}^T \Gamma^{-1} \tilde{\theta}, \tag{3–18}$$

where $V(e, r, t) \in \mathbb{R}$ is defined as

$$V = \frac{1}{2} e^T e + \frac{1}{2} r^T M(q) r. \tag{3–19}$$

After using Equation 3–13 and Property 2.3, the time derivative of Equation 3–18 is

$$\dot{V}_a = e^T \dot{e} + r^T \left(Y_1 \theta + Y_2 \tilde{\theta} \right) + r^T u_0 - \tilde{\theta}^T \Gamma^{-1} \dot{\hat{\theta}}. \tag{3–20}$$

After adding and subtracting $r^T(t) Y_1(q, \dot{q}) \hat{\theta}(t)$ the expression in Equation 3–20 can be expressed as

$$\dot{V}_a = e^T \dot{e} + r^T Y_1 \hat{\theta} + r^T u_o + \tilde{\theta}^T \left((Y_1 + Y_2)^T r - \Gamma^{-1} \dot{\hat{\theta}} \right). \tag{3–21}$$

After substituting the adaptive update law in Equation 3–12 the expression in Equation 3–21 reduces to

$$\dot{V}_a = e^T \dot{e} + r^T Y_1 \hat{\theta} + r^T u_o. \tag{3–22}$$

The term $Y_1(q, \dot{q}) \hat{\theta}(t)$ in Equation 3–22 can be expressed as

$$Y_1 \hat{\theta} = \alpha \hat{V}_m(q, \dot{q}) e + \alpha \hat{M}(q)(r - \alpha e) - \hat{F}_d(r - \alpha e), \tag{3–23}$$

where $\hat{V}_m(q, \dot{q})$, $\hat{M}(q)$, $\hat{F}_d \in \mathbb{R}^{n \times n}$ denote the estimates for the centripetal-Coriolis matrix, inertia matrix, and the viscous friction coefficient matrix respectively. By substituting $\dot{e}(t)$ from Equation 3–5 and using Equation 3–23, the expression in Equation 3–21 can be written as

$$\begin{aligned} \dot{V}_a &= r^T \left(I_n + \alpha \hat{V}_m(q, \dot{q}) - \alpha^2 \hat{M}(q) + \alpha \hat{F}_d \right) e \\ &\quad - \alpha e^T e + r^T \left(\alpha \hat{M}(q) - \hat{F}_d \right) r + r^T u_o \\ &= -\alpha e^T e + \sqrt{\alpha} r^T \Psi_1 e + r^T \Psi_2 r + r^T u_o, \end{aligned} \tag{3–24}$$

where $\Psi_1(t)$ and $\Psi_2(t)$ are introduced in Equation 3–16 and Equation 3–17, respectively. Substituting the expression in Equation 3–15 for $u_o(t)$ yields

$$\dot{V}_a = -\alpha e^T e + \sqrt{\alpha} r^T \Psi_1^T e + r^T \Psi_2 r - r^T \left(K_1 + \frac{\Psi_1^T \Psi_1}{2} + \frac{\Psi_2^T K_1^{-1} \Psi_2}{2} \right) r. \tag{3–25}$$

Applying nonlinear damping to Equation 3–25 yields

$$\begin{aligned} \dot{V}_a = &-\frac{\alpha}{2} e^T e - \frac{1}{2} r^T K_1 r - \frac{1}{2} \left\| \sqrt{\alpha} e - \Psi_1 r \right\|^2 \\ &- \frac{1}{2} r^T \left(K_1 - \Psi_2 \right)^T K_1^{-1} \left(K_1 - \Psi_2 \right) r. \end{aligned} \tag{3–26}$$

The expression in Equation 3–26 can be reduced to

$$\dot{V}_a \leq -\frac{\alpha}{2} e^T e - \frac{1}{2} r^T K_1 r. \tag{3–27}$$

The expressions in Equation 3–18, Equation 3–19, and Equation 3–27 can be used to show that $V_a(e, r, \tilde{\theta}, t) \in \mathcal{L}_\infty$; hence, $e(t)$, $r(t)$, and $\tilde{\theta}(t) \in \mathcal{L}_\infty$. Given that $e(t)$ and $r(t) \in \mathcal{L}_\infty$, standard linear analysis methods can be used to prove that $\dot{e}(t) \in \mathcal{L}_\infty$ (and hence, $e(t)$ is uniformly continuous) from Equation 3–5. Since $e(t)$ and $\dot{e}(t)$, $\in \mathcal{L}_\infty$, the property that $q_d(t)$ and $\dot{q}_d(t)$ exist and are bounded can be used along with Equation 3–4 and Equation 3–5 to conclude that $q(t)$ and $\dot{q}(t) \in \mathcal{L}_\infty$. Since $\tilde{\theta}(t) \in \mathcal{L}_\infty$, the expression in Equation 3–14 can be used to conclude that $\hat{\theta}(t) \in \mathcal{L}_\infty$. Since $\hat{\theta}(t)$, $q(t)$, and $\dot{q}(t) \in \mathcal{L}_\infty$, Property 3.1 can be used to conclude that $\hat{M}(q)$, $\hat{V}_m(q, \dot{q})$, and $\hat{G}(q) \in \mathcal{L}_\infty$. Since $\hat{M}(q)$, $\hat{V}_m(q, \dot{q})$, and $\hat{F}_d \in \mathcal{L}_\infty$, Equation 3–16 and Equation 3–17 can be used to concluded $\Psi_1(t)$ and $\Psi_2(t) \in \mathcal{L}_\infty$. Since $\Psi_1(t)$, $\Psi_2(t)$, and $r(t) \in \mathcal{L}_\infty$, Equation 3–15 can be used to conclude that $u_o(t) \in \mathcal{L}_\infty$. Since $q(t)$, $\dot{q}(t)$, $e(t)$, and $\dot{e}(t) \in \mathcal{L}_\infty$, Property 3.1, Property 3.2, Property 3.3, Equation 3–8, and Equation 3–9, can be used to conclude that $Y_1(t)$ and $Y_2(t) \in \mathcal{L}_\infty$. Since $Y_2(t)$ and $\hat{\theta}(t) \in \mathcal{L}_\infty$, the expression in Equation 3–10 can be used to concluded that $u_f(t) \in \mathcal{L}_\infty$. Since $u_f(t)$ and $u_o(t) \in \mathcal{L}_\infty$, the expression Equation 3–11 can be used to concluded that $u(t) \in \mathcal{L}_\infty$. Since $q(t)$, $\dot{q}(t)$, $r(t)$, $Y_1(t)$, $Y_2(t)$, and $u(t) \in \mathcal{L}_\infty$, Property 3.1 and Equation 3–7, can be used to conclude that $\dot{r}(t) \in \mathcal{L}_\infty$ (and

hence $r(t)$ is uniformly continuous). Due to the fact that $e(t)$ and $r(t) \in \mathcal{L}_2$ and uniformly continuous, Barbalat's Lemma can be used to conclude that $\|e(t)\|$ and $\|r(t)\| \to 0$ as $t \to \infty$.

3.4 Cost Functional Minimization

The ability of the controller to minimize a meaningful cost can be examined through the following theorem.

Theorem 3.2: The feedback law given by

$$u_o^* = -\beta R^{-1} r, \tag{3–28}$$

with the scalar gain constant selected as $\beta \geq 2$, and the adaptive update law given in Equation 3–12, minimizes the meaningful cost functional

$$J = \lim_{t \to \infty} \left\{ \beta \tilde{\theta}^T(t) \Gamma^{-1} \tilde{\theta}(t) + \int_0^t \left(l + u_o^T R u_o \right) \quad d\sigma \right\}, \tag{3–29}$$

where $l\left(x, \hat{\theta}\right) \in \mathbb{R}$ is determined to be

$$l = -2\beta \left[e^T \dot{e} + r^T Y_1 \hat{\theta} \right] + \beta^2 r^T R^{-1} r, \tag{3–30}$$

for the system given in Equation 3–13.

Proof: The cost function in Equation 3–29 is considered to be meaningful if it is a positive function of the control and the states. From Equation 3–29, the cost function is a positive function if $l\left(x, \hat{\theta}\right)$ in Equation 3–30 is positive. To examine the sign of $l\left(x, \hat{\theta}\right)$, the expressions in Equation 3–15, Equation 3–22, and Equation 3–27 are used to determine that

$$e^T \dot{e} + r^T Y_1 \hat{\theta} - r^T R^{-1} r \leq -\frac{\alpha}{2} e^T e - \frac{1}{2} r^T K_1 r. \tag{3–31}$$

Multiplying both sides by -2β yields

$$-2\beta \left[e^T \dot{e} + r^T Y_1 \hat{\theta} - r^T R^{-1} r \right] \geq 2\beta \left[\frac{\alpha}{2} e^T e + \frac{1}{2} r^T K_1 r \right]. \tag{3–32}$$

The expression in Equation 3–32 can be rewritten as

$$\begin{aligned} -2\beta\left[e^T\dot{e}+r^TY_1\hat{\theta}-r^TR^{-1}r\right]+\beta\left(\beta-2\right)r^TR^{-1}r \\ \geq 2\beta\left[\frac{\alpha}{2}e^Te+\frac{1}{2}r^T\beta r\right]+\beta\left(\beta-2\right)r^TR^{-1}r. \end{aligned} \tag{3–33}$$

Based on Equation 3–30, the expression in Equation 3–33 can be simplified as

$$l \geq 2\beta\left[\frac{\alpha}{2}e^Te+\frac{1}{2}r^Tr\right]+\beta\left(\beta-2\right)r^TR^{-1}r. \tag{3–34}$$

The inequality in Equation 3–34 indicates that $l\left(x,\hat{\theta}\right)$ is positive since $R\left(t\right)$ is positive definite and $\beta \geq 2$. Therefore $J\left(t\right)$ is a meaningful cost; penalizing $e\left(t\right)$, $r\left(t\right)$, and the actuation.

To show that $u_o^*\left(t\right)$ minimizes $J\left(t\right)$, the auxiliary signal $v\left(t\right) \in \mathbb{R}^n$ is defined as

$$v = u_o + \beta R^{-1}r. \tag{3–35}$$

Substituting Equation 3–30 and Equation 3–35 into Equation 3–29 yields

$$\begin{aligned} J = \lim_{t\to\infty}\Bigg\{\beta\tilde{\theta}^T\left(t\right)\Gamma^{-1}\tilde{\theta}\left(t\right)+\int_0^t \beta^2r^TR^{-1}r-2\beta\left[e^T\dot{e}+r^TY_1\hat{\theta}\right]\quad d\sigma \\ +\int_0^t\left(v-\beta R^{-1}r\right)^TR\left(v-\beta R^{-1}r\right)\quad d\sigma\Bigg\}. \end{aligned} \tag{3–36}$$

After adding and subtracting the integral of $2\beta r^TY_2\tilde{\theta}$ and $2\beta r^Tu_o$ and using Equation 3–14 and Equation 3–35, the expression in Equation 3–36 can be written as

$$\begin{aligned} J = \lim_{t\to\infty}\Bigg\{\beta\tilde{\theta}^T\left(t\right)\Gamma^{-1}\tilde{\theta}\left(t\right)+\int_0^t v^TRv\ \ d\sigma+2\beta\int_0^t \beta r^TR^{-1}r-v^Tr\ \ d\sigma \\ +2\beta\int_0^t r^T\left(v-\beta R^{-1}r\right)\quad d\sigma-2\beta\int_0^t e^T\dot{e}+r^T\left[Y_1\theta+Y_2\tilde{\theta}+u_o\right]\quad d\sigma \\ +2\beta\int_0^t r^T\left(Y_1+Y_2\right)\tilde{\theta}\ \ d\sigma\Bigg\}. \end{aligned} \tag{3–37}$$

Canceling common terms, and using Equation 3–20, the expression in Equation 3–37 can be simplified as

$$J = \lim_{t\to\infty} \left\{ \beta\tilde{\theta}^T(t)\Gamma^{-1}\tilde{\theta}(t) + \int_0^t v^T R v \ \ d\sigma - 2\beta \int_0^t \dot{V}_a + \tilde{\theta}^T\Gamma^{-1}\dot{\hat{\theta}} \ \ d\sigma \right. \tag{3–38}$$
$$\left. + 2\beta \int_0^t r^T (Y_1 + Y_2)\tilde{\theta} \ \ d\sigma \right\}.$$

Substituting Equation 3–12 into Equation 3–38 yields

$$J = \lim_{t\to\infty} \left\{ \beta\tilde{\theta}^T(t)\Gamma^{-1}\tilde{\theta}(t) + \int_0^t v^T R v \ \ d\sigma \right. \tag{3–39}$$
$$\left. -2\beta \int_0^t \dot{V} + \frac{d}{dt}\left(\frac{1}{2}\tilde{\theta}^T\Gamma^{-1}\tilde{\theta}\right) \ \ d\sigma \right\}.$$

After integrating Equation 3–39, $J(t)$ can be expressed as

$$J = \beta\tilde{\theta}^T(0)\Gamma^{-1}\tilde{\theta}(0) + 2\beta V(0) + \lim_{t\to\infty} \left\{ -2\beta V(T) + \int_0^t v^T R v \ \ d\sigma \right\}.$$

By substituting Equation 3–28 into Equation 3–24 it is trivial to show that $u_o^*(t)$ stabilizes the system. Based on the analysis in Section 3.3, $\|e(t)\|$ and $\|r(t)\| \to 0$ as $t \to \infty$. Therefore, $V(t) \to 0$ as $t \to \infty$ and $J(t)$ is minimized if $v(t) = 0$. Therefore, the control law $u_o(t) = u_o^*(t)$ is optimal and minimizes the cost functional Equation 3–29.

3.5 Simulation and Experimental Results

3.5.1 Simulation

To examine the performance of the controller in Equation 3–11 a numerical simulation was performed. The simulation is based on the dynamics for a two-link robot given in Equation 2–95 with no disturbance $\tau_d(t)$. The desired trajectory is given as

$$q_{d_1} = q_{d_2} = \frac{1}{2}\sin(2t), \tag{3–40}$$

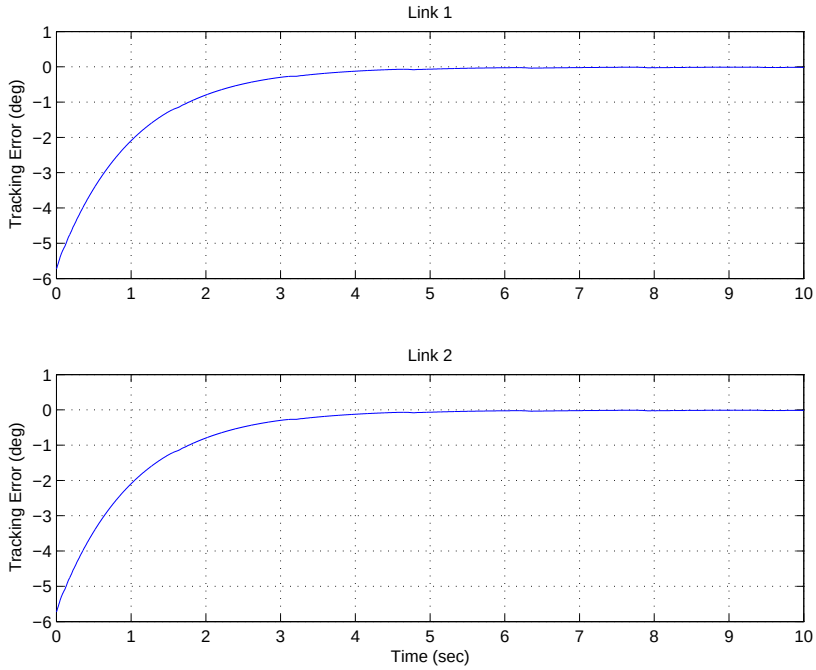

Figure 3-1. The simulated tracking errors for the adaptive inverse optimal controller.

and the initial conditions of the robot were selected as

$$q_1(0) = q_2(0) = 5.72\ deg$$

$$\dot{q}_1(0) = \dot{q}_2(0) = 51.56\ deg/\sec .$$

The control gains were selected as

$$\alpha = 1 \qquad K_1 = 5I_2 \qquad \Gamma = 5000I_5$$

$$\beta = 2.$$

The tracking errors and control torques are shown in Figure 3-1 and Figure 3-2, respectively. Figure 3-1 shows that the errors asymptotically converge to zero, while Figure 3-2 shows the bounded input torque. The estimates for θ are shown in Figure 3-3. Figure 3-4 indicates that $l\left(x, \hat{\theta}\right)$ is positive, and Figure 3-5 indicates that the cost is meaningful.

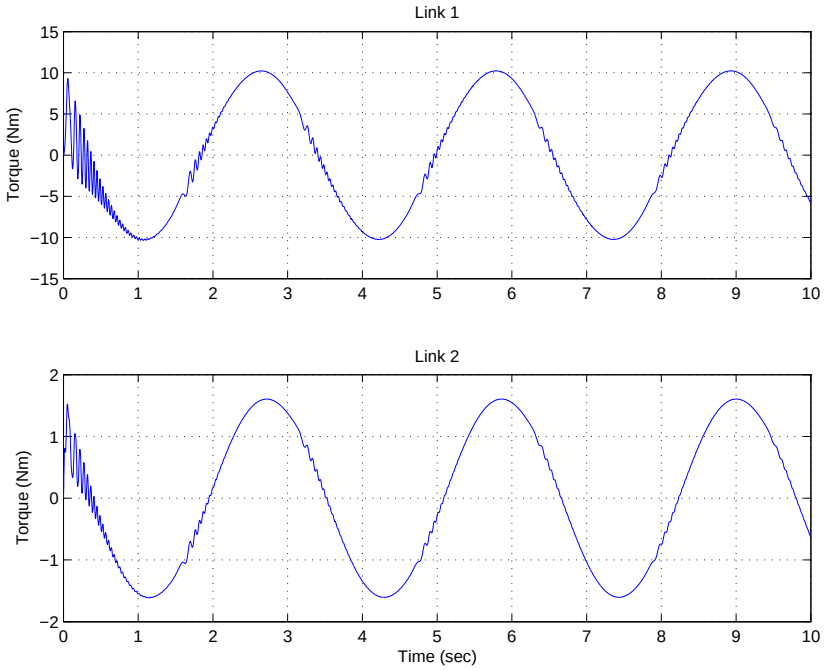

Figure 3-2. The simulated torques for the adaptive inverse optimal controller.

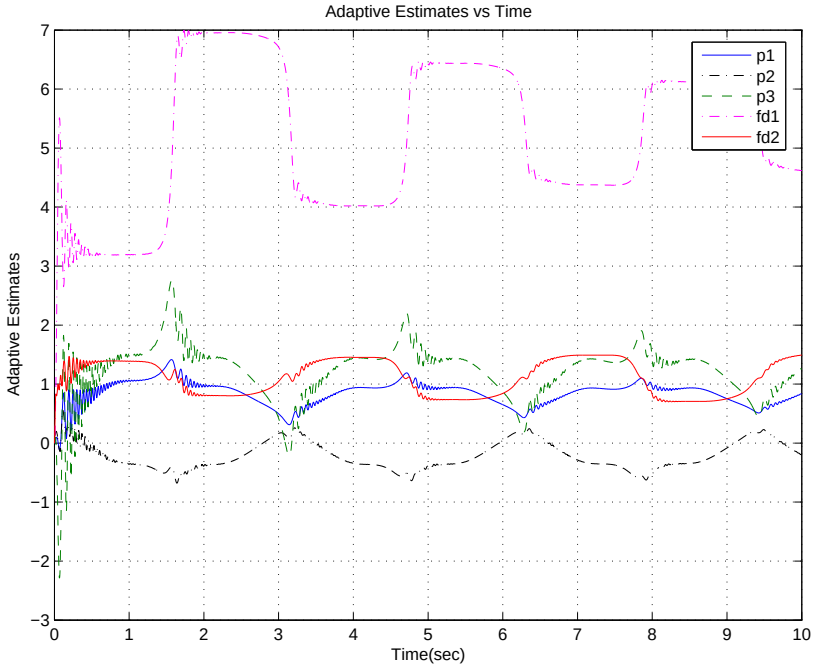

Figure 3-3. Unknown system parameter estimates for the adaptive inverse optimal controller.

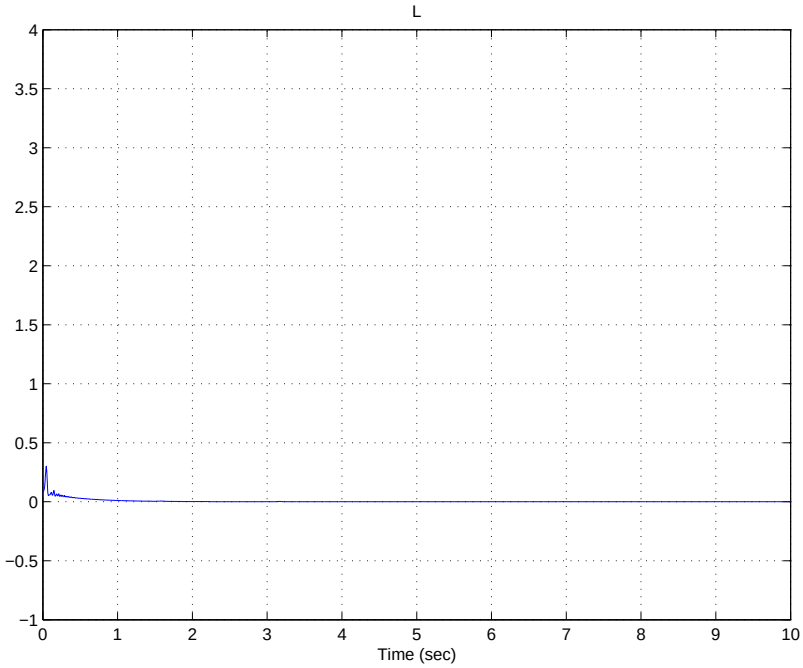

Figure 3-4. The value of $l\left(x,\hat{\theta}\right)$ from Equation 3–30.

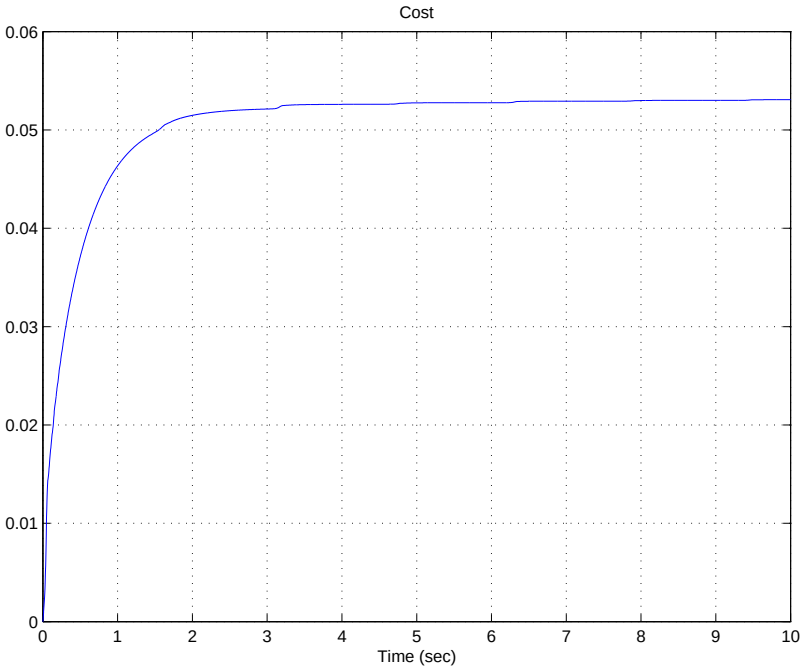

Figure 3-5. The integral part of the cost functional in Equation 3–29.

3.5.2 Experiment

To test the validity of the controller proposed in Equation 3–11 an experiment was performed on the two-link robot testbed as described Section 2.9. The control objective is to track the desired time-varying trajectory by using the developed adaptive inverse optimal control law. To achieve this control objective, the control gains α, defined as a scalar in Equation 3–5 was implemented (with non-consequential implications to the stability result) as diagonal gain matrices. Specifically, the control gains were selected as

$$\begin{gathered} \alpha = diag\left\{1.6,\ .9\right\} \quad K_1 = diag\left\{55,\ 10\right\} \\ \beta = 4, \end{gathered} \tag{3–41}$$

and the adaptation gains were selected as

$$\Gamma = diag\left([5, 5, 5, 5, 5]\right).$$

The desired trajectories for this experiment were chosen as follows:

$$q_{d_1} = q_{d_2} = 60\sin(2t)\left(1 - \exp\left(-0.01t^3\right)\right). \tag{3–42}$$

The experiment was run a second time with a slower desired trajectory, chosen as follows:

$$q_{d_1} = q_{d_2} = 60\sin(0.5t)\left(1 - \exp\left(-0.01t^3\right)\right). \tag{3–43}$$

For this trajectory β was set equal to 5.5. Data from the experiments is displayed in Table 3-1.

Figure 3-6 and Figure 3-7 depict the tracking errors and control torques for one experimental trial for the adaptive inverse optimal controller for the trajectory given in Equation 3–42. Figure 3-8 and Figure 3-9 depict the tracking errors and control torques for one experimental trial for the adaptive inverse optimal controller for the trajectory given in Equation 3–43.

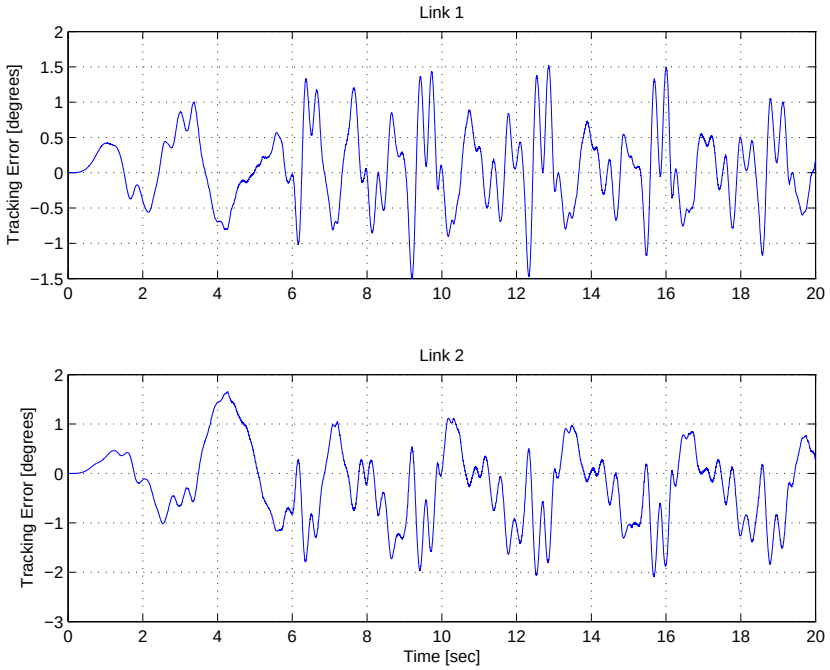

Figure 3-6. Tracking errors resulting from implementing the adaptive inverse optimal controller.

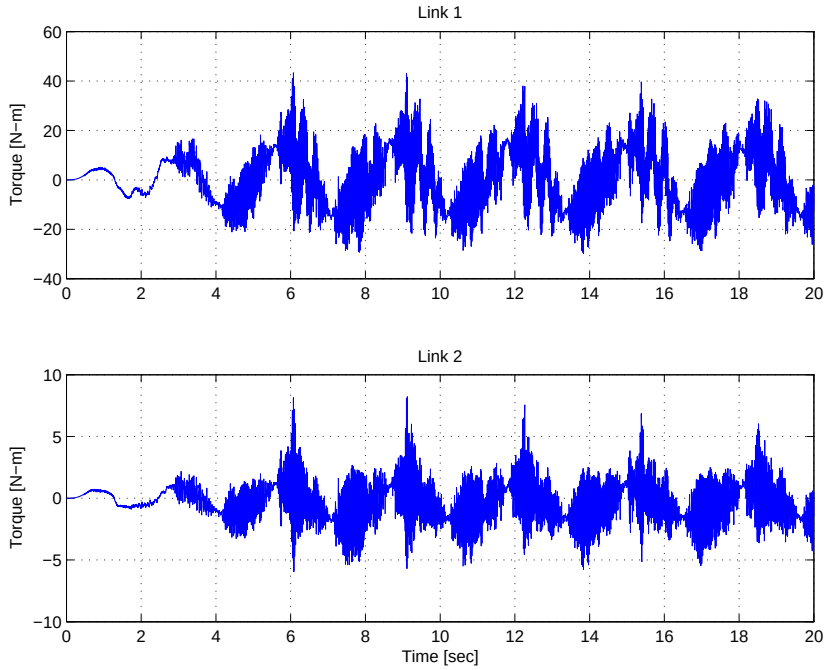

Figure 3-7. Torques resulting from implementing the adaptive inverse optimal controller.

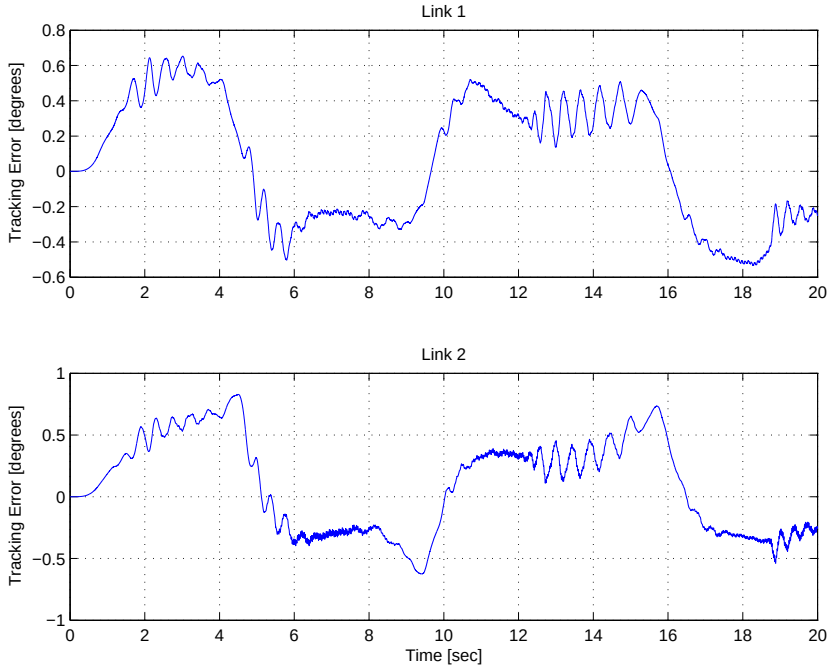

Figure 3-8. Tracking errors resulting from implementing the adaptive inverse optimal controller for a slower trajectory.

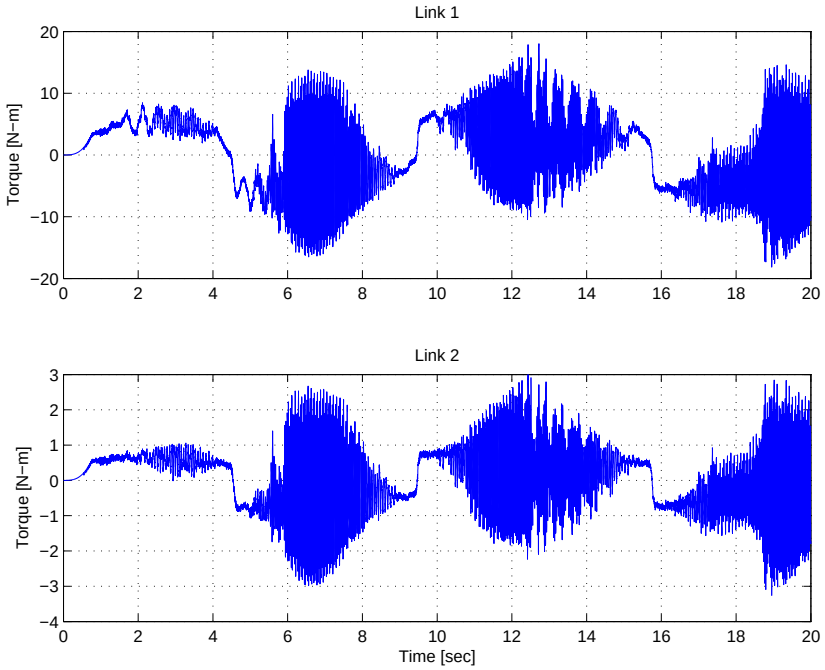

Figure 3-9. Torques resulting from implementing the adaptive inverse optimal controller for a slower trajectory.

Table 3-1. Tabulated values for the adaptive inverse optimal controller

	Trajectory in Equation 3–42	Trajectory in Equation 3–43
Max Steady State Error (deg)- Link 1	1.5213	0.5337
Max Steady State Error (deg)- Link 2	2.0865	0.7342
RMS Error (deg) - Link 1	0.5553	0.3605
RMS Error (deg) - Link 2	0.8176	0.3954
RMS Torque (Nm) - Link 1	11.4267	6.0446
RMS Torque (Nm) - Link 2	1.5702	0.9610

3.5.3 Discussion

This controller had maximum steady state errors (defined as the last 10 seconds of the experiment) on the order 1.5 degrees for the first link and 2 degrees for the second link, well above the errors in Section 2.9. In an effort to reduce the errors the frequency of the trajectory was reduced, and β was increased. These modifications resulted in sub-degree tracking, still approximately 10 times greater than the controllers discussed in Section 2.9. The reason was due to the α gain. The α gain in Equation 3–5, tends to be one of the most important tuning gains. It behaves like the proportional gain in a PID controller. Increasing α tends to result in faster convergence and reduced steady state error. In this case, α appears in other terms besides Equation 3–5. In Equation 3–15, α appears to the third power. The α terms in Equation 3–15 are then multiplied by $r(t)$ in Equation 3–15 which results in α to the third power multiplied by $\dot{e}(t)$ and α to the forth power multiplied by $e(t)$. So an α of 10, which generally would not be unreasonable, would result in a gain of $1,000$ multiplied by a velocity error and $10,000$ multiplied by a position error. This makes the controller very sensitive to noise and fast trajectories, as well as difficult to implement due to large torques. To do so, the value of α had to be decreased, which resulted in poor tracking performance. Some solutions to this would be to alter the controller design to reduce the power of α, as well as to eliminate the need for velocity measurements which would mitigate the effect noisy measurements has on the

controller. This experiment was only run once because there was no need to demonstrate repeatability.

CHAPTER 4
INVERSE OPTIMAL CONTROL OF A NONLINEAR EULER-LAGRANGE SYSTEM USING OUTPUT FEEDBACK

In this chapter, an adaptive output feedback inverse optimal controller is designed. Output feedback based controllers are more desirable than full-state feedback controllers, because the necessary sensors for full-state feedback may not always be available, and using numerical differentiation to obtain velocities can be problematic if position measurements are noisy. Using the error system developed in (31–34), an adaptive output feedback IOC is developed based on the theoretical foundation presented in (22; 25; 40). The developed controller minimizes a meaningful performance index (i.e., a positive function of the states and control input) as the generalized coordinates of a nonlinear Euler-Lagrange system globally asymptotically track a desired time-varying trajectory despite LP uncertainty in the dynamics. Like the previously developed controller, the considered class of systems does not adhere to the model given in Equation 3–1. A Lyapunov analysis is provided to prove the stability of the developed controller and to determine a meaningful cost functional. Experimental results are included to illustrate the performance of the controller.

The remainder of this chapter is organized as follows. In Section 4.1, the model is given along with several of its properties. In Section 4.2, the control objective is stated and an error system is formulated. In Section 4.3, the stability of the controller is proven. In Section 4.4, a meaningful cost is developed and shown to be minimized by the control. In Section 4.5, it is shown how the controller can be implemented using only position measurements. In Section 4.6, experimental results are presented.

4.1 Dynamic Model and Properties

The class of nonlinear dynamic systems considered in this chapter is assumed to follow the model given in Equation 3–2. In addition to Properties 2.1, 2.2, 2.3, 3.1, 3.2, and 3.4, the following property will be exploited in the subsequent development.

Property 4.1: The desired trajectory is assumed to be designed such that $q_d(t)$, $\dot{q}_d(t)$, $\ddot{q}_d(t)$, and $\dddot{q}_d(t) \in \mathbb{R}^n$ exist, and are bounded.

Property 4.2: The centripetal-Coriolis matrix satisfies the following relationship:

$$V_m(q,\xi)\, v = V_m(q,v)\, \xi \qquad \forall \xi, v \in \mathbb{R}^n.$$

Property 4.3: There exists a positive scalar constant $\zeta_v \in \mathbb{R}$ such that:

$$\|V_m(q,\dot{q})\| \leq \zeta_v \|\dot{q}\|.$$

To aid the subsequent control design and analysis, the vector function $Tanh(\cdot) \in \mathbb{R}^n$ and the matrix function $Cosh(\cdot) \in \mathbb{R}^{n\times n}$ are defined as follows:

$$Tanh(\xi) = \left[\begin{array}{ccc} \tanh(\xi_1), & \cdots, & \tanh(\xi_n) \end{array} \right]^T,$$

and

$$Cosh(\xi) = diag\left\{ \begin{array}{ccc} \cosh(\xi_1), & \cdots, & \cosh(\xi_n) \end{array} \right\},$$

where $\xi = [\xi_1, ..., \xi_n]^T \in \mathbb{R}^n$; and $diag\{\cdot\}$ denotes the operation of forming a matrix with zeros everywhere except for the main diagonal.

Assumption 4.1: The positive constants ζ_m, ζ_g, and ζ_{c2} are assumed to exist for all $\xi, v \in \mathbb{R}^n$ such that (31)

$$\begin{aligned} \|M(\xi) - M(v)\| &\leq \zeta_m \|Tanh(\xi - v)\|, \\ \|G(\xi) - G(v)\| &\leq \zeta_g \|Tanh(\xi - v)\|, \\ \|V_m(\xi,\dot{q}) - V_m(v,\dot{q})\| &\leq \zeta_{c2} \|\dot{q}\| \|Tanh(\xi - v)\|. \end{aligned} \tag{4–1}$$

4.2 Control Development

As in the previous chapters, the control objective is to ensure that the generalized coordinates of a system track a desired time-varying trajectory despite uncertainties in the dynamic model, while minimizing a performance index. To quantify the tracking objective,

a position tracking error denoted by $e(t) \in \mathbb{R}^n$, is defined as

$$e \triangleq q_d - q. \tag{4–2}$$

To facilitate the subsequent control design and stability analysis, a filtered tracking error, denoted by $\eta(t) \in \mathbb{R}^n$, is defined as (31; 47)

$$\eta = \dot{e} + \alpha_1 Tanh(e) + \alpha_2 Tanh(e_f), \tag{4–3}$$

where α_1, $\alpha_2 \in \mathbb{R}$ are positive, constant gains, and $e_f(t) \in \mathbb{R}^n$ is an auxiliary filter variable designed as (31; 47)

$$\dot{e}_f = -\alpha_3 Tanh(e_f) + \alpha_2 Tanh(e) - k_1 Cosh^2(e_f)\eta \tag{4–4}$$

$$e_f(0) = 0,$$

where $k_1 \in \mathbb{R}$ is a positive constant control gain, and $\alpha_3 \in \mathbb{R}$ is a positive constant filter gain. The subsequent development exploits the hyperbolic filter structure developed in (47) and (31) to overcome the problem of injecting higher order terms in the controller and to facilitate the development of sufficient gain conditions used in the subsequent stability analysis. By taking the time derivative of $\eta(t)$ and premultipling by $M(q)$ the following open-loop error system can be obtained:

$$M(q)\dot{\eta} = M(q)\ddot{e} + \alpha_1 M(q) Cosh^{-2}(e)\dot{e} + \alpha_2 M(q) Cosh^{-2}(e_f)\dot{e}_f. \tag{4–5}$$

After utilizing Equation 4–2 - Equation 4–4, the expression in Equation 4–5, can be rewritten as

$$\begin{aligned} M(q)\dot{\eta} = {} & M(q)(\ddot{q}_d - \ddot{q}) - \alpha_2 k_1 M(q) Cosh^{-2}(e_f) Cosh^2(e_f)\eta \\ & + \alpha_1 M(q) Cosh^{-2}(e)(\eta - \alpha_1 Tanh(e) - \alpha_2 Tanh(e_f)) \\ & + \alpha_2 M(q) Cosh^{-2}(e_f)(-\alpha_3 Tanh(e_f) + \alpha_2 Tanh(e)). \end{aligned}$$

Substituting the dynamics in Equation 3–2 for $M(q)\ddot{q}(t)$ yields

$$\begin{aligned} M(q)\dot{\eta} = M(q)\ddot{q}_d - V_m(q,\dot{q})\eta - \alpha_2 k_1 M(q)\eta + F_d\dot{q} + G(q) \\ + \alpha_1 M(q) Cosh^{-2}(e)(\eta - \alpha_1 Tanh(e) - \alpha_2 Tanh(e_f)) \\ + \alpha_2 M(q) Cosh^{-2}(e_f)(-\alpha_3 Tanh(e_f) + \alpha_2 Tanh(e)) \\ + V_m(q,\dot{q})(\dot{q}_d + \alpha_1 Tanh(e) + \alpha_2 Tanh(e_f)) - u. \end{aligned} \tag{4–6}$$

After utilizing Property 4.2 the expression in Equation 4–6 can be expressed as

$$M(q)\dot{\eta} = -V_m(q,\dot{q})\eta - \alpha_2 k_1 M(q)\eta + \chi + Y_d\theta + \tilde{Y} - u, \tag{4–7}$$

where $\chi(e, e_f, \eta, t) \in \mathbb{R}^n$ and $\tilde{Y}(e, e_f, \eta, t) \in \mathbb{R}^n$ are defined as

$$\begin{aligned} \chi = \alpha_1 M(q) Cosh^{-2}(e)(\eta - \alpha_1 Tanh(e) - \alpha_2 Tanh(e_f)) \\ + \alpha_2 M(q) Cosh^{-2}(e_f)(-\alpha_3 Tanh(e_f) + \alpha_2 Tanh(e)) \\ + V_m(q, \dot{q}_d + \alpha_1 Tanh(e) + \alpha_2 Tanh(e_f))(\alpha_1 Tanh(e) + \alpha_2 Tanh(e_f)) \\ + V_m(q,\dot{q}_d)(\alpha_1 Tanh(e) + \alpha_2 Tanh(e_f)) \\ - V_m(q,\eta)(\dot{q}_d + \alpha_1 Tanh(e) + \alpha_2 Tanh(e_f)), \end{aligned} \tag{4–8}$$

and

$$\tilde{Y} = M(q)\ddot{q}_d + V_m(q,\dot{q}_d)\dot{q}_d + G(q) + F_d\dot{q} - Y_d\theta \tag{4–9}$$

$$Y_d\theta = M(q_d)\ddot{q}_d + V_m(q_d,\dot{q}_d)\dot{q}_d + G(q_d) + F_d\dot{q}_d. \tag{4–10}$$

By exploiting the fact that the desired trajectory is bounded, and using Properties 2.1, 3.1, 4.3, and the properties of hyperbolic functions, $\chi(e, e_f, \eta, t)$ of Equation 4–8 can be upper bounded as

$$\|\chi\| \leq \zeta_1 \|x\|, \tag{4–11}$$

where $\zeta_1 \in \mathbb{R}$ is some positive bounding constant that depends on the mechanical parameters and the desired trajectory, and $x \in \mathbb{R}^{3n}$ is defined as

$$x = \begin{bmatrix} Tanh\left(e\right)^T & Tanh\left(e_f\right)^T & \eta \end{bmatrix}^T.$$

Furthermore, by utilizing the fact that the desired trajectory is bounded and Assumption 4.1, it can be shown that $\tilde{Y}\left(e, e_f, \eta, t\right)$ of Equation 4–9 can be upper bounded as

$$\left\| \tilde{Y} \right\| \leq \zeta_2 \left\| x \right\|, \tag{4–12}$$

where $\zeta_2 \in \mathbb{R}$ is also some positive bounding constant that depends on the mechanical parameters and the desired trajectory. The terms in Equation 4–9 and Equation 4–10 are developed to facilitate the development of the optimal control law. Although both terms contain the same unknown parameters, Equation 4–10 depends purely on the desired trajectory, while Equation 4–9 depends on the actual current trajectory. Based on the segregation of these two terms, the total control $u(t)$ is made up of two parts: $u_f(t)$ and $u_o(t)$. The feedforward control term $u_f(t)$ is based on Equation 4–10 and is independent of the state of the system and therefore the optimization.. The feedback law $u_o(t)$ is based on Equation 4–9 and the open-loop error system and is later shown to minimize a meaningful cost (i.e., a cost that puts a positive penalty on the states and actuation). The total control is defined as

$$u_f = Y_d \hat{\theta} \tag{4–13}$$

$$u = u_f - u_o = Y_d \hat{\theta} - u_o, \tag{4–14}$$

where u_o, $u_f \in \mathbb{R}^n$, and $\hat{\theta}\left(t\right) \in \mathbb{R}^p$ is an estimate for θ. The parameter estimate $\hat{\theta}\left(t\right)$ in Equation 4–13 and Equation 4–14 is generated by the adaptive update law

$$\dot{\hat{\theta}} = \Gamma Y_d^T \eta, \tag{4–15}$$

where $\Gamma \in \mathbb{R}^{p\times p}$ is a constant, positive definite, symmetric, gain matrix. Substituting Equation 4–14 into Equation 4–7 yields

$$M\left(q\right)\dot{\eta} = -V_m\left(q,\dot{q}\right)\eta - \alpha_2 k_1 M\left(q\right)\eta + \chi + Y_d\tilde{\theta} + \tilde{Y} + u_o, \tag{4–16}$$

where the parameter estimate error $\tilde{\theta}\left(t\right) \in \mathbb{R}^p$ is defined as

$$\tilde{\theta} = \hat{\theta} - \theta. \tag{4–17}$$

Based on Equation 4–16 and the subsequent stability analysis, the control input $u_o\left(t\right)$ is designed as

$$u_o = R^{-1}Tanh\left(e_f\right) = k_1 Cosh\left(e_f\right)^2 Tanh\left(e_f\right). \tag{4–18}$$

4.3 Stability Analysis

The stability of the controller given in Equation 4–13 - Equation 4–15, and Equation 4–18 can be examined through the following theorem.

Theorem 4.1: The adaptive update law given by Equation 4–15 and the feedback law given by Equation 4–18 ensures global asymptotic tracking of the system in Equation 4–16 in the sense that

$$\|e(t)\| \to 0 \qquad \|\eta(t)\| \to 0 \quad as \quad t \to \infty,$$

provided the control gain k is selected as

$$k_1 = \frac{1}{\alpha_2 m_1}\left(1 + k_2\left(\zeta_1 + \zeta_2 + 1\right)^2\right), \tag{4–19}$$

where m_1, ζ_1, and ζ_1 are constants defined in Equation 2–2, Equation 4–11, and Equation 4–12, respectively, and $k_2 \in \mathbb{R}$ is a control gain that must satisfy the following sufficient condition:

$$k_2 > \frac{1}{4\lambda_1}, \tag{4–20}$$

where $\lambda_1 \in \mathbb{R}$ is defined as follows:

$$\lambda_1 = \min \left\{ \begin{array}{ccc} 1 & \alpha_1 & \alpha_3 \end{array} \right\}.$$

Proof: Let $V_a(e, r, \tilde{\theta}, t) \in \mathbb{R}$ denote a positive definite, radially unbounded function defined as

$$V_a = V + \frac{1}{2}\tilde{\theta}^T \Gamma^{-1} \tilde{\theta}, \tag{4–21}$$

where $V(e, r, t) \in \mathbb{R}$ is defined as

$$V = \sum_{i=1}^{n} \ln\left(\cosh\left(e_i\right)\right) + \sum_{i=1}^{n} \ln\left(\cosh\left(e_{f_i}\right)\right) + \frac{1}{2}\eta^T M\left(q\right)\eta, \tag{4–22}$$

where $e_i\left(t\right) \in \mathbb{R}$ and $e_{f_i}\left(t\right) \in \mathbb{R}$ are the i^{th} elements of the $e\left(t\right)$ and $e_f\left(t\right)$ vectors respectively. After using Equation 4–16 and Property 2.3, the time derivative of Equation 4–21 is

$$\begin{aligned} \dot{V}_a = & Tanh\left(e\right)^T \dot{e} + Tanh\left(e_f\right)^T \dot{e}_f - \tilde{\theta}^T \Gamma^{-1} \dot{\hat{\theta}} \\ & + \eta^T \left[-\alpha_2 k_1 M\left(q\right)\eta + \chi + Y_d \tilde{\theta} + \tilde{Y}\right] + \eta^T u_0. \end{aligned} \tag{4–23}$$

After substituting the adaptive update law in Equation 4–15 the expression in Equation 4–23 reduces to

$$\dot{V}_a = Tanh\left(e\right)^T \dot{e} + Tanh\left(e_f\right)^T \dot{e}_f + \eta^T u_0 + \eta^T \left[-\alpha_2 k_1 M\left(q\right)\eta + \chi + \tilde{Y}\right]. \tag{4–24}$$

After substituting Equation 4–3 and Equation 4–4, Equation 4–24 can be expressed as

$$\begin{aligned} \dot{V}_a = & -\alpha_1 Tanh\left(e\right)^T Tanh\left(e\right) - \alpha_3 Tanh\left(e_f\right)^T Tanh\left(e_f\right) \\ & + \eta^T Tanh\left(e\right) - \eta^T \alpha_2 k_1 M\left(q\right)\eta + \eta^T \left[\chi + \tilde{Y}\right] \\ & - k_1 Tanh\left(e_f\right)^T Cosh^2(e_f)\eta + \eta^T u_o. \end{aligned} \tag{4–25}$$

After using Equation 4–11, Equation 4–12, Equation 4–18, and Equation 4–19 the expression in Equation 4–25 can be written as

$$\dot{V}_a \leq -\alpha_1 Tanh\left(e\right)^T Tanh\left(e\right) - \alpha_3 Tanh\left(e_f\right)^T Tanh\left(e_f\right) - \eta^T \eta \\ - \left[k_2 \left(\zeta_1 + \zeta_2 + 1\right)^2 \left\|\eta\right\|^2 - \left(\zeta_1 + \zeta_2 + 1\right) \left\|\eta\right\| \left\|x\right\|\right]. \tag{4–26}$$

After completing the squares on the bracketed term, the expression in Equation 4–26 can be written as

$$\dot{V}_a \leq -\alpha_1 Tanh\left(e\right)^T Tanh\left(e\right) - \eta^T \eta - \alpha_3 Tanh\left(e_f\right)^T Tanh\left(e_f\right) + \frac{\left\|x\right\|^2}{4k_2}. \tag{4–27}$$

The expression in Equation 4–27 can be reduced to

$$\dot{V}_a \leq -\left[\lambda_1 - \frac{1}{4k_2}\right] \left\|x\right\|^2. \tag{4–28}$$

If k_2 is selected according to Equation 4–20, the inequality in Equation 4–28 can be reduced to

$$\dot{V}_a \leq -\lambda_2 \left\|x\right\|^2, \tag{4–29}$$

where $\lambda_2 \in \mathbb{R}$ is a positive constant.

The expressions in Equation 4–21, Equation 4–22, and Equation 4–29 can be used to show that $V_a(e, r, \tilde{\theta}, t) \in \mathcal{L}_\infty$; hence, $e(t)$, $e_f\left(t\right)$, $\eta(t)$, and $\tilde{\theta}(t) \in \mathcal{L}_\infty$. Given that $\eta(t) \in \mathcal{L}_\infty$, Equation 4–3 can be used to prove that $\dot{e}(t) \in \mathcal{L}_\infty$ (and hence, $e(t)$ is uniformly continuous). Since $e(t)$ and $\dot{e}(t)$, $\in \mathcal{L}_\infty$, the property that $q_d(t)$ and $\dot{q}_d(t)$ exist and are bounded can be used along with Equation 4–2 and Equation 4–3 to conclude that $q(t)$ and $\dot{q}(t) \in \mathcal{L}_\infty$. Since $\tilde{\theta}(t) \in \mathcal{L}_\infty$, the expression in Equation 4–17 can be used to conclude that $\hat{\theta}(t) \in \mathcal{L}_\infty$. Since, by the property that, $q_d(t)$, $\dot{q}_d(t)$, and $\ddot{q}_d(t) \in \mathcal{L}_\infty$, Property 3.1 can be used to conclude that $Y_d\left(q_d, \dot{q}_d, \ddot{q}_d\right) \in \mathcal{L}_\infty$. Since $Y_d\left(q_d, \dot{q}_d, \ddot{q}_d\right)$ and $\hat{\theta}(t) \in \mathcal{L}_\infty$, Equation 4–13 can be used to concluded that $u_f\left(t\right) \in \mathcal{L}_\infty$. Since $e_f\left(t\right)$, and $\eta(t)$, $\in \mathcal{L}_\infty$, Equation 4–18 can be used to conclude that $u_o\left(t\right) \in \mathcal{L}_\infty$. Since $u_f\left(t\right)$ and $u_o\left(t\right) \in \mathcal{L}_\infty$, the expression

Equation 4–14 can be used to concluded that $u(t) \in \mathcal{L}_\infty$. Since $q(t)$, $\dot{q}(t)$, $e(t)$, $e_f(t)$, $\eta(t)$, $Y_d(q_d, \dot{q}_d, \ddot{q}_d)$, $\tilde{\theta}(t)$, $u_o(t) \in \mathcal{L}_\infty$, Property 3.1 and Equation 4–16 can be used to conclude that $\dot{\eta}(t) \in \mathcal{L}_\infty$ (and hence $\eta(t)$ is uniformly continuous). Since $e(t)$, $e_f(t)$, and $\eta(t) \in \mathcal{L}_\infty$, Equation 4–4 can be used to conclude that $\dot{e}_f(t) \in \mathcal{L}_\infty$ (and hence $e_f(t)$ is uniformly continuous). From this it can be concluded that $x(t)$, $\dot{x}(t) \in \mathcal{L}_\infty$ (and hence $x(t)$ is uniformly continuous). The expression in Equation 4–29 can be used to concluded that $x(t) \in \mathcal{L}_2$. Barbalat's Lemma can be used to conclude that $\|x(t)\| \to 0$ as $t \to \infty$. Therefore $\|e(t)\|$ and $\|\eta(t)\| \to 0$ as $t \to \infty$.

4.4 Cost Functional Minimization

The ability of the controller to minimize a meaningful cost can be examined through the following theorem.

Theorem 4.2: The feedback law given by

$$u_o = R^{-1} Tanh(e_f), \tag{4–30}$$

and the adaptive update law given in Equation 4–15, minimizes the meaningful cost functional

$$J = \lim_{t \to \infty} \left\{ \tilde{\theta}(t)^T \Gamma^{-1} \tilde{\theta}(t) + \int_0^t l \ d\sigma \right\}, \tag{4–31}$$

where $l\left(x, \hat{\theta}\right) \in \mathbb{R}$ is determined to be

$$\begin{aligned} l = & -2\left[Tanh(e)^T \dot{e} + Tanh(e_f)^T \dot{e}_f\right] - 2\eta^T \left[-\alpha_2 k_1 M(q)\eta + \chi + \tilde{Y}\right] \\ & - 2\left[\dot{e} + \alpha_1 Tanh(e)\right]^T R^{-1} Tanh(e_f) - 2\alpha_2 Tanh(e_f)^T R^{-1} Tanh(e_f), \end{aligned} \tag{4–32}$$

for the system given in Equation 4–16.

Proof: The cost function in Equation 4–31 is considered to be meaningful if it is a positive function of the control and the states. From Equation 4–31, the cost function is a positive function if $l\left(x, \hat{\theta}\right)$ in Equation 4–32 is positive. To examine the sign of $l\left(x, \hat{\theta}\right)$, the expressions in Equation 4–18, Equation 4–24, and Equation 4–29 are used to

determine that

$$-\lambda_2 \|x\|^2 \geq Tanh\left(e\right)^T \dot{e} + Tanh\left(e_f\right)^T \dot{e}_f + \eta^T \left[-\alpha_2 k_1 M\left(q\right)\eta + \chi + \tilde{Y}\right] + \eta^T R^{-1} Tanh(e_f).$$

Substituting Equation 4–3 for $\eta\left(t\right)^T$ yields

$$-\lambda_2 \|x\|^2 \geq Tanh\left(e\right)^T \dot{e} + Tanh\left(e_f\right)^T \dot{e}_f + \eta^T \left[-\alpha_2 k_1 M\left(q\right)\eta + \chi + \tilde{Y}\right] + \left[\dot{e} + \alpha_1 Tanh(e)\right]^T R^{-1} Tanh(e_f) + \alpha_2 Tanh(e_f)^T R^{-1} Tanh(e_f).$$

Multiplying both sides by -2 yields

$$2\lambda_2 \|x\|^2 \leq -2\left[Tanh\left(e\right)^T \dot{e} + Tanh\left(e_f\right)^T \dot{e}_f\right] - 2\eta^T \left[-\alpha_2 k_1 M\left(q\right)\eta + \chi + \tilde{Y}\right] - 2\left[\dot{e} + \alpha_1 Tanh(e)\right]^T R^{-1} Tanh(e_f) - 2\alpha_2 Tanh(e_f)^T R^{-1} Tanh(e_f). \tag{4–33}$$

Based on Equation 4–32, the expression in Equation 4–33 can be simplified as

$$2\lambda_2 \|x\|^2 \leq l. \tag{4–34}$$

The inequality in Equation 4–34 indicates that $l\left(x, \hat{\theta}\right)$ is positive. Therefore $J\left(t\right)$ is a meaningful cost; penalizing $e\left(t\right)$, $\eta\left(t\right)$, $e_f\left(t\right)$, and hence, the control.

To show that $u_o\left(t\right)$ minimizes $J\left(t\right)$, Equation 4–32 is substituted into Equation 4–31 yielding

$$J = \lim_{t\to\infty} \left\{ \tilde{\theta}^T\left(t\right)\Gamma^{-1}\tilde{\theta}\left(t\right) - 2\int_0^t Tanh\left(e\right)^T \dot{e} + Tanh\left(e_f\right)^T \dot{e}_f + \eta^T \left[-\alpha_2 k_1 M\left(q\right)\eta + \chi + \tilde{Y}\right] \; d\sigma - 2\int_0^t \left[\dot{e} + \alpha_1 Tanh(e)\right]^T R^{-1} Tanh(e_f) + \alpha_2 Tanh(e_f)^T R^{-1} Tanh(e_f) \; d\sigma \right\}. \tag{4–35}$$

After adding and subtracting the integral of $2\eta^T Y_d \tilde{\theta}$, and substituting for $u_o(t)$, the expression in Equation 4–35 can be written as

$$J = \lim_{t\to\infty} \left\{ \tilde{\theta}^T(t)\,\Gamma^{-1}\tilde{\theta}(t) + 2\int_0^t \eta^T Y_d \tilde{\theta}\ d\sigma \right. \tag{4–36}$$
$$- 2\int_0^t Tanh(e)^T \dot{e} + Tanh(e_f)^T \dot{e}_f + \eta^T \left[-\alpha_2 k_1 M(q)\,\eta + \chi + \tilde{Y} + Y_d\tilde{\theta} \right]\ d\sigma$$
$$\left. - 2\int_0^t \left[\dot{e} + \alpha_1 Tanh(e)\right]^T R^{-1} Tanh(e_f) + \alpha_2 Tanh(e_f)^T u_o\ d\sigma \right\}.$$

Using Equation 4–3 and Equation 4–18, the expression in Equation 4–36 can be simplified as

$$J = \lim_{t\to\infty} \left\{ \tilde{\theta}^T(t)\,\Gamma^{-1}\tilde{\theta}(t) + 2\int_0^t \eta^T Y_d \tilde{\theta}\ d\sigma \right. \tag{4–37}$$
$$\left. - 2\int_0^t Tanh(e)^T \dot{e} + Tanh(e_f)^T \dot{e}_f + \eta^T \left[-\alpha_2 k_1 M(q)\,\eta + \chi + \tilde{Y} + Y_d\tilde{\theta} + u_o \right]\ d\sigma \right\}.$$

After using Equation 4–23, the expression in Equation 4–37 can be simplified to

$$J = \lim_{t\to\infty} \left\{ \tilde{\theta}^T(t)\,\Gamma^{-1}\tilde{\theta}(t) - 2\int_0^t \dot{V}_a + \tilde{\theta}^T\Gamma^{-1}\dot{\hat{\theta}} - \eta^T Y_d\tilde{\theta}\ d\sigma \right\}. \tag{4–38}$$

After using Equation 4–15, the expression in Equation 4–38 can be written as

$$J = \lim_{t\to\infty} \left\{ \tilde{\theta}^T(t)\,\Gamma^{-1}\tilde{\theta}(t) - 2\int_0^t \dot{V} + \frac{d}{dt}\left(\frac{1}{2}\tilde{\theta}^T\Gamma^{-1}\tilde{\theta}\right)\ d\sigma \right\}. \tag{4–39}$$

After integrating Equation 4–39, the cost functional can be expressed as

$$J = \tilde{\theta}^T(0)\,\Gamma^{-1}\tilde{\theta}(0) + 2V(0) + \lim_{t\to\infty}\{-2V(t)\}.$$

From the analysis in Section 4.3, $\|e(t)\|$ and $\|\eta(t)\| \to 0$ as $t \to \infty$. Therefore, $V(t) \to 0$ as $t \to \infty$, and $J(t)$ is minimized. Therefore, the control law $u_o(t)$ is optimal and minimizes the cost functional Equation 4–31.

4.5 Output Feedback Form of the Controller

To show that the control law proposed Equation 4–18 only requires position measurements, it is noted that the control input does not actually require the computation

of $e_f(t)$; rather, only $Tanh(e_f)$ and $Cosh^2(e_f)$. Let $y_i \in \mathbb{R}$ be defined as

$$y_i = \tanh\left(e_{f_i}\right). \tag{4–40}$$

From standard hyperbolic identities:

$$\cosh^2\left(e_{f_i}\right) = \frac{1}{1-\tanh^2\left(e_{f_i}\right)} = \frac{1}{1-y_i^2}. \tag{4–41}$$

If y_i can be calculated only from position measurements, then $\tanh\left(e_{f_i}\right)$ and $\cosh^2\left(e_{f_i}\right)$ can be calculated only from position measurements. Rewriting Equation 4–4 in terms of individual elements yields

$$\begin{aligned} \dot{e}_{f_i} &= -\alpha_3 \tanh(e_{f_i}) + \alpha_2 \tanh(e_i) - k_1 \cosh^2(e_{f_i})\eta_i \\ e_{f_i}(0) &= 0. \end{aligned} \tag{4–42}$$

Taking the time derivative of Equation 4–40, and substituting Equation 4–41 and Equation 4–42 yields

$$\begin{aligned} \dot{y}_i &= \cosh^{-2}\left(e_{f_i}\right)\dot{e}_{f_i} \\ &= \left(1-y_i^2\right)\left(-\alpha_3 y_i + \alpha_2 \tanh(e_i)\right) - k_1\left[\dot{e}_i + \alpha_1 \tanh(e_i) + \alpha_2 y_i\right] \\ y_i(0) &= 0. \end{aligned}$$

The auxiliary variable $y_i(t)$ can be generated from the following expression:

$$y_i = p_i - k_1 e_i, \tag{4–43}$$

where $p_i \in \mathbb{R}$ is an auxiliary variable generated from the following differential equation:

$$\begin{aligned} \dot{p}_i &= \left(1-\left(p_i - k_1 e_i\right)^2\right)\left[-\alpha_3\left(p_i - k_1 e_i\right) + \alpha_2 \tanh(e_i)\right] \\ &\quad - k_1\left[\alpha_1 \tanh(e_i) + \alpha_2\left(p_i - k_1 e_i\right)\right] \\ p_i(0) &= k_1 e_i(0). \end{aligned} \tag{4–44}$$

From Equation 4–44, it is obvious that $p_i(t)$ can be calculated using only position measurements. Due to the fact that $p_i(t)$ can be calculated using only position measurements, Equation 4–43 can be used to show that $y_i(t)$, and therefore $\tanh(e_{f_i})$ and $\cosh^2(e_{f_i})$, can be calculated using only position measurements. Due to the fact that $\tanh(e_{f_i})$ and $\cosh^2(e_{f_i})$ can be calculated using only position measurements, the expression in Equation 4–18 can be calculated using only position measurements.

To show that the adaptive update law given by Equation 4–15 only requires position measurements, Equation 4–3 is substituted into Equation 4–15, which is integrated by parts to form the following expression:

$$\hat{\theta} = \Gamma Y_d^T e + \Gamma \sigma \tag{4–45}$$
$$\dot{\sigma} = Y_d^T \left(\alpha_1 Tanh(e) + \alpha_2 y\right) - \dot{Y}_d^T e.$$

From Equation 4–45, it is obvious that $\hat{\theta}(t)$ can be calculated using only position measurements. Due to the fact that $\hat{\theta}(t)$ can be calculated using only position measurements, the expression in Equation 4–13 can be calculated using only position measurements. Due to the fact that the expressions in Equation 4–13 and Equation 4–18 can be calculated using only position measurements, the total control given in Equation 4–14 can be calculated using only position measurements.

4.6 Experimental Results

4.6.1 Experiment

To test the validity of the controller proposed in Equation 4–14 an experiment was performed on the two-link robot testbed as described Section 2.9. The modeled dynamics for the testbed are linear in the following parameters:

$$\theta = \begin{bmatrix} p_1 & p_2 & p_3 & F_{d1} & F_{d2} \end{bmatrix}^T.$$

The control objective is to track the desired time-varying trajectory by using the developed adaptive inverse optimal output feedback control law. To achieve this control

Table 4-1. Tabulated values for the 10 runs of the output feedback adaptive inverse optimal controller

Average Max Steady State Error (deg)- Link 1	0.0678
Average Max Steady State Error (deg)- Link 2	0.0973
Average RMS Error (deg) - Link 1	0.0261
Average RMS Error (deg) - Link 2	0.0323
Average RMS Torque (Nm) - Link 1	9.7256
Average RMS Torque (Nm) - Link 2	1.3959
Error Standard Deviation (deg) - Link 1	0.0001
Error Standard Deviation (deg) - Link 2	0.0030
Torque Standard Deviation (Nm) - Link 1	0.2184
Torque Standard Deviation (Nm) - Link 2	0.0446

objective, the control gains α_1, α_2, α_3, and k_1, defined as scalars in Equation 4–3 and Equation 4–4, were implemented (with non-consequential implications to the stability result) as diagonal gain matrices. Specifically, the control gains were selected as

$$\begin{aligned} \alpha_1 = diag\{50,\ 40\} \quad \alpha_2 = diag\{0.5,\ 4\} \\ \alpha_3 = diag\{65,\ 40\} \quad k_1 = diag\{200,\ 150\}, \end{aligned} \tag{4–46}$$

and the adaptation gains were selected as

$$\Gamma = diag([5, 5, 5, 5, 5]).$$

The desired trajectories for this experiment were chosen as follows:

$$q_{d_1} = q_{d_2} = 60\sin(2t)\left(1 - \exp\left(-0.01t^3\right)\right). \tag{4–47}$$

Each experiment was performed ten times, and data from the experiments is displayed in Table 4-1.

Figure 4-1 depicts the tracking errors for one experimental trial. The control torques and adaptive estimates for the same experimental trial are shown in Figures. 4-2 and 4-3, respectively.

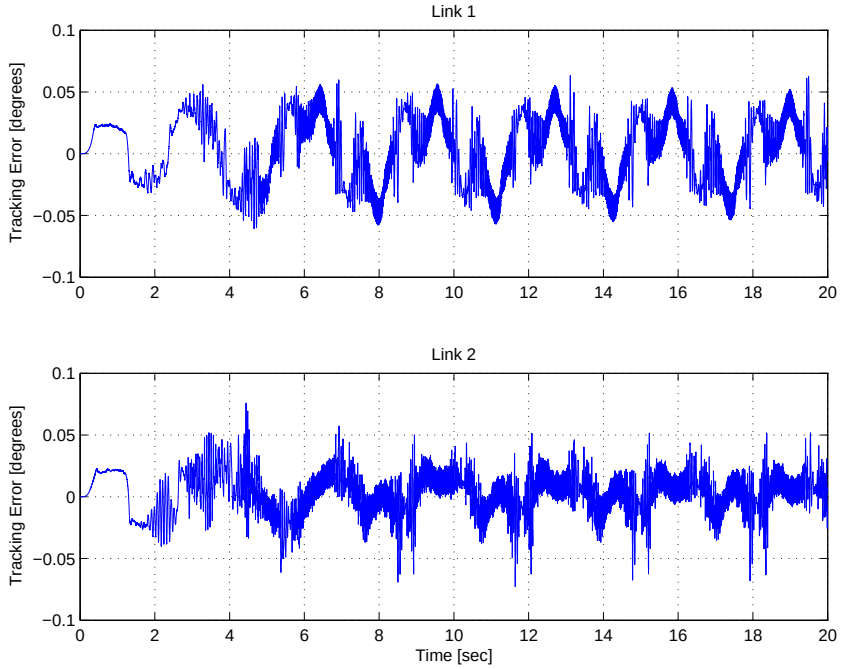

Figure 4-1. Tracking errors resulting from implementing the output feedback adaptive inverse optimal controller.

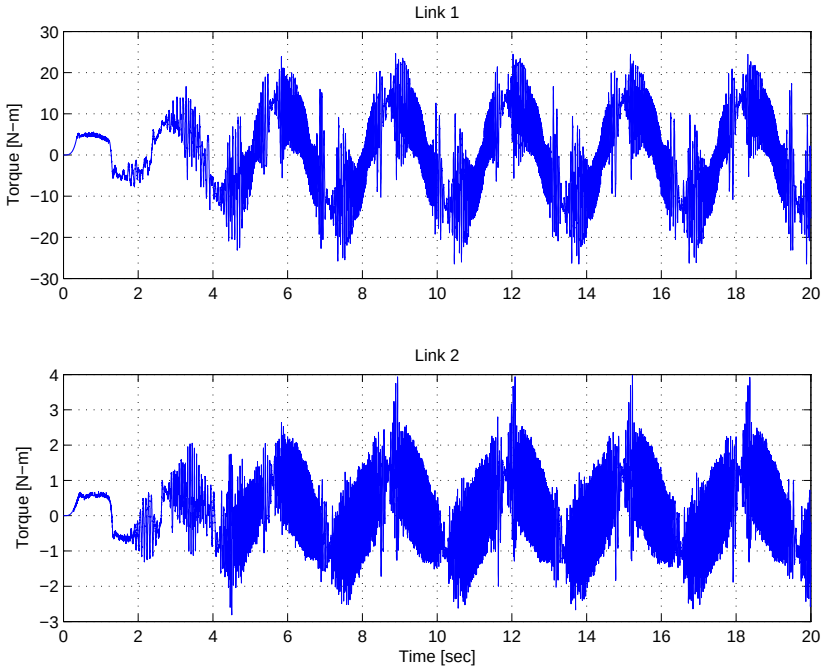

Figure 4-2. Torques resulting from implementing the output feedback adaptive inverse optimal controller.

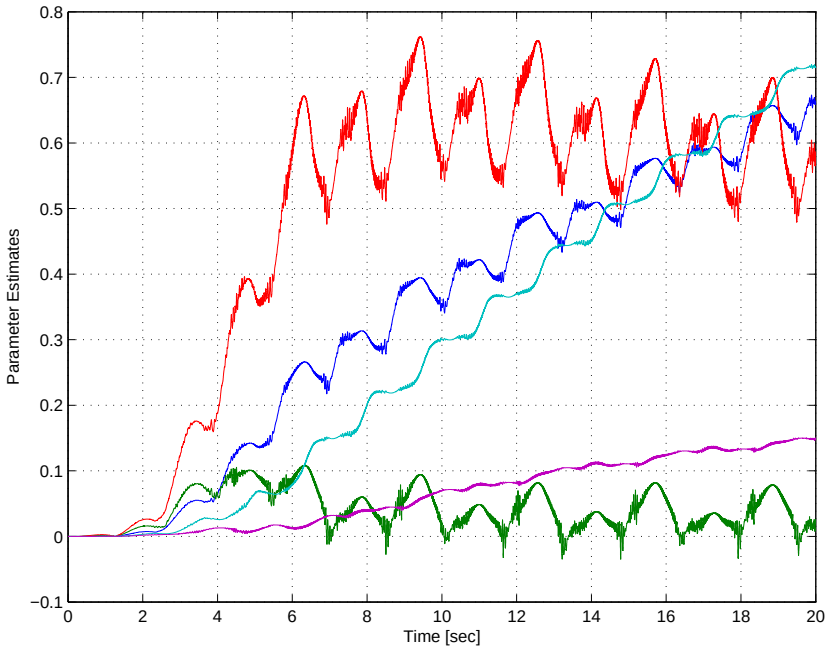

Figure 4-3. Unknown system parameter estimates for the output feedback adaptive inverse optimal controller.

4.6.2 Discussion

Compared to the results in Section 3.5 the results are improved. The controller was able keep the average maximum steady state (defined as the last 10 seconds of the experiment) errors below 0.07 degrees for the first link and 0.1 degrees for the second link. The average RMS error was 0.0261 degrees for the first link and 0.0323 degrees for the second link. The average RMS torque was 9.7256 Nm for the first link and 1.3959 Nm for the second link.

CHAPTER 5
CONCLUSION

In this dissertation, optimal controllers are designed for uncertain nonlinear Euler-Lagrange systems. The optimal control problems in this dissertation are separated into two main parts: 1) direct optimal control, where the cost functional was chosen a priori; and 2) inverse optimal control, where a meaningful cost functional was determined after the control design. These two design methods were approached using different control techniques.

In Chapter 2, a control scheme is developed for a class of nonlinear Euler-Lagrange systems that enables the generalized coordinates to asymptotically track a desired time-varying trajectory despite general uncertainty in the dynamics such as additive bounded disturbances and parametric uncertainty that do not have to satisfy a LP assumption. The main contribution of this work is that the RISE feedback method augmented with an auxiliary control term is shown to minimize a quadratic performance index based on a HJB optimization scheme. Like the influential work in (6–12; 36; 37) the result in this effort initially develops an optimal controller based on a partially feedback linearized state-space model assuming exact knowledge of the dynamics. The optimal controller is then combined with a feedforward NN and RISE feedback. A Lyapunov stability analysis is included to show that the NN and RISE identify the uncertainties, therefore the dynamics asymptotically converge to the state-space system that the HJB optimization scheme is based on. Numerical simulations and an experiment are included to support these results.

To circumvent having to solve an HJB equation, an adaptive inverse optimal controller is developed in Chapter 3 to achieve asymptotic tracking while minimizing a meaningful cost. In contrast to typical optimal controllers, inverse optimal controllers do not have an a priori chosen cost; rather the cost is calculated based on the Lyapunov function. This controller consists of an adaptive feedforward term and an feedback

term that is shown to minimize a meaningful cost. A Lyapunov stability analysis is used to show that the controller achieves asymptotic tracking and that the resulting cost functional is meaningful. A separate analysis is then used to show that the cost is minimized. Simulation and experimental results are provided to demonstrate the developed controller.

An output feedback adaptive IOC controller is designed in Chapter 4 due to the fact that output feedback controllers are more desirable than full-state feedback controllers. The controller is designed using a new error system and a DCAL feedforward adaptive term. A Lyapunov stability analysis is used to show that the developed controller not only stabilizes a system where the unknown matrices are functions of the states, and the input gain matrix is unknown, but minimizes a meaningful cost. Through an innovative filter design, the IOC is developed as an output feedback controller; requiring only position measurements for implementation. Experimental results are included to illustrate the improved performance of the controller over the full state feedback controller.

There are many possible avenues for future work. One possible direction is to include disturbances in the control design and to attempt to solve a Hamilton-Jacobi-Issacs (HJI) equation, rather than an HJB equation. The solution of HJI equations results in the solution of a differential game problem, that accounts for disturbances in the optimization. Another possible direction is the use of the RISE in inverse optimal design. In the controllers in Chapter 3 and Chapter 4, an adaptive feedforward term is used to compensate for LP uncertainty. The use of the RISE may result in inverse optimal controllers that can handle a broader class of systems.

APPENDIX A
SOLUTION OF RICCATI DIFFERENTIAL EQUATION

Lemma: If α_1, R, and K, introduced in Equation 2–5, Equation 2–12, and Equation 2–13, satisfy the following algebraic relationships

$$K = K^T = -\frac{1}{2}\left(Q_{12} + Q_{12}^T\right) > 0$$
$$Q_{11} = \alpha_1^T K + K\alpha_1,$$
$$R^{-1} = Q_{22},$$

then $P(q)$, satisfies the following differential equation:

$$z^T\left(PA + A^TP - PBR^{-1}B^TP + \dot{P} + Q\right)z = 0, \tag{A–1}$$

where $A\left(q,\dot{q}\right)$, $B\left(q\right)$ and $z\left(t\right)$ are introduced in Equation 2–11.

Proof: Substituting $A\left(q,\dot{q}\right)$, $B\left(q\right)$ and $P(q)$ into Equation A–1 yields

$$\begin{aligned} 0 = z^T\Bigg(&\begin{bmatrix} -K\alpha_1 & K \\ 0 & -V_m \end{bmatrix} + \begin{bmatrix} -\alpha_1^TK & 0 \\ K & -V_m^T \end{bmatrix} \\ &- \begin{bmatrix} 0 & 0 \\ 0 & R^{-1} \end{bmatrix} + \begin{bmatrix} 0 & 0 \\ 0 & \dot{M}\left(q\right) \end{bmatrix} + \begin{bmatrix} Q_{11} & Q_{12} \\ Q_{12}^T & Q_{22} \end{bmatrix}\Bigg)z. \end{aligned} \tag{A–2}$$

After applying Equation 2–3 in Property 2, Equation A–2 is satisfied if the following conditions are true:

$$\begin{bmatrix} -K\alpha_1 - \alpha_1^TK & K \\ K & -R^{-1} \end{bmatrix} = -\begin{bmatrix} Q_{11} & Q_{12} \\ Q_{12}^T & Q_{22} \end{bmatrix}.$$

Therefore, if α_1, R, and K are chosen as in Equation 2–14 - Equation 2–16, then $P\left(q\right)$ satisfies Equation A–1.

APPENDIX B
SOLUTION OF HAMILTON-JACOBI-BELLMAN EQUATION

Lemma: The value function $V(z,t) \in \mathbb{R}$

$$V = \frac{1}{2} z^T P z \tag{B–1}$$

satisfies the HJB equation. Then the optimal control $u(t)$ that minimizes Equation 2–12 subject to Equation 2–11 is

$$u(t) = -R^{-1} B^T \left(\frac{\partial V(z,t)}{\partial z} \right)^T = -R^{-1} e_2. \tag{B–2}$$

Proof: The HJB equation is given by

$$-\frac{\partial V(z,t)}{\partial t} = \min_u \left[H\left(z, u, \frac{\partial V(z,t)}{\partial z}, t \right) \right], \tag{B–3}$$

where the Hamiltonian is defined as

$$H\left(z, u, \frac{\partial V(z,t)}{\partial z}, t \right) = \min_u \left[L(z,u) + \frac{\partial V(z,t)}{\partial z} \dot{z} \right]. \tag{B–4}$$

To derive the optimal control law, the partial derivatives of the function $V(z,t)$ need to be evaluated. The time derivative of $V(z,t)$ can be expressed as

$$\frac{dV}{dt} = \frac{\partial V}{\partial t} + \frac{\partial V}{\partial z} \dot{z}. \tag{B–5}$$

The gradient of $V(z,t)$ with respect to the error state $z(t)$ is

$$\frac{\partial V}{\partial z} = z^T P + \frac{1}{2} z^T D, \tag{B–6}$$

where

$$D = \begin{bmatrix} \frac{\partial P}{\partial e_{11}} z & \cdots & \frac{\partial P}{\partial e_{1n}} z & 0 & \cdots & 0 \end{bmatrix} = \begin{bmatrix} D_1 & 0 \end{bmatrix}. \tag{B–7}$$

In Equation B–7, $D \in \mathbb{R}^{2n \times 2n}$ and $0 \in \mathbb{R}^{2n \times 1}$ is a zero vector and the notation $\frac{\partial P}{\partial e_{1i}}$ is used to represent the $2n \times 2n$ matrix whose elements are partial derivatives of the elements of $P(q)$ with respect to e_{1i}.

In order to determine a control that optimizes the Hamiltonian, its partial derivative with respect to $u(t)$ must be determined. Since $u(t)$ is unconstrained, Equation B–4 requires that

$$\frac{\partial H}{\partial u}\left(z, u, \frac{\partial V(z,t)}{\partial z}, t\right) = u^T R + \frac{\partial V}{\partial z} B = 0,$$

which gives an optimal control candidate

$$u(t) = -R^{-1} B^T \frac{\partial V^T}{\partial z}. \tag{B–8}$$

Since

$$\frac{\partial^2 H}{\partial u^2} = R > 0,$$

we know that Equation B–4 is minimized by $u(t)$. Substituting Equation B–6 and Equation B–7 into Equation B–8 gives

$$u(t) = -R^{-1} B^T \left(Pz + \frac{1}{2} D^T z\right) = -R^{-1} B^T P^T z = -R^{-1} e_2, \tag{B–9}$$

where the relation

$$B^T D^T = 0 D_1 + M 0 = 0,$$

is used.

A necessary and sufficient condition for optimality is that the chosen value function $V(z,t)$ satisfies Equation B–3. Substituting Equation B–4 into Equation B–3 yields

$$\frac{\partial V(z,t)}{\partial t} + \frac{\partial V(z,t)}{\partial z}\dot{z} + L(z, u^*) = 0. \tag{B–10}$$

Substituting Equation B–5 into Equation B–10 yields

$$z^T P \dot{z} + \frac{1}{2} z^T \dot{P} z + L(z, u) = 0. \tag{B–11}$$

Inserting Equation 2–11, Equation B–9, and $L(z,u)$ into Equation B–11 yields

$$z^T P A z + \frac{1}{2} z^T \left(\dot{P} + Q - P B R^{-1} B^T P^T\right) z = 0. \tag{B–12}$$

Since $z^T PAz = \frac{1}{2} z^T \left(A^T P + PA\right) z$, Equation B–12 can be written as

$$\frac{1}{2} z^T \left(\dot{P} + A^T P + PA + Q - PBR^{-1} B^T P^T\right) z = 0. \tag{B–13}$$

As shown in Appendix A, $P(q)$ satisfies Equation B–13, therefore $V(z,t)$ satisfies the HJB equation Equation B–3 and the optimal is given by Equation B–9.

APPENDIX C
BOUND ON $\tilde{N}(T)$

Lemma: The auxiliary error $\tilde{N}(t)$ defined in Equation 2–26 as

$$\tilde{N} \triangleq -\dot{V}_m e_2 - V_m \dot{e}_2 - \frac{1}{2}\dot{M} r + \dot{\bar{h}} + \alpha_2 \dot{M} e_2 + \alpha_2 M \dot{e}_2 + e_2 + \alpha_2 R^{-1} e_2, \tag{C–1}$$

$$- \|e_2\| \hat{\sigma} - \hat{W}^T \hat{\sigma} \|e_2\| x_d$$

can be upper bounded as follows:

$$\left\| \tilde{N}(t) \right\| \leq \rho(\|y\|) \|y\|,$$

where $y(t) \in \mathbb{R}^{3n}$ is defined as

$$y(t) \triangleq [e_1^T \quad e_2^T \quad r^T]^T, \tag{C–2}$$

and the bounding function $\rho(\|y\|) \in \mathbb{R}$ is a positive globally invertible nondecreasing function.

Proof: $\tilde{N}(q, \dot{q}, \ddot{q}_d, \dddot{q}_d, e_1, e_2, r) \in \mathbb{R}^n$ in Equation C–1 can be expressed as follows:

$$\begin{aligned}
\tilde{N} = & -\frac{1}{2}\dot{M}(q) r + \dot{M}(q) \left[\alpha_1 (e_2 - \alpha_1 e_1) + \alpha_2 e_2\right] + \dot{M}(q) \ddot{q}_d + M(q) \dddot{q}_d \\
& + M(q) \left[\alpha_1 (r - \alpha_2 e_2 - \alpha_1 (e_2 - \alpha_1 e_1)) + \alpha_2 (r - \alpha_2 e_2)\right] - \dot{M}(q_d) \ddot{q}_d \\
& + V_m(q, \dot{q}) \left[\ddot{q}_d - r + \alpha_2 e_2 + \alpha_1 e_2 - \alpha_1^2 e_1\right] - \dot{V}_m(q_d, \dot{q}_d) \dot{q}_d - V_m(q_d, \dot{q}_d) \ddot{q}_d \\
& - M(q_d) \dddot{q}_d + \dot{V}_m(q, \dot{q}) \dot{q} + \dot{G}(q) - \dot{G}(q_d) + \dot{F}(\dot{q}) - \dot{F}(\dot{q}_d) + e_2 + \alpha_2 R^{-1} e_2
\end{aligned}$$

where the following were used:

$$\begin{aligned}
\dot{e}_1 &= e_2 - \alpha_1 e_1, \\
\ddot{e}_1 &= r - \alpha_2 e_2 - \alpha_1 (e_2 - \alpha_1 e_1), \\
\dot{e}_2 &= r - \alpha_2 e_2, \\
\ddot{q} &= \ddot{q}_d - r + \alpha_2 e_2 + \alpha_1 e_2 - \alpha_1^2 e_1.
\end{aligned}$$

Let $N\left(q, \dot{q}, \ddot{q}_d, \dddot{q}_d, e_1, e_2, r\right) \in \mathbb{R}^n$ be defined as

$$\begin{aligned} N \triangleq & -\frac{1}{2}\dot{M}(q)r + \dot{M}(q)\left[\alpha_1\left(e_2 - \alpha_1 e_1\right) + \alpha_2 e_2\right] + \dot{G}\left(q\right) \\ & + M(q)\left[\alpha_1\left(r - \alpha_2 e_2 - \alpha_1\left(e_2 - \alpha_1 e_1\right)\right) + \alpha_2\left(r - \alpha_2 e_2\right)\right] \\ & + \dot{M}(q)\ddot{q}_d + M(q)\dddot{q}_d + \dot{V}_m(q,\dot{q})\dot{q} + \dot{F}\left(\dot{q}\right) + e_2 + \alpha_2 R^{-1} e_2 \\ & + V_m(q,\dot{q})\left[\ddot{q}_d - r + \alpha_2 e_2 + \alpha_1 e_2 - \alpha_1^2 e_1\right]. \end{aligned}$$

The auxiliary error $\tilde{N}(t)$ can be written as the sum of errors pertaining to each of its arguments as follows:

$$\begin{aligned} \tilde{N}(t) &= N\left(q, \dot{q}, \ddot{q}_d, \dddot{q}_d, e_1, e_2, r\right) - N\left(q_d, \dot{q}_d, \ddot{q}_d, \dddot{q}_d, 0, 0, 0\right) \\ &= N\left(q, \dot{q}_d, \ddot{q}_d, \dddot{q}_d, 0, 0, 0\right) - N\left(q_d, \dot{q}_d, \ddot{q}_d, \dddot{q}_d, 0, 0, 0\right) \\ &+ N\left(q, \dot{q}, \ddot{q}_d, \dddot{q}_d, 0, 0, 0\right) - N\left(q, \dot{q}_d, \ddot{q}_d, \dddot{q}_d, 0, 0, 0\right) \\ &+ N\left(q, \dot{q}, \ddot{q}_d, \dddot{q}_d, 0, 0, 0\right) - N\left(q, \dot{q}, \ddot{q}_d, \dddot{q}_d, 0, 0, 0\right) \\ &+ N\left(q, \dot{q}, \ddot{q}_d, \dddot{q}_d, 0, 0, 0\right) - N\left(q, \dot{q}, \ddot{q}_d, \dddot{q}_d, 0, 0, 0\right) \\ &+ N\left(q, \dot{q}, \ddot{q}_d, \dddot{q}_d, e_1, 0, 0\right) - N\left(q, \dot{q}, \ddot{q}_d, \dddot{q}_d, 0, 0, 0\right) \\ &+ N\left(q, \dot{q}, \ddot{q}_d, \dddot{q}_d, e_1, e_2, 0\right) - N\left(q, \dot{q}, \ddot{q}_d, \dddot{q}_d, e_1, 0, 0\right) \\ &+ N\left(q, \dot{q}, \ddot{q}_d, \dddot{q}_d, e_1, e_2, r\right) - N\left(q, \dot{q}, \ddot{q}_d, \dddot{q}_d, e_1, e_2, 0\right). \end{aligned}$$

Applying the Mean Value Theorem to $\tilde{N}(t)$ results in the following expression:

$$\begin{aligned}\tilde{N}(t) = & \frac{\partial N(\sigma_1, \dot{q}_d, \ddot{q}_d, \dddot{q}_d, 0, 0, 0)}{\partial \sigma_1}|_{\sigma_1 = v_1} (q - q_d) \\ & + \frac{\partial N(q, \sigma_2, \ddot{q}_d, \dddot{q}_d, 0, 0, 0)}{\partial \sigma_2}|_{\sigma_2 = v_2} (\dot{q} - \dot{q}_d) \\ & + \frac{\partial N(q, \dot{q}, \sigma_3, \dddot{q}_d, 0, 0, 0)}{\partial \sigma_3}|_{\sigma_3 = v_3} (\ddot{q}_d - \ddot{q}_d) \\ & + \frac{\partial N(q, \dot{q}, \ddot{q}_d, \sigma_4, 0, 0, 0)}{\partial \sigma_4}|_{\sigma_4 = v_4} (\dddot{q}_d - \dddot{q}_d) \\ & + \frac{\partial N(q, \dot{q}, \ddot{q}_d, \dddot{q}_d, \sigma_5, 0, 0)}{\partial \sigma_5}|_{\sigma_5 = v_5} (e_1 - 0) \\ & + \frac{\partial N(q, \dot{q}, \ddot{q}_d, \dddot{q}_d, e_1, \sigma_6, 0)}{\partial \sigma_6}|_{\sigma_6 = v_6} (e_2 - 0) \\ & + \frac{\partial N(q, \dot{q}, \ddot{q}_d, \dddot{q}_d, e_1, e_2, \sigma_7)}{\partial \sigma_7}|_{\sigma_7 = v_7} (r - 0) \,,\end{aligned} \tag{C–3}$$

where

$$\begin{aligned} v_1 &\in (q_d, q) \\ v_2 &\in (\dot{q}_d, \dot{q}) \\ v_3 &\in (\ddot{q}_d, \ddot{q}_d) \\ v_4 &\in (\dddot{q}_d, \dddot{q}_d) \\ v_5 &\in (0, e_1) \\ v_6 &\in (0, e_2) \\ v_7 &\in (0, r) \,. \end{aligned}$$

From equation Equation C–3, $\tilde{N}(t)$ can be upper bounded as follows:

$$\begin{aligned}\left\|\tilde{N}(t)\right\| \leq & \left\|\frac{\partial N(\sigma_1, \dot{q}_d, \ddot{q}_d, \dddot{q}_d, 0, 0, 0)}{\partial \sigma_1}|_{\sigma_1=v_1}\right\| \|e_1\| \\ & + \left\|\frac{\partial N(q, \sigma_2, \ddot{q}_d, \dddot{q}_d, 0, 0, 0)}{\partial \sigma_2}|_{\sigma_2=v_2}\right\| \|e_2 - a_1 e_1\| \\ & + \left\|\frac{\partial N(q, \dot{q}, \ddot{q}_d, \dddot{q}_d, \sigma_5, 0, 0)}{\partial \sigma_5}|_{\sigma_5=v_5}\right\| \|e_1\| \\ & + \left\|\frac{\partial N(q, \dot{q}, \ddot{q}_d, \dddot{q}_d, e_1, \sigma_6, 0)}{\partial \sigma_6}|_{\sigma_6=v_6}\right\| \|e_2\| \\ & + \left\|\frac{\partial N(q, \dot{q}, \ddot{q}_d, \dddot{q}_d, e_1, e_2, \sigma_7)}{\partial \sigma_7}|_{\sigma_7=v_7}\right\| \|r\| .\end{aligned} \tag{C–4}$$

By noting that

$$\begin{aligned} v_1 &= q - c_1 (q - q_d) \\ v_2 &= \dot{q} - c_2 (\dot{q} - \dot{q}_d) \\ v_5 &= e_1 (1 - c_5) \\ v_6 &= e_2 (1 - c_6) \\ v_7 &= r (1 - c_7) . \end{aligned}$$

where $c_i \in (0, 1) \in \mathbb{R}$, $i = 1, 2, 5, 6, 7$ are unknown constants, the following upper bounded can be developed:

$$\begin{aligned} \left\|\frac{\partial N(\sigma_1, \dot{q}_d, \ddot{q}_d, \dddot{q}_d, 0, 0, 0)}{\partial \sigma_1}|_{\sigma_1=v_1}\right\| &\leq \rho_1(e_1) \\ \left\|\frac{\partial N(q, \sigma_2, \ddot{q}_d, \dddot{q}_d, 0, 0, 0)}{\partial \sigma_2}|_{\sigma_2=v_2}\right\| &\leq \rho_2(e_1, e_2) \\ \left\|\frac{\partial N(q, \dot{q}, \ddot{q}_d, \dddot{q}_d, \sigma_5, 0, 0)}{\partial \sigma_5}|_{\sigma_5=v_5}\right\| &\leq \rho_5(e_1, e_2) \\ \left\|\frac{\partial N(q, \dot{q}, \ddot{q}_d, \dddot{q}_d, e_1, \sigma_6, 0)}{\partial \sigma_6}|_{\sigma_6=v_6}\right\| &\leq \rho_6(e_1, e_2) \\ \left\|\frac{\partial N(q, \dot{q}, \ddot{q}_d, \dddot{q}_d, e_1, e_2, \sigma_7)}{\partial \sigma_7}|_{\sigma_7=v_7}\right\| &\leq \rho_7(e_1, e_2, r). \end{aligned}$$

The bound on $\tilde{N}(t)$ can be further reduced to:

$$\begin{aligned}\left\|\tilde{N}(t)\right\| \leq \rho_1(e_1)\left\|e_1\right\| + \rho_2(e_1,e_2)\left\|e_2-\alpha_1 e_1\right\| \\ + \rho_5(e_1,e_2)\left\|e_1\right\| + \rho_6(e_1,e_2)\left\|e_2\right\| \\ + \rho_7(e_1,e_2,r)\left\|r\right\|.\end{aligned} \tag{C–5}$$

Using the inequality

$$\left|\left|e_2-\alpha_1 e_1\right|\right| \leq \left\|e_2\right\| + \alpha_1\left\|e_1\right\|,$$

the expression in Equation C–5 can be further upper bounded as follows:

$$\begin{aligned}\left\|\tilde{N}(t)\right\| \leq \left[\rho_1(e_1) + \alpha_1\rho_2(e_1,e_2) + \rho_5(e_1,e_2)\right]\left\|e_1\right\| \\ + \left[\rho_2(e_1,e_2) + \rho_6(e_1,e_2)\right]\left\|e_2\right\| + \rho_7(e_1,e_2,r)\left\|r\right\|.\end{aligned}$$

Using the definition of $y(t) \in \mathbb{R}^{3n}$ in Equation C–2, $\tilde{N}(t)$ can be expressed in terms of $y(t)$ as follows:

$$\begin{aligned}\left\|\tilde{N}(t)\right\| \leq \left[\rho_1(e_1) + \alpha_1\rho_2(e_1,e_2) + \rho_5(e_1,e_2)\right]\left\|y(t)\right\| \\ + \left[\rho_2(e_1,e_2) + \rho_6(e_1,e_2)\right]\left\|y(t)\right\| \\ + \rho_7(e_1,e_2,r)\left\|y(t)\right\|.\end{aligned}$$

Therefore,

$$\left\|\tilde{N}(t)\right\| \leq \rho\left(\left\|y\right\|\right)\left\|y\right\|,$$

where $\rho\left(\left\|y\right\|\right)$ is some positive globally invertible nondecreasing function. The inclusion of the additional terms in Equation 2–67 is trivial due to the fact that $proj\left(\cdot\right) \leq \left\|e_2\right\|$, and all other terms are bounded by assumption or design.

APPENDIX D
BOUND ON $L(T)$ - PART 1

Lemma: Define the auxiliary function $L(t)$ as Equation 2–36. If the following sufficient conditions in Equation 2–33 then

$$\int_0^t L(\tau)d\tau \leq \beta_1 \left\|e_2(0)\right\| - e_2(0)^T N_D(0). \tag{D–1}$$

Proof: Integrating both sides of Equation 2–36 yields

$$\int_0^t L(\tau)d\tau = \int_0^t r(\tau)^T \left(N_D(\tau) - \beta_1 sgn(e_2)\right) d\tau. \tag{D–2}$$

Substituting Equation 2–6 into Equation D–2,

$$\begin{aligned}\int_0^t L(\tau)d\tau = \int_0^t \frac{de_2(\tau)}{d\tau}^T N_D(\tau)d\tau - \int_0^t \beta \frac{de_2(\tau)}{d\tau}^T sgn(e_2)d\tau \\ + \int_0^t \alpha_2 e_2(\tau)^T \left(N_D(\tau) - \beta_1 sgn(e_2)\right) d\tau.\end{aligned} \tag{D–3}$$

After integrating the first integral in Equation D–3 by parts, the expression in Equation D–3 can be written as

$$\begin{aligned}\int_0^t L(\tau)d\tau = \int_0^t \alpha_2 e_2(\tau)^T \left(N_D(\tau) - \beta_1 sgn(e_2)\right) d\tau - \int_0^t e_2(\tau)^T \frac{dN_D(\tau)}{d\tau} d\tau \\ -\beta_1 \left\|e_2(t)\right\| + \beta_1 \left\|e_2(0)\right\| + e_2(t)^T N_D(t) - e_2(0)^T N_D(0).\end{aligned} \tag{D–4}$$

After rearranging the terms in Equation D–4 as

$$\begin{aligned}\int_0^t L(\tau)d\tau \leq \beta_1 \left\|e_2(0)\right\| - e_2(0)^T N_D(0) + \left\|e_2(t)\right\| (\zeta_1 - \beta_1) \\ + \int_0^t \alpha_2 \left\|e_2(\tau)\right\| \left(\zeta_1 + \frac{1}{\alpha_2}\zeta_2 - \beta_1\right) d\tau,\end{aligned} \tag{D–5}$$

the inequality in Equation D–5 can be obtained if β_1 satisfies Equation 2–33.

APPENDIX E
BOUND ON $L(T)$ - PART 2

Lemma: Let the function $L(t)$ as Equation 2–82. If the following sufficient conditions in Equation 2–79 then

$$\int_0^t L(\tau)d\tau \leq \beta_1 \left\|e_2(0)\right\| - e_2(0)^T N_B(0). \tag{E–1}$$

Proof: Integrating both sides of Equation 2–82 yields

$$\begin{aligned}\int_0^t L(\tau)d\tau = \int_0^t (-\beta_2 \left\|e_2(\tau)\right\|^2 + \frac{de_2(\tau)}{d\tau}^T N_{B_2}(\tau) \\ + r(\tau)^T(N_{B_1}(\tau) + N_D(\tau) - \beta_1 sgn(e_2)))d\tau.\end{aligned} \tag{E–2}$$

Substituting Equation 2–6 into Equation E–2,

$$\begin{aligned}\int_0^t L(\tau)d\tau = \int_0^t \frac{de_2(\tau)}{d\tau}^T N(\tau)d\tau - \int_0^t \beta_1 \frac{de_2(\tau)}{d\tau}^T sgn(e_2)d\tau \\ + \int_0^t \alpha_2 e_2(\tau)^T \left(N_{B_1}(t) + N_D(t) - \beta_1 sgn(e_2)\right) d\tau \\ - \int_0^t \beta_2 \left\|e_2(t)\right\|^2 d\tau.\end{aligned} \tag{E–3}$$

Integrating the first integral in Equation E–3 by parts, and by using the fact that

$$\begin{aligned}\frac{dN(\tau)}{d\tau} &= \frac{dN_D(\tau)}{d\tau} + \frac{dN_B(\tau)}{d\tau} \\ &= \frac{dN_D(\tau)}{d\tau} + \frac{\partial N_B(\tau)}{\partial x_d}\frac{d\dot{x}_d}{dt} + \frac{\partial N_B(\tau)}{\partial vec\left(\hat{W}\right)}\frac{dvec\left(\hat{W}\right)}{dt} + \frac{\partial N_B(\tau)}{\partial vec\left(\hat{V}\right)}\frac{dvec\left(\hat{V}\right)}{dt}.\end{aligned}$$

The expression in Equation E–3 can be written as

$$\int_0^t L(\tau)d\tau = \int_0^t \alpha_2 e_2(\tau)^T \left(N_{B_1}(t) + N_D(t) - \beta_1 sgn(e_2)\right) dt \tag{E–4}$$
$$- \int_0^t \beta_2 \left\|e_2(t)\right\|^2 d\tau - \frac{1}{\alpha_2}\int_0^t \alpha_2 e_2(\tau)^T \left(\frac{\partial N_B(\tau)}{\partial x_d}\frac{dx_d}{dt} + \frac{dN_D(\tau)}{d\tau}\right) d\tau$$
$$- \int_0^t e_2(\tau)^T \left(\frac{\partial N_B(\tau)}{\partial vec\left(\hat{W}\right)}\frac{dvec\left(\hat{W}\right)}{dt} + \frac{\partial N_B(\tau)}{\partial vec\left(\hat{V}\right)}\frac{dvec\left(\hat{V}\right)}{dt}\right) d\tau$$
$$-\beta_1 \left\|e_2(t)\right\| + \beta_1 \left\|e_2(0)\right\| + e_2(t)N(t) - e_2(0)N(0).$$

After rearranging the terms in Equation E–4 as

$$\int_0^t L(\tau)d\tau \leq \beta_1 \left\|e_2(0)\right\| - e_2(0)N(0) \tag{E–5}$$
$$+ \int_0^t \alpha_2 \left\|e_2(\tau)\right\| \left(\zeta_1 + \zeta_2 + \frac{1}{\alpha_2}\zeta_3 + \frac{1}{\alpha_2}\zeta_4 - \beta_1\right) d\tau$$
$$+ \int_0^t \left\|e_2(\tau)\right\|^2 (\zeta_5 - \beta_2) + \left\|e_2(t)\right\| (\zeta_1 + \zeta_2 - \beta_1)\, d\tau,$$

the inequality in Equation E–5 can be obtained if β_1 and β_2 satisfy Equation 2–79.

APPENDIX F
REVIEW OF ADAPTIVE INVERSE OPTIMAL CONTROL:

Given a system of the form

$$\dot{x} = f(x) + g(x)\, u, \tag{F–1}$$

where $x(t) \in \mathbb{R}^n$ denotes the state vector, $u(t) \in \mathbb{R}^m$, denotes the control vector, $f(x) \in \mathbb{R}^n$ is a smooth vector valued function and $g(x) \in \mathbb{R}^{n\times m}$ is a smooth matrix valued function, the optimal control problem is to determine the control $u^*(t) \in \mathbb{R}^m$ which minimizes a cost

$$J(u) \triangleq \int_0^\infty L(x,u)\, dt, \tag{F–2}$$

subject to the dynamic constraints in Equation F–1, where $L(z,u) \in \mathbb{R}$ is the Lagrangian. A necessary and sufficient condition for an optimal solution to exist, is the existence of a function $V(x,t) \in \mathbb{R}$, called the value function, which satisfies the Hamilton-Jacobi-Bellman (HJB) equation

$$0 = \frac{\partial V(x,t)}{\partial t} + \min_u \left[L(x,u) + \frac{\partial V(x,t)}{\partial x} \right] \dot{x}.$$

In general the HJB equation, a nonlinear partial differential equation, can not be solved analytically. In an effort to circumvent the need to solve the HJB equation, inverse optimal control was developed. Furthermore, adaptive inverse optimal control was developed to allow the design of inverse optimal controllers for systems with unknown parameters. Consider a system of the form

$$\dot{x} = f(x) + F(x)\,\theta + g(x)\, u, \tag{F–3}$$

where $f(x) \in \mathbb{R}^n$ denotes a known smooth vector function and $F(x) \in \mathbb{R}^{n\times p}$, $g(x) \in \mathbb{R}^{n\times m}$ are known, smooth matrix valued functions, $\theta \in \mathbb{R}^p$ is a vector of unknown constants, and $u(t) \in \mathbb{R}^m$ denotes the control vector. A positive definite, radially unbounded function $V_a(x,\theta) \in \mathbb{R}$ is called an adaptive control Lyapunov function for Equation F–3 if it is a

control Lyapunov function for the modified system

$$\dot{x} = f(x) + F(x)\left(\theta + \Gamma\left(\frac{\partial V_a}{\partial \theta}\right)^T\right) + g(x)\,u, \tag{F–4}$$

where $\Gamma \in \mathbb{R}^{p\times p}$ is positive definite. The function $V_a(x,\theta)$ is a control Lyapunov function for Equation F–4 if there exists a smooth control law $u(\theta,x)$, with $u(\theta,0) = 0$, which satisfies

$$\frac{\partial V}{\partial x}\left[f(x) + F(x)\left(\theta + \Gamma\left(\frac{\partial V_a}{\partial \theta}\right)^T\right) + g(x)\,u\right] \leq 0. \tag{F–5}$$

If there exists a control Lyapunov function for Equation F–4 (which means an adaptive control Lyapunov function for Equation F–3), and a feedback control law of the form

$$u = -R(x,\theta)^{-1}\left(\frac{\partial V_a}{\partial x}g\right)^T, \tag{F–6}$$

where $R(x,\theta) \in \mathbb{R}^{m\times m}$ is a positive definite and symmetric matrix that stabilizes Equation F–4, then the feedback control law

$$u^* = -\beta R\left(x,\hat{\theta}\right)^{-1}\left(\frac{\partial V_a}{\partial x}g\right)^T \quad \beta \in \mathbb{R} \geq 2,$$

where $\hat{\theta} \in \mathbb{R}^p$ is an estimate for θ, with the parameter update law

$$\dot{\hat{\theta}} = \Gamma\left(\frac{\partial V_a}{\partial x}F\right)^T, \tag{F–7}$$

minimizes the cost functional

$$J = \beta \lim_{t\to\infty}\left\|\theta - \hat{\theta}\right\|^2_{\Gamma^{-1}} + \int_0^\infty \left(l\left(x,\hat{\theta}\right) + u^T R(x,\theta)\,u\right)\quad dt, \tag{F–8}$$

where $l\left(x,\hat{\theta}\right) \in \mathbb{R}$ is defined as

$$l = -2\beta\left[\frac{\partial V_a}{\partial x}\left(f + F\left(\hat{\theta} + \Gamma\frac{\partial V_a}{\partial \hat{\theta}}^T\right) + gu\right)\right] + \beta(\beta-2)\frac{\partial V_a}{\partial x}gR^{-1}\left(\frac{\partial V_a}{\partial x}g\right)^T.$$

The cost functional $J(t)$ is considered meaningful in the sense that it imposes a positive penalty on the state and actuation. The adaptive inverse optimal control problem can be

summarized as follows: if an adaptive control Lyapunov function and a stabilizing control law of the form in Equation F–6 can be found for the system in Equation F–3, then that control law minimizes the cost functional in Equation F–8.

REFERENCES

[1] R. Freeman and P. Kokotovic, "Optimal nonlinear controllers for feedback linearizable systems," in *Proceedings of the American Controls Conference*, Seattle, WA, 1995, pp. 2722–2726.

[2] Q. Lu, Y. Sun, Z. Xu, and T. Mochizuki, "Decentralized nonlinear optimal excitation control," *IEEE Transactions on Power Systems*, vol. 11, no. 4, pp. 1957–1962, 1996.

[3] M. Sekoguchi, H. Konishi, M. Goto, A. Yokoyama, and Q. Lu, "Nonlinear optimal control applied to STATCOM for power system stabilization," in *Proceedings of the IEEE/PES Transmission and Distribution Conference and Exhibition*, Yokohama, Japan, 2002, pp. 342–347.

[4] V. Nevistic and J. A. Primbs, "Constrained nonlinear optimal control: a converse HJB approach," California Institute of Technology, Pasadena, CA 91125, Tech. Rep. CIT-CDS 96-021, 1996.

[5] J. A. Primbs and V. Nevistic, "Optimality of nonlinear design techniques: A converse HJB approach," California Institute of Technology, Pasadena, CA 91125, Tech. Rep. CIT-CDS 96-022, 1996.

[6] R. Johansson, "Quadratic optimization of motion coordination and control," *IEEE Transactions on Automatic Control*, vol. 35, no. 11, pp. 1197–1208, 1990.

[7] Y. Kim, F. Lewis, and D. Dawson, "Intelligent optimal control of robotic manipulator using neural networks," *Automatica*, vol. 36, no. 9, pp. 1355–1364, 2000.

[8] Y. Kim and F. Lewis, "Optimal design of CMAC neural-network controller for robot manipulators," *IEEE Transactions on Systems, Man, and Cybernetics: Part C*, vol. 30, no. 1, pp. 22–31, Feb. 2000.

[9] M. Abu-Khalaf and F. Lewis, "Nearly optimal HJB solution for constrained input systems using a neural network least-squares approach," in *Proceedings of the IEEE Conference on Decision and Control*, Las Vegas, NV, 2002, pp. 943–948.

[10] T. Cheng and F. Lewis, "Fixed-final time constrained optimal control of nonlinear systems using neural network HJB approach," in *Proceedings of the IEEE Conference on Decision and Control*, San Diego, CA, 2006, pp. 3016–3021.

[11] ——, "Neural network solution for finite-horizon H-infinity constrained optimal control of nonlinear systems," in *Proceedings of the IEEE International Conference on Control and Automation*, Guangzhou, China, 2007, pp. 1966–1972.

[12] T. Cheng, F. Lewis, and M. Abu-Khalaf, "A neural network solution for fixed-final time optimal control of nonlinear systems," *Automatica*, vol. 43, no. 3, pp. 482–490, 2007.

[13] P. M. Patre, W. MacKunis, C. Makkar, and W. E. Dixon, "Asymptotic tracking for systems with structured and unstructured uncertainties," *IEEE Transactions on Control Systems Technology*, vol. 16, no. 2, pp. 373–379, 2008.

[14] ——, "Asymptotic tracking for systems with structured and unstructured uncertainties," in *Proceedings of the IEEE Conference on Decision and Control*, San Diego, CA, 2006, pp. 441–446.

[15] M. Krstic and H. Deng, *Stabilization of Nonlinear Uncertain Systems*. New York: Springer, 1998.

[16] M. Krstic and P. Tsiotras, "Inverse optimality results for the attitude motion of a rigid spacecraft," in *Proceedings of the American Controls Conference*, Albuquerque, NM, 1997, pp. 1884–1888.

[17] M. Krstic and Z.-H. Li, "Inverse optimal design of input-to-state stabilizing nonlinear controllers," in *Proceedings of the IEEE Conference on Decision and Control*, San Diego, CA, 1997, pp. 3479–3484.

[18] N. Kidane, Y. Yamashita, H. Nakamura, and H. Nishitani, "Inverse optimization for a nonlinear system with an input constraint," in *SICE 2004 Annual Conference*, Sapporo, Japan, 2004, pp. 1210–1213.

[19] T. Fukao, "Inverse optimal tracking control of a nonholonomic mobile robot," in *Proceedings of the IEEE/RSJ International Conference on Intelligent Robots and Systems*, Sendai, Japan, 2004, pp. 1475–1480.

[20] R. Freeman and J. Primbs, "Control lyapunov functions: new ideas from an old source," in *Proceedings of the IEEE Conference on Decision and Control*, Kobe, Japan, 1996, pp. 3926–3931.

[21] P. Gurfil, "Non-linear missile guidance synthesis using control lyapunov functions," *Proceedings of the Institution of Mechanical Engineers, Part G: Journal of Aerospace Engineering*, vol. 219, no. 2, pp. 77–88, 2005.

[22] Z. Li and M. Krstic, "Optimal design of adaptive tracking controllers for nonlinear systems," in *Proceedings of the American Controls Conference*, Albuquerque, New Mexico, 1997, pp. 1191–1197.

[23] X.-S. Cai and Z.-Z. Han, "Inverse optimal control of nonlinear systems with structural uncertainty," *IEE Proceedings of Control Theory and Applications*, vol. 152, no. 1, pp. 79–84, 2005.

[24] J. L. Fausz, V.-S. Chellaboina, and W. Haddad, "Inverse optimal adaptive control for nonlinear uncertain systems with exogenous disturbances," in *Proceedings of the IEEE Conference on Decision and Control*, San Diego, CA, 1997, pp. 2654–2659.

[25] W. Luo, Y. Chu, and K. Ling, "Inverse optimal adaptive control for attitude tracking of spacecraft," *IEEE Transactions on Automatic Control*, vol. 50, no. 11, pp. 1639–1654, Nov. 2005.

[26] L. Sonneveldt, E. Van Oort, Q. P. Chu, and J. A. Mulder, "Comparison of inverse optimal and tuning functions designs for adaptive missile control," *Journal of Guidance, Control, and Dynamics*, vol. 31, no. 4, pp. 1176–1182, 2008.

[27] K. Ezal, P. V. Kokotovic, A. R. Teel, and T. Basar, "Disturbance attenuating output-feedback control of nonlinear systems with local optimality," *Automatica*, vol. 37, no. 6, pp. 805–817, 2001.

[28] Z. Qu, J. Wang, C. E. Plaisted, and R. A. Hull, "Output-feedback near-optimal control of chained systems," in *Proceedings of the American Controls Conference*, Minneapolis, MN, 2006, pp. 4975–4980.

[29] T. Perez and H. Haimovich, *Constrained Control and Estimation*. Berlin: Springer, 2005, ch. Output Feedback Optimal Control with Constraints, pp. 279–294.

[30] F. L. Lewis and V. L. Syrmos, *Optimal Control*. New York: John Wiley and Sons, 1995.

[31] F. Zhang, D. M. Dawson, M. S. de Queiroz, and W. E. Dixon, "Global adaptive output feedback tracking control of robot manipulators," *IEEE Transactions on Automatic Control*, vol. 45, no. 6, pp. 1203–1208, 2000.

[32] W. E. Dixon, E. Zergeroglu, and D. M. Dawson, "Global robust output feedback tracking control of robot manipulators," *Robotica*, vol. 22, no. 4, pp. 351–357, 2004.

[33] E. Zergeroglu, W. E. Dixon, D. Haste, and D. M. Dawson, "A composite adaptive output feedback tracking controller for robotic manipulators," *Robotica*, vol. 17, pp. 591–600, 1999.

[34] T. Burg, D. M. Dawson, and P. Vedagarbha, "A redesigned dcal controller without velocity measurements: Theory and demonstration," *Robotica*, vol. 15, no. 4, pp. 337–346, 1997.

[35] Z. Qu and J. Xu, "Model-based learning controls and theircomparisons using Lyapunov direct method," *Asian Journal of Control*, vol. 4, no. 1, pp. 99–110, 2002.

[36] M. Abu-Khalaf, J. Huang, and F. Lewis, *Nonlinear H-2/H-Infinity Constrained Feedback Control*. London: Springer, 2006.

[37] F. L. Lewis, *Optimal Control*. New York: John Wiley and Sons, 1986.

[38] P. M. Patre, W. MacKunis, K. Kaiser, and W. E. Dixon, "Asymptotic tracking for uncertain dynamic systems via a multilayer neural network feedforward and rise

feedback control structure," *IEEE Transactions on Automatic Control*, vol. 53, no. 9, pp. 2180–2185, 2008.

[39] R. Ortega, A. Lora, P. J. Nicklasson, and H. J. Sira-Ramirez, *Passivity-based Control of Euler-Lagrange Systems: Mechanical, Electrical and Electromechanical Applications*. London: Springer, 1998.

[40] M. Krstic and P. V. Kokotovic, "Control lyapunov functions for adaptive nonlinear stabilization," *Systems and Control Letters*, vol. 26, no. 1, pp. 17–23, 1995.

[41] B. Xian, D. M. Dawson, M. S. de Queiroz, and J. Chen, "A continuous asymptotic tracking control strategy for uncertain nonlinear systems," *IEEE Transactions on Automatic Control*, vol. 49, no. 7, pp. 1206–1211, 2004.

[42] H. K. Khalil, *Nonlinear Systems*. New Jersey: Prentice-Hall, 2002.

[43] F. L. Lewis, "Nonlinear network structures for feedback control," *Asian Journal of Control*, vol. 1, no. 4, pp. 205–228, 1999.

[44] F. Lewis, J. Campos, and R. Selmic, *Neuro-Fuzzy Control of Industrial Systems with Actuator Nonlinearities*. Philadelphia: SIAM, 2002.

[45] W. E. Dixon, A. Behal, D. M. Dawson, and S. P. Nagarkatti, *Nonlinear Control of Engineering Systems: a Lyapunov-Based Approach*. Boston: Birkhuser, 2003.

[46] M. S. Loffler, N. P. Costescu, and D. M. Dawson, "Qmotor 3.0 and the Qmotor robotic toolkit: a pc-based control platform," *IEEE Control Systems Magazine*, vol. 22, no. 3, pp. 12–26, 2002.

[47] W. E. Dixon, E. Zergeroglu, D. M. Dawson, and M. W. Hannan, "Global adaptive partial state feedback tracking control of rigid-link flexible-joint robots," in *Proceedings of the IEEE/ASME International Conference on Advanced Intelligent Mechatronics*, Atlanta, GA, 1999, pp. 281–286.

BIOGRAPHICAL SKETCH

Keith Dupree was born in 1982 in Port Jefferson, New York. He received his Bachelor of Science degree in aerospace engineering with a minor in physics in May of 2005, his Masters of Science in mechanical engineering in May of 2007, and his Master of Science in electrical and computer engineering in August of 2008, and his Doctor of Philosophy in mechaincal engineering in May of 2009; all from the University of Florida. His research interests include nonlinear controls, image processing, state estimation, and optimal control.